

University of Alberta

Modelling of solvent extraction of coal

by

Diana Carolina Figueroa

A thesis submitted to the Faculty of Graduate Studies and Research

in partial fulfillment of the requirements for the degree of

Master of Science

in

Chemical Engineering

Chemical and Materials Engineering Department

©Diana Carolina Figueroa Murcia

Spring 2012

Edmonton, Alberta

Permission is hereby granted to the University of Alberta Libraries to reproduce single copies of this thesis and to lend or sell such copies for private, scholarly or scientific research purposes only. Where the thesis is converted to, or otherwise made available in digital form, the University of Alberta will advise potential users of the thesis of these terms.

The author reserves all other publication and other rights in association with the copyright in the thesis and, except as herein before provided, neither the thesis nor any substantial portion thereof may be printed or otherwise reproduced in any material form whatsoever without the author's prior written permission.

ABSTRACT

Modelling of solvent extraction was studied using 1,2,3,4-tetrahydronaphthalene (tetralin) and Poplar coal (lignite). A kinetic model was developed taking into account temperature, mass transfer limitations and dominating events (physical or chemical) during coal liquefaction. It was found there is no influence of coal particle size (53 – 1000 μ m) and coal to solvent ratio (1:2 – 1:8) on the extraction yield. After 15 minutes or longer extraction time, two regions were identified, physical and chemical dissolution. The physical dissolution is dominant at low temperatures and chemical dissolution is dominant at high temperatures.

Physical and chemical dissolution were modelled using separate terms. The term for physical dissolution employed a limiting concentration and was of the form $C_{s\text{-physical}}(1 - e^{-k_p t})$. The term for chemical dissolution also included a limiting concentration and was of the form $(C_{s\text{-reactive}} - C_{s\text{-physical}})(1 - e^{-k_r t})$. The description of chemical dissolution was further refined to predict the coal soluble, coal insoluble and light fraction.

ACKNOWLEDGEMENT

First of all I would to thank my parents and my brother for their immense support, love and encouragement.

Also I would to thank Oscar for his moral support and encouragement during this experience.

I would like to acknowledge the advice, support, guidance of my supervisors Dr Arno de Klerk and Dr Rajender Gupta.

I also thank Dr Moshfiqur Rahman for his help during the development of the experimental techniques.

My sincere acknowledgement to Mariangel for her support during the development of this project, for her friendship and for making this experience more enjoyable.

Additionally, I would to thank Hector, Rosa and Roberto for valuable contributions to this project.

This work is enabled by the generous support of Sherritt Technologies and the Canadian government through the NSERC-CRD program.

TABLE OF CONTENTS

	Page
1. INTRODUCTION	9
2. OBJECTIVES – HYPOTHESES	12
3. OVERVIEW OF SOLVENT EXTRACTION OF COAL	13
3.1. Coal composition	13
3.2. Coal Liquefaction	14
3.3. Temperature regions in solvent extraction	14
4. OVERVIEW OF KINETIC MODELING OF THE SOLVENT EXTRACTION OF COAL	19
4.1. Commonly employed terms and experimental techniques	19
4.2. Kinetic models based on solvent-class lumping	20
4.3. Other kinetic models based on chromatography and related networks	29
5. MODELLING PHYSICAL DISSOLUTION OF COAL	34
5.1. Relevance of particle size, nature of solvent and coal and coal to solvent ratio	34
5.2. Experimental	36
5.3. Results and discussions	39
5.4. Performance of published models	46
5.5. Modeling of physical dissolution	51
5.6. Conclusion	54
5.7. Recommendations	54
6. MODELING OF CHEMICAL DISSOLUTION OF COAL	55
6.1. Relevance of a fundamental model	55
6.2. Preliminary tests	55
6.3. Low temperature regime	59
6.4. High temperature regime	60
6.5. Discussions	80
6.6. Conclusions	86
6.7. Recommendations	86
7. GENERAL CONCLUSIONS	88
8. BIBLIOGRAPHY	90
9. APPENDIXES	94

LIST OF FIGURES

	Page
Figure 1 Free radicals mechanism formation for tetralin.....	17
Figure 2 Solvent extraction sequence from Cronauer et al (1978).....	20
Figure 3 Set of series-parallel non-reversible reactions.....	21
Figure 4 Reaction mechanism model proposed by Shalabi et al.	23
Figure 5 Experimental vs. predicted data (kinetic model) obtained by Shalabi et al.....	24
Figure 6 Reactions path ways proposed by Li et al.	25
Figure 7 Reaction mechanism proposed by Pradhan et al.	27
Figure 8 Plots of experimental data vs. data predicted using different catalyst.....	28
Figure 9 Models proposed for high temperature range by Mohan and Silla.....	30
Figure 10 Model 2 at low temperature range by Mohan and Silla.....	30
Figure 11 Model 3 proposed by Mohan and Silla.	31
Figure 12 Model 4 proposed by Mohan and Silla.	31
Figure 13 Vector representation of Naphthalene.....	32
Figure 14 Effect of coal particle size on extraction yield during solvent extraction of lignite (3 hours) with tetralin at 100 and 300 °C.	42
Figure 15 Effect of coal type on extraction yield during solvent extraction of three types of coal (3 hours) with tetralin at 100 and 300 °C.	43
Figure 16 Effect of coal to solvent ratio on extraction yield during solvent extraction of lignite (1 hour) with tetralin at 100°C.....	44
Figure 17 Effect of time on extraction yield during solvent extraction of lignite (355-1000 µm particles) with tetralin at 100, 200 and 300 °C.	45
Figure 18 Effect of time on extraction yield during solvent extraction of lignite (355-1000 µm particles) with tetralin at 300, 350 and 450 °C.	46
Figure 19 Isothermal extraction path proposed by Giri and Sharma.....	47
Figure 20 Isothermal kinetic model proposed by Giri and Sharma.....	48
Figure 21 Shrinking core model proposed by Giri and Sharma.....	50
Figure 22 Deterministic model in the modelling of coal dissolution at low temperatures.....	53
Figure 23 Correlation between maximum concentration at physical dissolution and temperature.	53
Figure 24 Pyrolysis of coal under nitrogen atmosphere obtained using Thermo-Gravimetric Analysis (TGA).....	56
Figure 25 H/C ratio of solid residue measured using Elemental Analysis.	57
Figure 26 H/C ratio of solid residue using Elemental Analysis (extended time for extractions at low temperature).....	58
Figure 27 1H-NMR of the extracted coal dissolved in tetralin.....	59
Figure 28 Experimental data for solvent extraction of coal at 350°C.....	62
Figure 29 Experimental data for solvent extraction of coal at 450°C.....	63
Figure 30 n-Heptane and Toluene insoluble at 350°C.....	64
Figure 31 n-Heptane and Toluene insoluble at 450°C.....	65
Figure 32 Model A based on the Model 1 proposed by Ceylan and Olcay.....	66

Figure 33 Model B based on the Model 2 proposed by Ceylan and Olcay.....	66
Figure 34 Model C based on the Model 3 proposed by Ceylan and Olcay	66
Figure 35 Model 1 at 350°C	70
Figure 36 Model 1 at 450°C	71
Figure 37 Model 2 at 350°C	72
Figure 38 Model 2 at 450°C	73
Figure 39 Model 3 at 350°C	74
Figure 40 Model 3 at 450°C	75
Figure 41 Model 4 at 350°C	77
Figure 42 Model 4 at 450°C	78
Figure 43 Model 5 at 350°C	79
Figure 44 Model 5 at 450°C	80

LIST OF TABLES

	Page
Table 1 Ultimate and proximate analysis of coals.....	37
Table 2 Petrographic analysis	38
Table 3 Initial conditions for study of particle size, effect of time and coal to solvent ratio.	39
Table 4 Summary of the rate constants calculated for literature models.....	67
Table 5 Summary of the parameters calculated for the models proposed	83

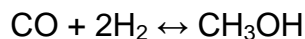
LIST OF SYMBOLS

k, k_1, k_2	Constant rate
t	Time
a	Amount of coal extract obtained at infinite time
x	Extract obtained at time t
n	Order of reaction
V	Volume of reactive core
C	Concentration of reactive molecules
dN	Molecules that disappear during time
r_c	Radius of the reactive core
R	Radius
α	Fractional conversion
dC/dt	Rate of dissolution
C_s	Limit concentration
$C(t)$	Concentration of species of interest at time t
$C_{s-physical}$	Maximum concentration during physical dissolution
k_p	Constant rate of physical dissolution
$C_{s-reactive}$	Maximum concentration during reactive dissolution
k_r	Constant rate of reactive dissolution
a,b,c,d	Stoichiometric factors
P	Toluene insoluble fraction
A	n-Heptane insoluble fraction
O	Light fraction
I	Undissolved coal

1. INTRODUCTION

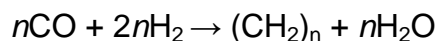
Coal is the most abundant fossil fuel available and one of the main carbon based energy resources in Alberta. The potential of coal for generating added value fuels, as products of liquefaction of coal, is enormous. Coal liquids can be upgraded to chemicals and fuels and are worthy replacements for crude oil derived products in some markets. Of specific interest is the solvent extraction of coal, which has the potential of combining the high carbon efficiency of direct liquefaction with milder operating conditions than has historically been employed for the production of coal liquids (1). During combustion of coal, inorganic matter present in coal produces ash; this constitutes a major concern when coal is used as an energy source. Inorganic matter can be removed during the solvent extraction process, obtaining ash free coal (2).

There are two main classes of liquefaction: indirect and direct liquefaction. The process of indirect liquefaction consists in the gasification of the coal at 1300K in the presence of steam and oxygen to produce a synthesis gas that consists mainly of carbon monoxide and hydrogen. Afterwards, this synthesis gas is cleaned from impurities, adjusted to the H₂/CO ratio and then converted to liquid fuels via methanol synthesis or Fisher-Tropsch synthesis. Methanol synthesis is carried out by reacting the synthesis gas over a catalyst (e.g. CuO, ZnO, Al₂O₃) (3). The reaction is shown below in *Equation 1*.



Equation 1 Methanol synthesis
Equation taken from (3)

The process of methanol synthesis can be classified into vapour-phase low-pressure synthesis and liquid-phase low-pressure synthesis. The liquid-phase synthesis technology has been lately developed, and it is employed when the synthesis gas is rich in CO (4). The Fisher -Tropsch synthesis is a very versatile process in which the synthesis gas can be transformed to a wide range of linear alkenes, olefins and alcohols. The process mainly consist of reacting CO and H₂ (components of the syngas) using a catalyst (5). The reaction between the CO and H₂ is a polymerization reaction to produce hydrocarbon polymers that can be represented with the following reaction (see *Equation 2*) :



Equation 2 Fisher Tropsch synthesis
Equation taken from (5)

Depending on the metal catalyst used, different molecular weights and products are obtained. For example Ni catalyst produces CH_4 , Fe and Re catalyst produce different amounts of alkenes, Ru produces olefins and Rh alcohols (5).

One of the most important characteristic of the indirect liquefaction is the wide range of sulphur and nitrogen free products including motor fuels, methanol, oxygenates (octane enhancers) and other chemicals that can be generated.

On the other hand, direct liquefaction converts solid coal into liquid fuels without producing the synthesis gas as in indirect liquefaction. This liquefaction method is the most energetically efficient and produces the highest oil yields (6). There are two ways to obtain liquid fuels from direct liquefaction: pyrolysis or hydrogenation (7). During pyrolysis coal is treated at elevated temperatures in an inert atmosphere or vacuum to produce gases, condensable liquid (tar) and char. Pyrolysis involves cleavage of chemical bond of coal macromolecules induced by thermal energy that leads to the formation of free radicals. Those free radicals are stabilized by an internal hydrogen source (rearrangement of molecules), obtaining lighter products (6). The hydrogenation process consists in the addition of hydrogen to the coal structure from an external source during thermal treatment of coal at high temperatures. The addition of hydrogen can be done from molecular hydrogen or from a hydrogen-donor solvent (i.e tetralin) in a process called solvent extraction (7). During solvent extraction the pyrolysis process is present, but the difference lies on the fact that, during solvent extraction the source of hydrogen to stabilize the free radicals comes from the molecular hydrogen or the hydrogen donated by the donor solvent. The yield of low molecular liquid products in solvent extraction, ultimately depends on the ability of the solvent to donate hydrogen atoms, otherwise the free radicals will stabilize themselves obtaining more stable products (8). Solvent extraction is also carried out using catalyst in order to increase the production yield. This process is known as catalytic liquefaction. The main advantage of adding a catalyst to the process is: less hydrogen and lower temperatures are required. Also disadvantages can be mentioned in the case of catalytic liquefaction, for example the cost related with the catalyst and the complexity of the reaction (9).

Since the solvent extraction process is a very complex series of reactions taking place, a good understanding of the way that the extraction proceed is of the utmost importance in improving the process.

The kinetics of coal liquefaction has been studied using different approaches in order to explain the process that best describes the reactions that coal undergoes during liquefaction. Most of the approaches are based on the lumping tool. The lumped tool, model the products that are generated from the liquefaction, in categories that have something in common or that have properties that are easily measurable. Those categories can be determined depending on the separation technique that will be used

to obtain the different products from the liquefaction process. The products can be extracted based on their solubility in other solvents (pentane, benzene, THF, etc.). For example, Liquid-Solid Chromatography (LSC) has been used in the separation process by Mohan and Silla obtaining six different fractions which set the starting point for their kinetic model (10). Defining the categories in terms of easily measurable categories is attractive from an experimental point of view. However, just because a category is easily measurable, does not imply that it provides a logical lumping based on the process fundamentals. When the lumping does not reflect the underlying chemistry, modelling runs the risk of becoming a parameter fitting exercise with little predictive capability or fundamental basis

A different lumping method has been proposed by Quann and Jaffe (11). This lumping can be made using a molecular-based representation of the products; it is more complex but more accurate. In this case a hydrocarbon molecule can be represented for a vector which is constituted by structural features and structural groups, characteristics of a molecule (11).

Lumping at a molecular level can be made using techniques such as LC Field Ionization MS and GC-MS (11). Fundamentally this is ideal, but practically it is unlikely that coals or coal liquids can be fully characterised compound by compound. This approach is the opposite extreme from very high level lumping, but becomes untenable as a practical approach.

When a kinetic model is proposed, a proper understanding of the chemical structure of coal and the solvent and also the chemical events occurring is of the utmost importance to obtain accurate results.

The scope of this project is to develop a predictive kinetic model that is able to explain the solvent extraction of coal process based on a time-temperature history of the coal-solvent system. Depending on time and temperature, the products formed and the yield of products will vary due to changes on solvent properties, mass transfer limitations and free radicals formation and stabilization rate. The model needs to accurately reflect the reaction mechanism of coal during liquefaction process. It is unlikely that a simplistic single region model will be able to capture the transition from solvation dominated liquefaction to reaction dominated liquefaction. Our aim is to develop a model that is firmly grounded in the fundamentals. Of course, this is an ambitious goal and the present study represents only the first steps in achieving this objective.

2. OBJECTIVES – HYPOTHESES

Specific objective:

- Develop a predictive kinetic model for coal liquefaction.

Objectives:

- Perform experimental investigation of solvent extraction of coal with tetralin as model system to obtain data needed for the modelling of the process.

The aim of this study is to prove if the following hypotheses are valid:

- Mass transfer limits the liquefaction process. Mass transfer limitations depend on particle size. These limitations can be observed as yield losses and the formation of high molecular weight products (recombination of free radicals, i.e., self-stabilization).
- The kinetic description used for solvent extraction of coal cannot be formulated as a state function. The kinetic model should be formulated based on a time-temperature profile, where the time-temperature history affects dissolution.

3. OVERVIEW OF SOLVENT EXTRACTION OF COAL

In order to formulate a predictive kinetic model for coal liquefaction, it is important to understand what really happens during the liquefaction process. Interactions between coal and solvent have to be understood as well as the phenomena that drive the process of obtaining liquid fuels from coal liquefaction.

3.1. Coal composition

Coal is a material that was formed by plants and remains of plants (such as pollen). Over geological time, the material underwent chemical and physical changes to form the coal as we know it nowadays. Plants are mainly constituted of cellulose and lignin, which under high temperatures and short times or low temperatures and long periods of time can form coal structures. Since coal originates from plant debris, its predominant elements are carbon, hydrogen and oxygen and in lesser proportions also nitrogen and sulfur (12). Inorganic compounds are found in coal composition; such as clays, shales, carbonates, sulfides, silica and pyrites (9).

The mineral matter present in coal can act as a catalyst during the liquefaction process; however the coal liquefaction can be carried out without using a catalyst. When mineral matter is present in the coal structure this can be used as an advantage to increase the yield. Also the presence of sulfur or pyrite in coal is related with an increase in coal conversion (6).

Based on the carbon content all coals can be classified in the following categories (ascending order of carbon content): peat, lignite, subbituminous coal, bituminous coal and anthracite. Lignites and subbituminous coal are called low rank coals, while bituminous and anthracite, are well known as high rank coals. Depending on coal rank, the composition of coal may vary; for example the sulphur content can vary from 1 wt.% to high concentration. The nitrogen content may vary from 0.5 to slightly over 2% (9). In the case of bituminous coals, their structure mainly consists of an aggregate of condensed aromatic and aliphatic rings linked by single bonds (13).

The microscopic constituents of coal are a series of macerals. Macerals are divided in three different groups: vitrinite, exinite and inertinite. Vitrinite and exinite constitute the reactive macerals of coal, while inertinite behaves as inert infusible diluents (8).

In order to characterize the coal, two analysis can be carried out, the proximate and the ultimate analysis. The proximate analysis determines moisture content, volatile matter content, ash content and fixed carbon (8). The ultimate analysis determines the elemental composition of the coal, in which carbon, hydrogen, nitrogen, sulphur

(organic) and oxygen are determined quantitatively (8). Oxygen content in the ultimate analysis is determined by difference. (12).

3.2. Coal Liquefaction

Coal liquefaction is a combination of physical and chemical processes to obtain liquid products from coal using a solvent. Liquefaction of coal is achieved by incorporation of hydrogen into the coal structure through a hydrogenation process. During this process, along with the chemical process also physical phenomena occur.

Physical phenomena occur when the solvent removes extractable material from coal, and depend on solvent characteristics, coal permeability and the nature of the extractable molecules. Physical phenomena are present in the first step of liquefaction in which, small molecules are dragged out from the coal structure due to interactions between the solvent and the molecules extracted. At this moment the small molecules become soluble in the solvent and present in the liquid phase. This phenomenon is observed in coal usually at temperatures below 350°C. As temperature increases some macromolecules can be dissolved in the liquid phase as well. Other molecules undergo thermal fission at their weakest bond, forming fragmented radicals. This case is observed in methylene and benzylether bonds (6).

Chemical process, such as adding hydrogen to the coal structure, imply cleavage of covalent bonds (thermally or catalytically) to obtain low molecular weight products. Hydrogen capping is a key process during liquefaction. If the pyrolytically generated radicals are rapidly capped by hydrogen (i.e. hydrogen addition to free radicals), light molecular weight products are generated (14). The free radicals formed can be capped with hydrogen from the hydrogen donor solvent, or by transfer of hydrogen on a catalyst or from dissolved H₂ when reactor is pressurized with H₂. The stabilized smaller molecules, which are smaller than those originally present in the coal structure, are now soluble in the solvent. On the other hand, when hydrogen is not available for transfer, the free radicals recombine to form heavier products (6).

3.3. Temperature regions in solvent extraction

Liquefaction of coal occurs at temperatures above 350° when the coal substance is actively decomposing. At temperatures below 350°C hydrogenation of coal does not produce liquids of interest, instead what is obtained, is a coal more soluble in pyridine.

When coal is heated in an inert atmosphere (no presence of oxygen for this practical case), at high temperatures, the coal is decomposed, producing water, tar and gas. An inert residue is left at the end of the process.

Devolatilization of coal begins in the range between (~350°C - 500°C) and proceeds rapidly, but, in fact, decomposition of coal starts at lower temperature. Studies made by Berkowitz using Thermogravimetric Analysis showed that three regions can be identified when coal is heated up until 550°C. These regions are as follows (8):

First Stage (below 200°C)

Rate of decomposition of coal at this stage is very slow and it is characterized by the release of 'chemically combined' water, oxides of carbon and hydrogen sulfide. Molecules as benzoic acid decompose producing CO₂ and also at this stage reactions occur, which produce water. The decomposition reactions at low temperature take place at a low rate, but, modify the coal structure and therefore subsequent thermal behaviour of coal is influenced (8).

At low temperature in the presence of a solvent, the coal structure swells due to interaction with the solvent and some of the compounds in the coal dissolves in the solvent. In this regime, only solubility (physical effects) affects the liquid yield. As the temperature is increased, some labile bonds may start rupturing to initiate free radical reactions. Small changes may start occurring at around 100 °C (15), but decomposition reactions become noticeable at around 150-175 °C.

Second Stage (begins between ~350°C - 400°C and ends near 550°C) "The active stage"

At this temperature range almost 75% of volatile matter, including all tar and lighter condensable hydrocarbons, are evolved. The volatile matter evolved, which does not pre-exist in the coal matrix waiting to be released, actually is formed by thermally breaking some of the bonds in the coal structure which will form combustible gases such as hydrogen, carbon monoxide, methane, lighter hydrocarbons and other incombustible gases like carbon dioxide and water vapour (9), (12).

At this stage fragmentation of coal molecule and random recombination of free radicals generated during the heat treatment depends on the conditions such as pressure and heating rate. These conditions will set the path at which different products are formed as a result of coal decomposition (9).

At around 350°C, the weak bonds of the crosslinking section of the coal macromolecule (most of them formed by methylene, sulfide, and disulfide bonds) break down due to thermal effects. Also it has been said that these breakdown is related with cleavage of ether (16) (17) and benzylic ether bonds (18). This concept is based on the observations of the liquefied products obtained, in which an increasing amount of phenolic groups is noticeable in comparison with the parental coal (18). Free radicals are formed during these thermal decomposition reactions.

The mechanism of coal liquefaction is a free radical process characterized by 3 steps: initiation, propagation and termination. The initiation step is a thermal decomposition of the coal molecule, in which the free radicals are formed. In this case, C-O bonds (i.e. ether, hydroxyl) are the first ones to break down due to their lower bond dissociation energies. Those free radicals can undergo “ β scission, addition to available aromatic systems, disproportionation, combination, and hydrogen abstraction either from a hydroaromatic or aliphatic structure in the coal or from the hydroaromatic solvent” (19). Release of hydrogen and attack of hydrogen donor solvent to coal molecule is due to free radical initiation. The formation of free radicals is due to thermal effects during the dissolution process of coal. The propagation can proceed in three different ways (20):

- Radical transfer: abstraction of a hydrogen atom from another radical yielding a new radical. The abstraction of a hydrogen atom from the solvent depends on the weakness of C-H bonds present in the solvent.
- Radical decomposition: the radical decomposes itself, producing an unsaturated compound.
- Radical addition: Generation of high molecular species due to reaction between a radical and an unsaturated compound (20).

At the termination stage, free radicals are stabilized by subtraction of a hydrogen atom from the donor solvent (21). If there is not availability of hydrogen atoms, repolymerization of the free radical can take place. In such a case the products that will be obtained are higher in molecular weight. In *Figure 1* the mechanism of tetralin to donate hydrogen atoms is shown, in the case of tetralin present with coal, the termination step will be the capping of the free radicals formed of the coal structure with the hydrogen atoms formed in the steps of initiation and propagation of the mechanism of tetralin to naphthalene.

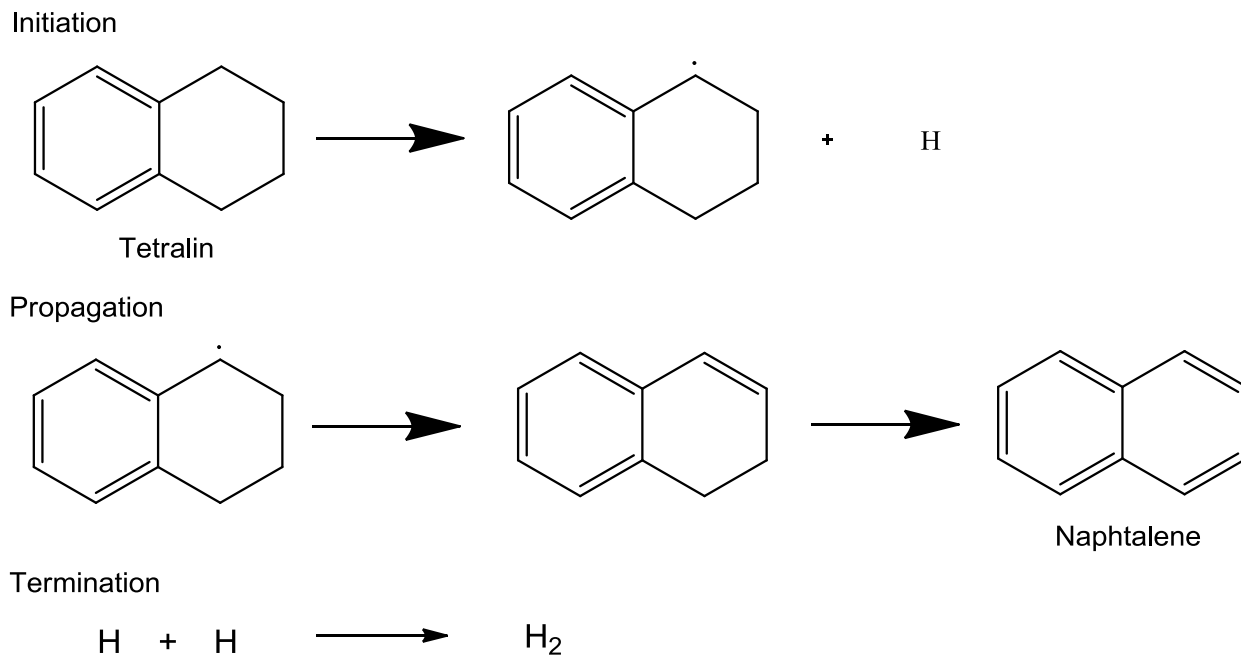


Figure 1 Free radicals mechanism formation for tetralin
Drawing taken from (22)

At 390°C, short reaction times were studied by Provine et al for bituminous and subbituminous coals using tetralin as hydrogen donor solvent (without the use of gaseous hydrogen in the atmosphere). The results showed that more aromatic than aliphatic material was extracted in the earliest stages of liquefaction (18).

Shalabi et al pointed out that as a result of the initial thermal reactions during liquefaction; the products obtained are largely asphaltenes and preasphaltenes. This statement, made by Shalabi et al, is not realistic. Asphaltenes and preasphaltenes are products that are measured by an indirect technique, based on solubility. Asphaltene and preasphaltenes are just a fraction of the wide range of products that are obtained as a result of thermal effects during the liquefaction.

When hydrogenation of those products goes further, species like oil and gases (lighter in molecular weight) are obtained (23). Retrograde reactions may occur (bond forming) as tar and coke and consequently yield losses are observed (18).

Final Stage (from 550°C - ~950°C)

The weight loss of coal at this stage is slower compared to second stage. At this stage the elimination of heteroatoms (principally hydrogen and oxygen) can be observed and the process ends when the char is transformed into a graphitic solid. The most

important by-products obtained in this stage are: water, oxides of carbon, hydrogen, methane, traces of C₂ hydrocarbons and many inorganic compounds (8) (12).

4. OVERVIEW OF KINETIC MODELING OF THE SOLVENT EXTRACTION OF COAL

Below an overview of the main contributions to kinetic modeling of coal liquefaction will be summarized. Since this is a very broad field, the aim of this chapter is to highlight the main approaches and discuss the deficiencies observed, other than listing all the contributions available in literature.

4.1. Commonly employed terms and experimental techniques

Due to the complexity of the products obtained during the solvent extraction of coal, the approach that is widely used to build mechanistic models is based on categories of products that have been classified based on similarities. Usually the similarities are based on the solubility and/or insolubility of the products obtained in certain organic solvents (10). The products that obtained are: asphaltenes and preasphaltenes.

Preasphaltene is a major fraction of heavy material present in coal liquids, characterized by a higher aromaticity and polarity compared to asphaltene fraction. Preasphaltenes are soluble in pyridine and insoluble in benzene and toluene (24) (25).

Asphaltenes are material of the highest molecular weight and most complexity obtained after coal liquefaction. Asphaltene are soluble in organic solvents such as tetrahydrofuran (THF) or methylene chloride, but insoluble in solvents such as pentane, hexane or n-heptane (26) (27).

The experimental procedure that is followed by most of the authors, after the liquefaction process, is as follows (28), (29), (23):

- Washing of the reactor with THF or with the same solvent that was used in the liquefaction.
- Use a filtration system or a Soxhlet extractor to separate the solid and the liquid fraction.
- Then the liquid fraction is processed with different solvents, such as benzene, toluene, hexane, heptanes, pentane to obtain different lumped categories.

An example of an extraction strategy using n-pentane, benzene and pyridine to obtain fractions such as asphaltene, preasphaltenes and oils (among others) is shown in *Figure 2*.

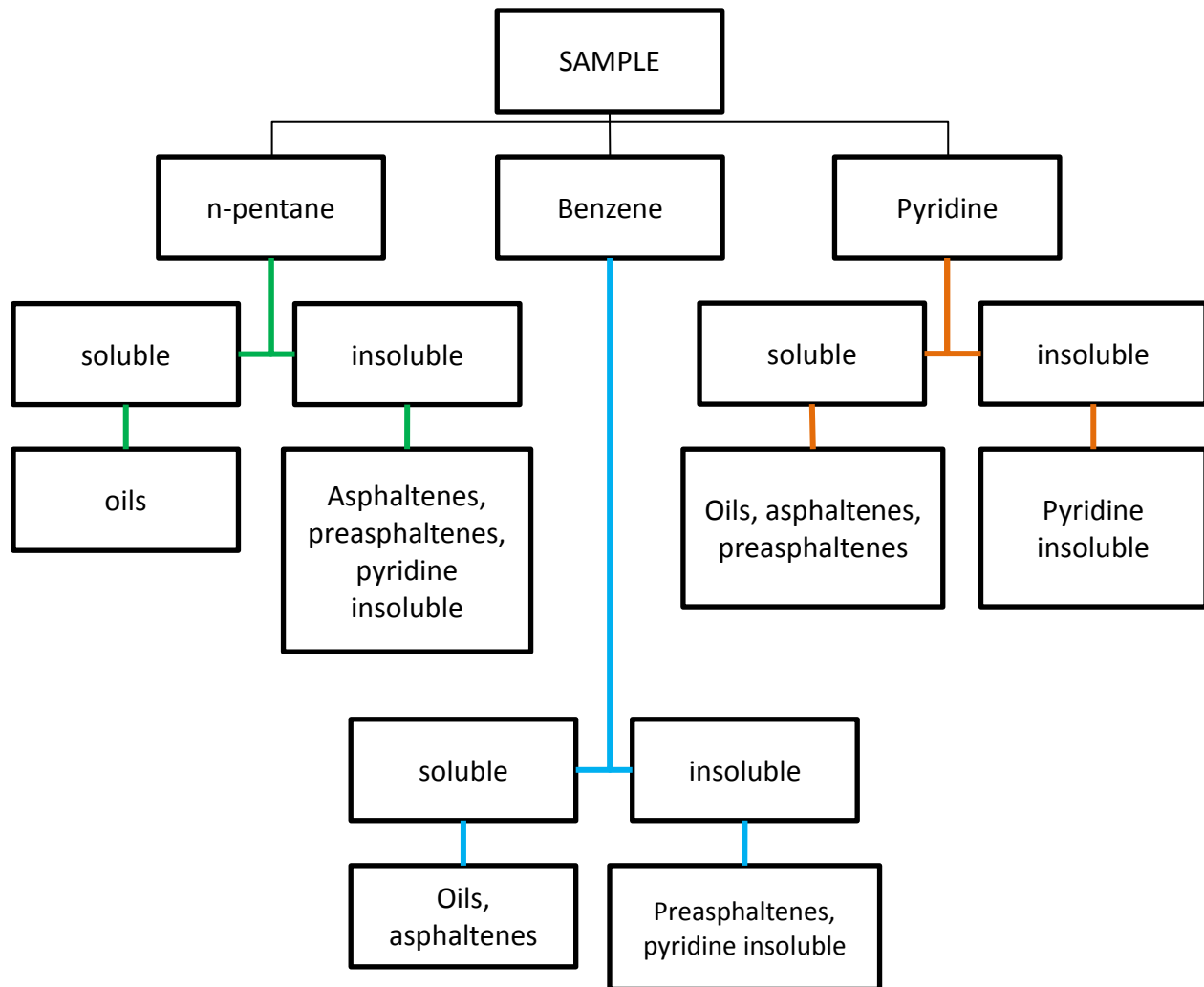


Figure 2 Solvent extraction sequence from Cronauer et al (1978).
Drawing taken from (29)

When the fractions are obtained, mass balance has to be done in order to obtain the quantities obtained for each fraction. These data are the 'feed data' for modeling. Models can be proposed analyzing the data obtained from the mass balance during different periods of time and/or at different temperatures. That can elucidate the behaviour of the fractions that will be part of the kinetic model.

4.2. Kinetic models based on solvent-class lumping

Depending on the extraction strategy of the products obtained from the liquefaction, different kinetics models can be proposed. As mentioned before, one of the most common techniques is the solubilization of the liquid obtained in different solvents. The lumping criteria for the categories are mainly based on analytical capability and by

product value (26). In this methodology the groups or categories that are usually obtained in the model are preasphaltenes, asphaltenes and oils. Preasphaltenes and asphaltenes can be precipitated using different solvents. For example preasphaltenes can be precipitated using toluene or benzene. The use of different solvents to extract preasphaltenes and asphaltenes will determine the yield and the composition of the products (27).

The molecular structure and amounts of those products will depend on the liquefaction conditions, solvent used, coal rank and strategy of extraction with different solvents (30). For example, Chong et al studied the preasphaltenes and asphaltenes using two different processes: solvent extraction and hydroliquefaction. The solvent extraction was carried out using cyclohexanone as solvent in nitrogen atmosphere. Hydroliquefaction was carried out with no presence of solvent, hydrogen atmosphere and pyrite as catalyst. Preasphaltenes and asphaltenes were precipitated using benzene and hexane, respectively. The precipitation method was the same either for solvent extraction or hydroliquefaction process. It was concluded from this study that preasphaltenes and asphaltenes obtained from hydroliquefaction differ in structural parameters and molecular weight, from those obtained from solvent extraction. (31).

Series, parallel and series-parallel of irreversible and/or reversible reactions mechanism models have been proposed in order to explain the kinetic behaviour of the coal liquefaction.

An example of series and parallel reaction mechanisms is shown in *Figure 3*, proposed by Cronauer et al.:

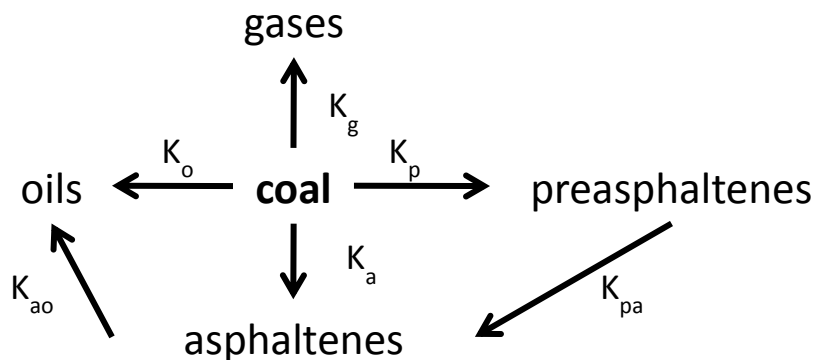


Figure 3 Set of series-parallel non-reversible reactions.
Drawing taken from (29)

This model differs from the models that have been proposed in the way that is not strictly a series model; instead, it considers parallel reactions as gases and asphaltenes formation. This model was proposed for a subbituminous coal (Belle Ayr) with two

solvents hydrogenated anthracene oil (HAO) and hydrogenated phenanthrene (HPh). Coal to solvent ratio was 1:1.5. The experiments were carried out in a continuous stirred reactor (1000 – 1500 rpm). Operation temperature range was established between 400 and 470°C (400-425-450-460-470). The slurry sample, obtained after the second 60 minutes cycle, was filtered and the cake was treated with n-pentane, benzene and pyridine to obtain the different fractions (preasphaltenes, asphaltenes and oils). The predicted yields of the different fractions by the model developed do not reflect in an accurate way the experimental data. Gas production is the only one that is observed that the model predict in a better way independent of the solvent used for the extraction. Since the activation energies are obtained from the constant determined using the kinetic model proposed, the activation energies values were very low (pointed out by the authors). This is not a surprise, because of the kinetic model does not describe in an accurate way the reactions occurring during coal liquefaction (29).

Series and series-parallel kinetics models (see *Figure 4*) were proposed in the case of Shalabi et al. The studies were carried out in a 300 cm³ batch reactor using a high A bituminous coal (Madisonville No 9) and tetralin as a solvent. A volume of 190 cm³ of tetralin was charged in the reactor and purged with helium. The contents were heated until desired temperature (350 – 375 - 400°C) was reached. Afterwards, a mixture of coal and tetralin (ratio 1:1.2 by weight) is pumped in the reactor. The final ratio coal/tetralin is 1:10. The liquefaction reaction was quenched at room temperature and the gas products were collected and analyzed using gas chromatography. The liquid products were treated with different solvents such as benzene, THF and n-pentane. In this case, three models, which include the same fractions (A, reactive maceral part of coal; B, asphaltenes; C, preasphaltenes and D, oils+gases), differ in the suggested mechanism of the model. The Model 1 is a purely series mechanism, meanwhile Model 2 includes parallel steps. Model 2 differs from Model 1 in the step when the oil and gas are formed. Formation of oil and gas in Model 2 is possible directly from the preasphaltenes and also from asphaltenes. Model 3 differs from the other two models in the role of the preasphaltenes. In this model preasphaltenes are formed directly from the reactive fraction of the coal and also are the precursors for the formation of asphaltenes and oil and gas. Oil and gas formation is a direct step from the reactive part of the coal, as it was pointed out in Model 2 (23).

The aspects that can be highlighted in this study are:

- Incorporation of the concept of a reactive fraction is necessary (Stewart, 1976) to adequately model the data since the final concentration of unreacted coal will not be zero.
- Pure series model did not provide an adequate representation for the donor solvent liquefaction process

- The deviation of the experimental data from the predicted values (i.e. residuals) is smaller in Model 3. This was expected by the authors, since Model 3 includes more parameters. From a mathematical point of view, the inclusion of parameters allows more variation in the data set to be accounted for by the regression scheme (23).

The weaknesses observed in this study are:

- In all models the gaseous products are lumped with oil products. Formation of oils is largely due to hydrogenation of heavy hydrocarbon moieties (preasphaltenes and asphaltenes). Gaseous products are formed through the reaction and formed at different stages of the liquefaction from different molecules. The path of formation of oils is different from gaseous products, for that reason it should not be lumped.
- In this study undissolved coal is not taking into account. This can be interpreted as at infinite time all the amount of coal loaded will become soluble. The fact is that, there is a portion of coal (i.e. fusinite) that would not become soluble even at infinite time. The undissolved coal fraction should be reflected in the modelling of coal liquefaction.

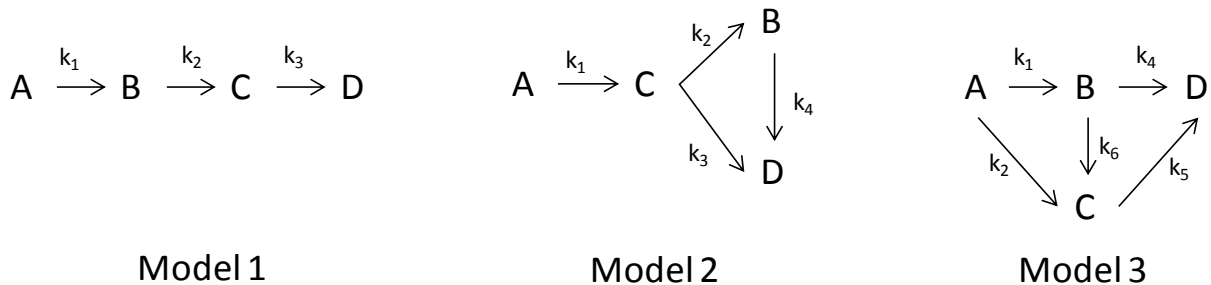


Figure 4 Reaction mechanism model proposed by Shalabi et al.
Drawing taken from (23)(23)

The results obtained by Shalabi et al fitting the experimental data and the models proposed shown the poorest fitting in the case of Model 1, meaning that a purely series mechanism model cannot explain the liquefaction process of coal. Adding a single extra step in the case of Model 2 the fitting is better for the case of unreacted coal and asphaltenes. The results obtained for Model 3 show that this mechanism proposed can predict the behaviour of the coal liquefaction. These results can be observed in *Figure 5*.

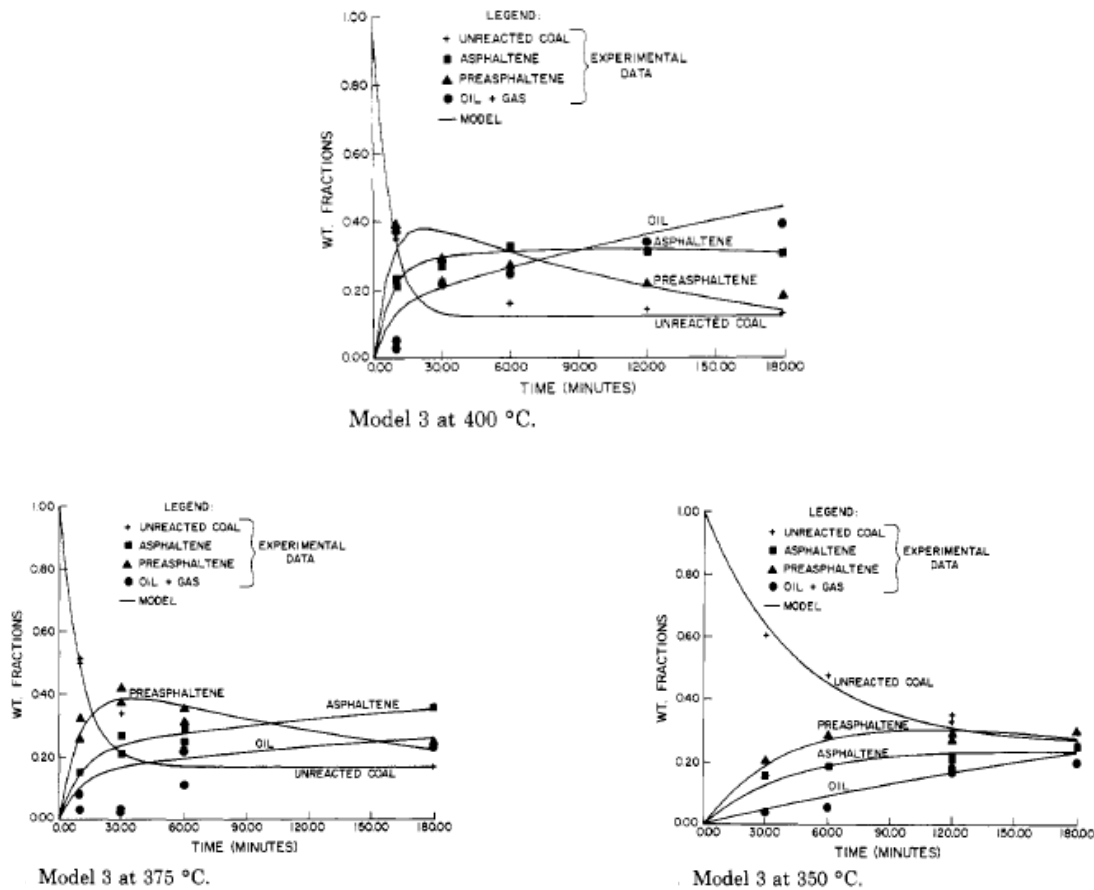


Figure 5 Experimental vs. predicted data (kinetic model) obtained by Shalabi et al. Drawing taken from (23)

From the experimental results obtained (see Figure 5) formation of asphaltenes and preasphaltenes is clearly observed. At the very beginning of the reactions, the concentration of asphaltenes and preasphaltenes starts to rise along with a decrease in the reactive fraction of the coal. Presence of iron or iron sulfur species in the coal may act as heterogeneous catalyst, which can explain the unexpected amounts of lighter products such oil (in this study this was observed especially at 400°C) and the formation of oils and gas also (at higher temperatures) can be explained by the properties of asphaltenes and preasphaltenes (23).

When the constant rates are calculated, it can be observed that none of them follow the Arrhenius-type temperature behaviour. It is recognized by the authors that Model 3 is based in a “rudimentary sense on the presumed chemistry of the liquefaction process”, so it cannot be considered as an appropriate kinetic model. For that reason the constant rates do not show a characteristic behaviour since those were obtained merely by a best fit exercise. It is also stated by the authors that based on the results of this study it

is necessary to establish a kinetic model based on the fundamental chemistry of the system (23).

Li et al proposed a kinetic model based on solubility of the products as well, but differ from the other proposals in the way that the fractions obtained by solubilisation in different solvents were then, lumped in categories based on reactivity of those groups (32).

The experimental part of this study was carried out as follows: bituminous coal (particle size less than 100 mesh) was liquefied with coal liquefaction cycle-oil at a solvent/coal ratio of 1.22/1, in an autoclave of 500 mL. The autoclave was loaded and then flushed twice with hydrogen. The reaction conditions of the process were: cold pressure 8 MPa, 400 rpm and heating rate of 5°C/min. For non-isothermal experiments the temperature range was from 370°C to 430°C, in the case of isothermal experiments the temperature was held at 430°C. After liquefaction, four fractions were obtained: oil (n-hexane soluble), asphaltene (toluene soluble but n-hexane insoluble), preasphaltene (THF soluble but toluene insoluble), and residues (THF insoluble) by Soxhlet extraction (32).

The kinetic model was built up based on successive reaction pathways, which are composed by parallel and series irreversible reactions of first order (see Figure 6).

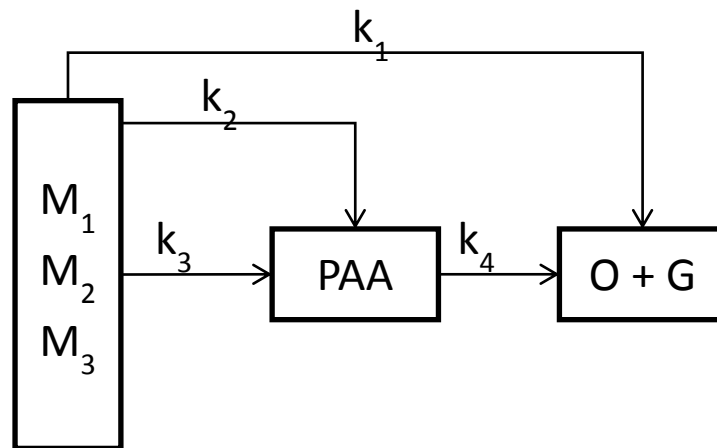


Figure 6 Reactions path ways proposed by Li et al.
Drawing taken from (32).

A very interesting assumption that was made in this study was to divide the coal in three groups based on their reactivity, Easy Reactive (M_1), Hard Reactive (M_2) and Unreactive (M_3). This is a different approach since coal is usually considered as a whole in kinetic modeling. This can be advantageous since coal is not a homogeneous substance (also characterized by different macerals having different H/C ratios) in terms of its molecular composition. So if this premise is considered the kinetic model built up

by taking into account the reactivity classes of coal, would generate a more accurate model (32).

As can be observed in *Figure 6*, preasphaltenes and asphaltenes were lumped in the same category (denoted by PAA) to simplify calculations, the same approximation was done in the case of gas and oils produced during the process, since the yield of gaseous products released, was very low. Influences of particle size, mass transfer and hydrogen pressure were ignored (32).

It was observed in the behaviour of PAA (preasphaltenes + asphaltenes) that its concentration increases during the heating up assays and also at the beginning of isothermal assays, then concentration decreases latter in isothermal mode. The formation of PAA from coal is favoured at low temperatures, but formation of oils and gas products (O+G) from PAA is favoured at higher temperature (32).

From the rate constants obtained in the study, it was observed that the constant rates obtained at heating up stage are larger than those at isothermal stage, therefore it can be stated that the reactions occurring at both stages are different. In the heating up stage, volatile matter, which are small molecules with high reactivity, are cracked and hydrogenated at mild conditions, this can be “translated” in a high reaction rate. In the case of the path that describes the reaction mechanism, it was observed that the reaction rate of coal to PAA is larger than PAA to (O+G) in both stages, meaning that the reaction PAA to (O+A) is the rate determining process. From this study it is worth to highlight the issue that two different regions were identified during the liquefaction process, with different constant rates. The lumping of preasphaltenes and asphaltenes under the same category to simplify calculations does not provide an accurate approximation of the model, considering that those products originate at different reaction conditions (32).

Based on the similar laboratory conditions, in reference to equipment used, the study of Pradhan et al offers a comparison point to the study I am proposing. Pradhan et al, used tubing bomb autoclaves immersed in a sand bath to evaluate the liquefaction process of coal under catalytic effects. For this study Wyodak coal (subbituminous) and tetralin using a coal to solvent ratio of 1:4 (3 grams of coal and 12 grams of tetralin) were used. Coal particle size was set at -20-100 mesh, but it was found that particle size did not affect product distribution. After charging coal and solvent, the reactor is pressurized at 6.9 MPa and shaken at 100cycles/min for premixing components. Then reactor is immersed in the sand bath. After reaction completion, the microreactor was quenched at room temperature using air (26).

The reason why Wyodak coal was chosen lies in the fact that the content of pyrite is low, so it would not interfere with the effect of the three catalysts studied: sulfated iron

oxide ($\text{Fe}_2\text{O}_3/\text{SO}_4$), sulphated iron-molybdenum ($\text{Mo}/\text{Fe}_2\text{O}_3/\text{SO}_4$) and iron oxide (Fe_2O_3) (26).

The reaction mechanism proposed is a model based on series and parallel reactions of coal to oils, as can be observed in *Figure 7*.

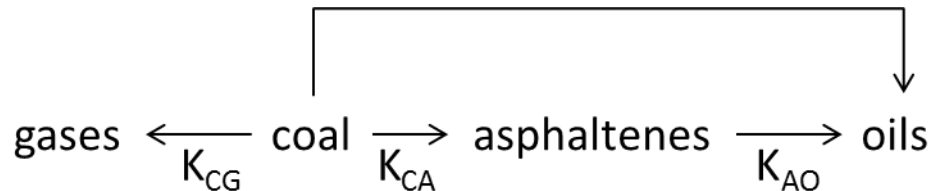


Figure 7 Reaction mechanism proposed by Pradhan et al.
Drawing taken from (26)

It is pointed out by the authors that this model proposed is similar to Radomyski and Szczygiel who found that series-parallel sets are more efficient than only series or only parallel reactions. The rate constants from the differential equation were obtained from a derivative free nonlinear regression program *AR* from the BMDP library (26).

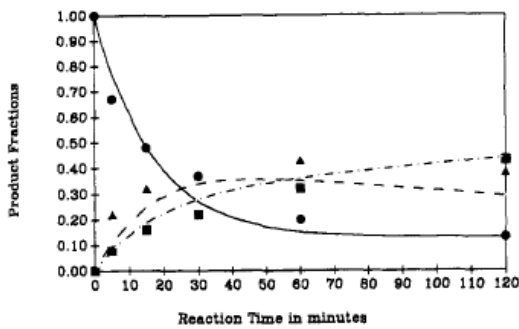
Reactions in the model are considered irreversible and with a pseudo first order reaction rate constant. In order to determine the maximum conversion, three (without catalyst) runs were conducted over a test period of 3 hours. The maximum conversion obtained in each case was 76%, 87%, and 93% (all on maf basis) at the temperature 648, 673, and 698 K respectively (26).

To quantify the products obtained after liquefaction, three measurements were made per each run: coal remaining, fraction converted to asphaltenes and fraction to oils (26).

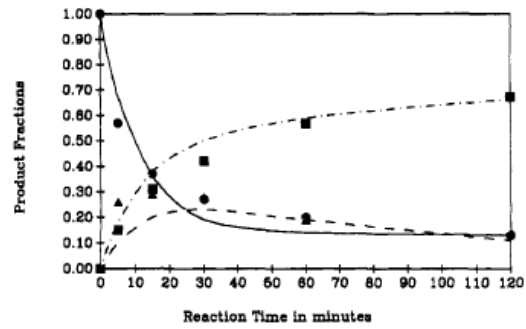
The findings in this study were (26):

- Reactions at very early stages (at around 5 min) are predominately thermal and produce amounts of preasphaltic material (significant amounts of light components (pentane soluble) are formed at very short times)
- The nature of the formation of oils from asphaltenes was found exclusively catalytic.
- The formation of asphaltenes from coal was found to be strictly related to thermal effects.
- The formation of oil directly from coal was found to be influenced by sulphate presence in the catalyst.

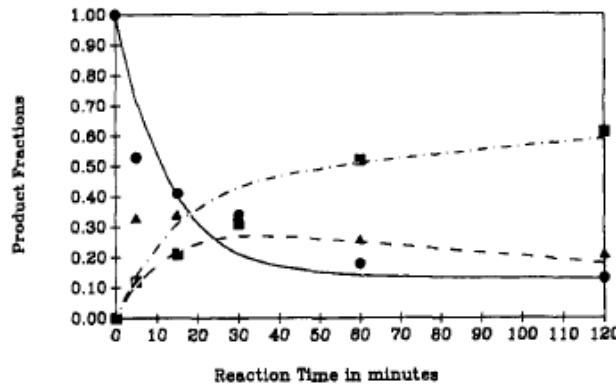
- Addition of molybdenum to the sulphated catalyst increased the rate of formation of coal to oil.



Catalyst: Mo/Fe₂O₃/SO₄ + S



Catalyst: Fe₂O₃ + S



Catalyst: Fe₂O₃/SO₄ + S

Figure 8 Plots of experimental data vs. data predicted using different catalyst. Unreacted coal (●), asphaltenes (▲) and oils (■). Predicted fractions unreacted coal(—) asphaltenes (- -) and (-.-) oils. Drawing taken from (26)

In *Figure 8*, it is observed that the model predicts the values for the product fractions close to those obtained experimentally. Weaknesses in the model can be noticed to predict the asphaltene fraction, especially at the very beginning of the process. As it was stated in this study, thermal effects occur at the beginning of the process, and then the catalytic effects take place. This might suggest that this model does not reflect in an accurate way the thermal effects during liquefaction (26).

The statistical analysis for the significance of data was made through an F test for the ratio of variance explained by the regression to estimated error variance. The authors clarify that F test is valid for linear regression, while the regression used in the study was a non-linear regression (26).

This study presents a very interesting approximation to the phenomena occurring during liquefaction, in terms of thermal and catalytic driven paths in the reaction mechanism. The catalytic paths depend on the pyrite content of the coals, which is different to the coals in my study. Besides this difference, the experimental part is very close to the experimental procedure used in my study of the kinetics. This results advantageous as this study can be employed as a reference for trial procedures (26).

4.3. Other kinetic models based on chromatography and related networks

Chromatography

Let's consider what happens when the mechanism is more specific in terms of fractions: is it enough to propose a purely series mechanism or not? Is it enough to propose irreversible or reversible reactions?

A very interesting case was studied by Mohan and Silla (10), using liquid-solid chromatography (LSC), as extraction technique. LSC provided five different fractions: multifunctionals (M), aromatics (A), hydroxyls (H), nitrogens (N) and ethers (E). The experimental part was carried out as follows: The hydrogen donor solvent for the experiments was tetralin (technical grade). A concentrated coal and tetralin slurry was pumped into the reactor (with the aim to avoid heat up times) in which tetralin was previously introduced. After the slurry injection the coal/tetralin ratio is 1/10. Stirring conditions were set up at 1500 rpm and 1300 rpm at which it has been reported that mass transfer effects are negligible. The temperature range of all experiments was from 330 until 450 °C and carried out at different residence times, the shortest being 5 minutes until 60 minutes. Times below 5 minutes were not studied since slurry injection takes 1 minute and the reaction quenching 2 minutes. On the other hand, after 60 minutes limited additional conversion was found. After reaction is quenched at room temperature, the products were collected and centrifuged. The reactor was washed with THF and the washed products were mixed with the sediment product of centrifugation. To recover the THF soluble fraction of the sediment and the washed products from the reactor, a Soxhlet extraction system was implemented and the extract obtained combined with the centrifuged liquids. Afterwards, in order to eliminate non reacted tetralin and by-products of the reacted tetralin, the extract was distilled at 125°C and 8 cm Hg (11 KPa). The bottom and distilled products were analyzed separately. The bottoms, Solvent Refined Coal (SRC), were analyzed using liquid-solid chromatography (LSC) (10).

Three reaction mechanistic models were proposed based on the five fractions obtained from LSC. Due to differences observed in the concentration-time profile of one of the fractions (multifunctionals) at low temperature range (defined by the authors as 330 -

390°C) and high temperature range (defined by the authors as 390 – 450°C), two models were proposed for the high temperature range and one for low temperature range (10).

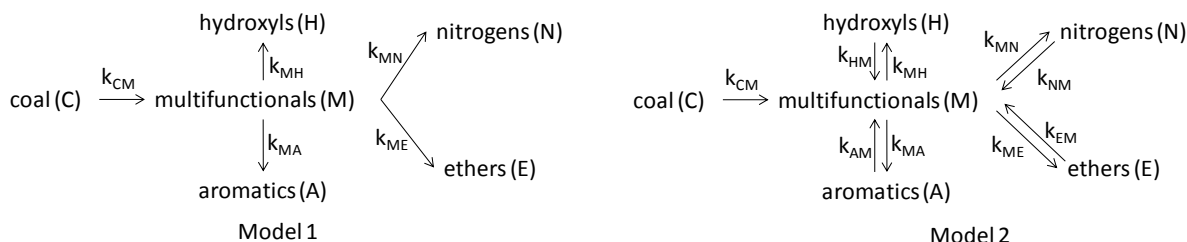


Figure 9 Models proposed for high temperature range by Mohan and Silla. Drawing taken from (10).

As can be observed in *Figure 9*, Model 1 and Model 2 are a set of series-parallel reactions. Those models just differ in the reversible reactions that multifunctional compounds undergo in Model 2. The results of the mechanism and kinetics proposed are shown in *Figure 10*.

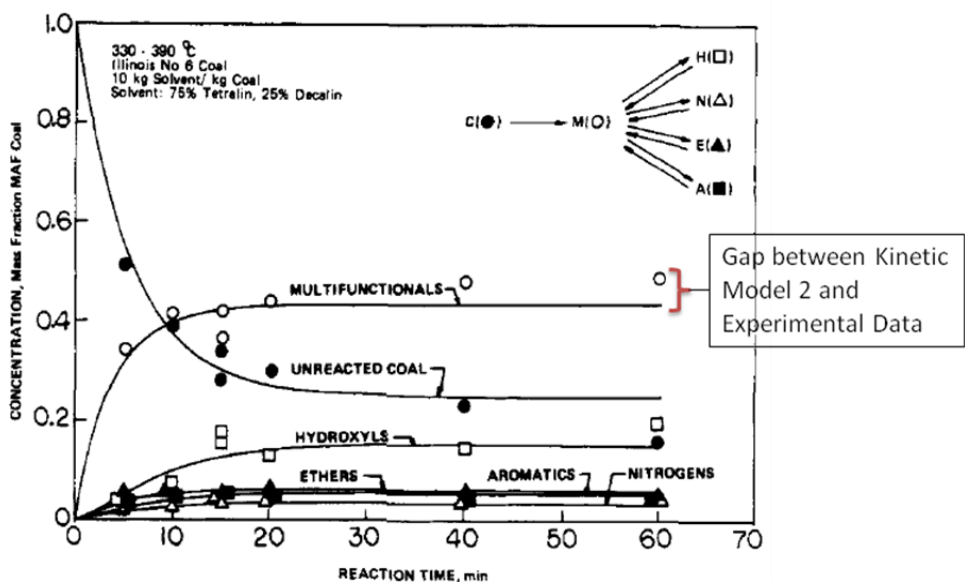


Figure 10 Model 2 at low temperature range by Mohan and Silla. Drawing taken from (10)

Model 2 fits the data better than Model 1 in the high temperature range, meaning that reverse reactions describe the coal liquefaction better. Mathematically, that can be explained because more parameters are included into the model. Kinetically, Model 2

can describe the phenomena better since it was found out that reverse reactions are faster than forward reactions. This explains the high concentration of the multifunctional compounds observed experimentally. Kinetic model 2 fits the experimental data for low temperature reactions also, but the behaviour of the concentration of the multifunctional compounds does not reach the maximum concentration (see *Figure 10*) and that can be explain by the fact that the formation rate of multifunctional compounds is slower at low temperature range. Since Model 2 does not fit the data very well at low temperature range, a kinetic model 3 (see *Figure 11*) was proposed in which all the compounds are formed directly from coal. It is not clear what chemical fundamentals the authors employed to propose Model 3 (10).

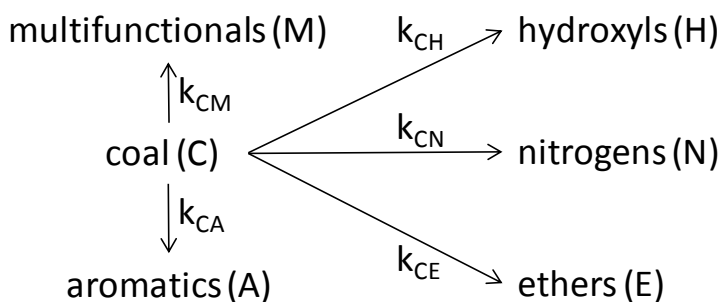


Figure 11 Model 3 proposed by Mohan and Silla.
Drawing taken from (10)

A theoretical approximation was made to compare the model using the fractions obtained using LSC and the typical fractions obtained using different solvents. The fractions obtained in the LSC, were grouped using a theoretical approximation in preasphaltenes, asphaltenes and oils. Reaction mechanism models were proposed using preasphaltenes, asphaltenes and oils. The model that best fits the model was the data is the model shown in *Figure 11* (10).

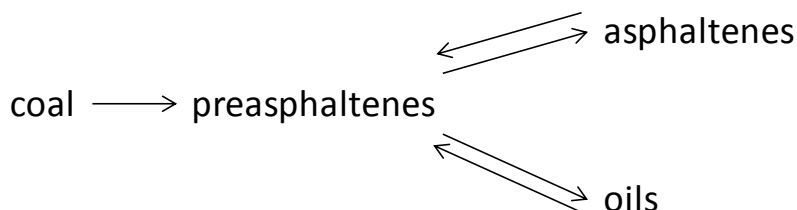


Figure 12 Model 4 proposed by Mohan and Silla.
Drawing taken from (10)

Similarities between kinetic model 2 and kinetic model 4 (based on solubility) were found. Model 4 (see *Figure 12*) has been proposed in which reversible reactions of

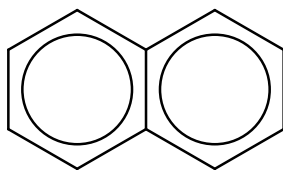
asphaltenes, preasphaltenes and oils are present as Model 2. Furthermore, both models have been found to fit the data either in the low region temperature (330-390 °C) and high region temperature (denominated by the authors) (390-450 °C) (10).

Since the LSC allows one to distinguish more lumped fractions (from a mathematically point of view this increase the number of parameters to take into account) and have fractions with better chemical similarity within each, this study shows an interesting option. As it was concluded in the section for solvent extraction, including reversible reactions into the reaction mechanism enables a better kinetic description of the phenomena occurring during liquefaction (10).

Rule based on relation networks

This structure oriented lumping has been applied to the study of the complex mixtures that are present in petroleum. This methodology states that hydrocarbon molecules can be described as a vector and be lumped based on structural groups present in the molecules. To do so, techniques such as LC-Field Ionization MS, GC-MS can be used (11).

In order to get a representation of the molecules involved during the cracking process, this complex mixture obtained can be represented using a small set of groups (i.e. atomic elements). These groups are represented by a vector and a stoichiometric matrix (structural groups). For the case of kinetic modeling it is necessary that the structure used, gives a convenient description of the molecule. The structures in this study are called "structure vectors", which can describe most of the molecules present but not the specific arrangement within a molecule. In this case a hydrocarbon molecule can be represented for a vector which is constituted by structural features and structural groups, characteristics of a molecule and a matrix that contains a set of atomic elements (C, N, S and O). An example is shown in *Figure 13* in which naphthalene is represented by a vector. The structural group A6 represents a six carbon aromatic ring and the A4 represents a four carbon aromatic ring attached to an A6 structural group. For that reason in the vector those groups are represented by 1 (11)



A6	A4	A2	N6	N5	N4	N3	N2	N1	R	br	me	IH	AA	NS	RS	AN	NN	NO	RO	KO	
1	1	0	0	0	0	0	0	0	0	0	0	0	0	0	0	0	0	0	0	0	0

Figure 13 Vector representation of Naphthalene.
Drawing taken from (11)

One of the advantages of this methodology is that reactions of specific chemical bonds are followed as a lump. The grouping of those sets of reactions is done based on NMR analysis (carbon types). Even catalytic mechanisms can be represented and included in the process model and are modelled taking into consideration the molecular transformations (11).

The disadvantage of this methodology is that all the products obtained from coal liquefaction must be characterized at a structural level. This is impractical and almost impossible. First of all, as many molecules as possible that are present in the products, should be identified and then represented by a vector (as suggested by the methodology). This demands high precision and state of the art equipment to obtain accurate results. For that reason, I consider that this technique is not feasible within the scope of this project (11).

5. MODELLING PHYSICAL DISSOLUTION OF COAL

The solvent present during solvent extraction plays one of the most important roles in the liquefaction process. The solvent can act as a hydrogen donor, due to its donor ability, and/or dissolve the structure of the coal (6). The donor ability of a solvent depends mainly in the structure and functional groups present in the solvent. For example, tetralin is the solvent most widely used in the study of coal liquefaction. Its ability to donate hydrogen is derived from the presence of the aromatic structures coupled to the naphthenic ring. The aromatic structure provides additional stabilization of the carbon radical after hydrogen donation through π -electron system. This additional stabilization is not available in the case of a purely naphthenic solvent such as decalin which lacks any aromatic structure. The dissolving process also depends on the molecular structure of the solvent, those solvents with two or more aromatic rings, such as methylnaphthalene, dissolve a larger amount of coal than those with aliphatic structures. (6).

An important factor that has to be taken into account in the liquefaction of coal is the solubility parameter. This parameter is an indicator of molecular interactions for non-polar molecules, and considers dispersion forces, dipole moments and hydrogen bonding. In order to obtain an interaction of the constituents of a system, in this case coal and solvent, the value of the solubility parameter should be as similar as possible (33). Sanada and Honda have found during the solvent extraction of Yubari and Ashibetsu coals with different solvents such as chloroform, ethanol, benzene, cyclohexanone, acetophenone, among others a direct correlation between the solubility parameter and yield of extraction. As the solubility parameter increased, the extraction yield also increased, however at a value higher than 10 for the solubility parameter, it was observed that the extraction yield started decreasing (34).

5.1. Relevance of particle size, nature of solvent and coal and coal to solvent ratio

There are three aspects that need to be considered for proper modeling: particle size, nature of solvent and coal and coal to solvent ratio.. These three aspects are related with mass transfer limitations, characteristics of the products obtained and extraction yield.

Particle size

The particle size has been reviewed by different authors, but surprisingly, the results obtained by the authors do not agree between them. It has been stated by various authors that the particle size of coal does not influence the reaction yield when it is smaller than 100 mesh, in other cases it has been said that particle size does have an effect when the particle is smaller than 3 mm. Models like the shrinking core model developed by Giri and Sharma considers that particle size should matter. The shrinking core model basically states that the solvent removes the outer layers of the coal particle. If two coal particles of different size are compared in terms of the rate of dissolution, taking into account the shrinking core model, the result would be that the dissolution rate for the smallest particles is faster than the rate for larger particles (35). From the point of view of mass transfer, particle size also should matter. In this case the solubilization of molecules at low temperature becomes limited due to the forces that drive the extraction process of the molecules from the inside of the particle. To overcome this issue, preliminary experiments were made in order to determine the influence of particle. Addressing the particle size issue will help proper modelling of the coal liquefaction process.

Nature of coal

Depending on the coal composition and coal rank, different products can be obtained during the solvent extraction. Vitrain is the most soluble constituent of any particular coal and it is the easiest part to dissolve from the coal during solvent extraction. Fusinite is the least soluble part of coal and will remain in the solid phase in the residue after extraction. The petrographic composition of coal gives to coal special characteristics such as pore size, pore distribution and an open or a close structure. These special characteristics can drive the solvent extraction process, letting the solvent to enter the coal particle and extract material (36)

Coal to solvent ratio

The impact of the coal to solvent ratio needs to be determined before starting the kinetic work. The model has to capture the effect of dissolution without reaction. Dissolution at “infinite” dilution allows us to study the effect of the solvent on the coal, without the solvent properties being substantially affected by the dissolved coal. It will also be important to determine what fraction of the liquid yield reported for a specific coal to solvent ratio is due to truly dissolved coal molecules and which fraction is due to colloidal suspensions of small coal aggregates. These two forms of “yield” will require different modeling descriptions. On a more practical level, preliminary experiments were run to determine at which coal to solvent ratio the highest yield is obtained.

Temperature and time

According to the behaviour of coal and coal/solvent mixtures observed during thermal analysis, the temperature at which coal reaches the active stage can be determined. In the model this will be the threshold where reactive dissolution starts to become more prominent. It is postulated that the time allowed in contact with the solvent before reaching this threshold temperature is important in determining the local concentration of solvent in relation to the coal structure (i.e. diffusion limitation). Thermal decomposition depends on temperature only. However, the ability to stabilize the free radical fragments once they are formed depends on the presence (or absence) of the solvent. The reaction network during free radical propagation is therefore dependent on both time and temperature.

The following experiments were conducted to study the relevance of the particle size, nature of solvent and coal and coal to solvent ratio

5.2. Experimental

(For this section see *Appendix 1* for detailed equipment description)

Lignite (Poplar) and subbituminous coal (Coal Valley), both Albertan coals were used in the experimental investigation of the effect of particle size and coal to solvent ratio. In order to study the effect of the nature of coal, among the coals mentioned previously, a bituminous coal (Teck) was included in the study.

These coals were treated with 1,2,3,4 – tetrahydronaphtalene Reagentplus 99% (Tetralin) as hydrogen donor solvent, provided by Sigma Aldrich. The ultimate and proximate analyses of the coals are shown below in *Table 1*.

Table 1 Ultimate and proximate analysis of coals.

Description	lignite	subbituminous	bituminous
	(Poplar)	(Valley)	(Teck)
Ultimate analysis (wt.% daf)			
carbon	38.4	72.4	77.3
hydrogen	3.8	5.1	4.3
nitrogen	0.7	1.1	1.2
sulfur	0.5	0.4	0.6
oxygen	56.5	21	16.6
Proximate analysis (wt.%)			
moisture	28.8	5.5	1.9
ash	21.6	12.5	9.8
volatile matter	31.2	31.4	24.1
fixed carbon	18.4	50.6	64.2

The ultimate analysis was carried out in an Elemental Vario MICRO Cube using a sample size between 4 – 5 mg. The proximate analysis was performed following the ASTM methods such as: Moisture analysis (ASTM D 3173-11) (47), Ash content (ASTM D 3174) (48) and Volatile matter content (ASTM D 3175) (49). Fixed carbon was calculated using *Equation 3*.

$$\text{Fixed carbon} = 100 - (\text{Moisture}(\%) + \text{Ash}(\%) + \text{Volatiles}(\%))$$

Equation 3

Petrographic analysis was also performed by the company Pearson Coal Petrography. The results are shown in *Table 2*.

Table 2 Petrographic analysis

Description	Poplar coal	Valley coal	Teck coal
Reactive Components			
Vitrinite	57.20	67.80	55.8
Liptinite	4.20	7.50	0.9
Reactive Semifusinite	7.20	5.20	N.A.
<i>Total Reactives</i>	68.6	80.5	56.7
Inert Components			
Inert Semifusinite	7.20	5.20	37.8
Fusinite	4.20	5.80	N.A.
Inertodetrinite	7.80	1.70	N.A.
Macrinite	0.40	N.A.	N.A.
Mineral Matter	11.80	6.80	N.A.
<i>Total Inerts</i>	31.4	19.5	37.8

The solvent extraction of coal experiments were carried out in a stainless steel micro reactor of 15 mL of capacity. The microreactors were filled up to 2/3 of the total capacity. Subbituminous coal was vacuum dried overnight at 80°C, prior to liquefaction. No attempt to remove moisture content from lignite coal was made (due to its high content of moisture, authors say this might change the coal properties and affect extraction yield) (37). After loading the coal sample and solvent (at a pre-established coal to solvent ratio), the microreactors were purged with nitrogen (three times) to remove the air present inside the microreactors. The microreactors were pressurized to 2 MPa, for experiments at 100°C and to 4 MPa for experiments at 300°C. Four microreactors were attached to a holder which was coupled to an eccentric vertical shaker. The liquefaction process was carried out in a fluidized sand bath, heating the reaction mixture from room temperature up to the reaction temperature. After the predetermined reaction time, the reaction mixture was cooled down to 100°C with compressed air, afterwards the microreactor was depressurized and the mixture poured to a ceramic funnel, vacuum filtrated and both the microreactor and the coal residue were washed with tetrahydrofuran (THF) ≥99.0% provided by Sigma Aldrich.

The reaction conditions for each experiment were as follows (see *Table 3*):

Table 3 Initial conditions for study of particle size, effect of time and coal to solvent ratio.

	Time [hours]	Particle Size [mm]	Coal to solvent ratio [w/w]	Temperature [°C]
Effect of Particle size	3	53-75; 90-150; 250-33; 355- 1000; 1000- 2000	1:3	100 – 200 - 300
Nature of coal	1	355- 1000	1:3	100 - 300
Coal to solvent ratio	3	355- 1000	1:2; 1:3;1:8	100
Effect of time	1 – 30	355- 1000	1:3	100 – 200 - 300

All the results are expressed using the extraction yield, calculated on moisture ash free basis, as follows (see *Equation 4*)

$$\text{Extraction yield (\%)} = \frac{\text{Feed coal (maf)} - \text{Residue (maf)}}{\text{Feed coal (maf)}} \times 100$$

Equation 4

5.3. Results and discussions

The influence of the particle size, time and coal to solvent ratio was studied on the extraction yield of the process. The results are shown as follows:

Particle size

The trend of the influence of particle size on the extraction yield in *Figure 14* is not very clear. There is no correlation, neither at low temperature, nor at high temperature, contrary to the findings of Giri and Sharma. Giri and Sharma pointed out that the effect of particle size becomes relevant at low temperature but it is negligible at high temperature (38). The studies made by Curran et al at specific particle size ranges (74-140 μm (100-200 mesh) and 388-716 μm (28-48 mesh) also suggested that there is no difference in the extraction yield values obtained at these two particles sizes. The effect of particle size at extended times (4-41 hours) was studied by Asbury, the findings

shown there is no correlation between particle size and extraction yield but that an effect is observed in the case of particle sizes of the order of millimeters (39, 40) (41).¹

In my study it became apparent that the initial rate of extraction is very high. The fact that no particle size effect was observed does not imply that there was none, but rather that the extraction time was too long to observe any such effects if they were present. This seems to be the case with my studies and could offer an explanation of why particle size seemingly did not matter.

Nature of coal

From *Figure 15* is clearly observed that lignite coal (Poplar) is more easily dissolved at low temperatures and it is more reactive (in presence of Tetralin) than bituminous and subbituminous coals that were also examined. The extraction yield obtained for bituminous and subbituminous coal even at 300°C is less than 5% percent. Even though, the content of the most soluble maceral of coal (vitrinite) is very close for the 3 coals studied (see *Table 2*) there are other factors such as the pore distribution in the coal that can affect its dissolution at low temperature. Lignites are highly porous and due to their open structure, the reactivity of lignites can be increased. However it is not clear by the authors if the high porosity of lignites is referent to macroporosity or microporosity.

Furthermore the presence of more functional groups (such oxygenates: carboxylic acids and hydroxyl groups) than those present in bituminous and subbituminous coals, enable different reactions that can take place at low temperature (42).

Coal to solvent ratio

In this case 3 different situations were studied, a diluted system using a ratio of coal to solvent of 1:8, an intermediate case using a ratio of 1:3 and a third option using a ratio 1:2 in which a decrease in dissolution due to the availability of solvent can be observed. The null hypothesis, namely that the coal-to-solvent ratio had no effect on the extraction yield, was evaluated by a paired t-test. From *Figure 16* neither significant variation nor correlation between the coal to solvent ratio and the extraction yield is observed. At 95% significance the paired t-test failed to reject the null hypothesis of equal means (p-values greater than 0.08). Pearson product-moment correlation coefficient (r) was 0.23 indicating very weak correlation between the variables. Therefore there is no limitation for dissolution of coal, at least, between coal to solvent ratios of 1:2 to 1:8.

¹ A version of this section has been accepted for publication. Pap.-Am. Chem. Soc., Div. Fuel Chem., 56:2 (2011) 304-305.

Temperature and time

There is no significant influence of time on the extraction yield at low temperatures (100°C) as can be observed in *Figure 17*. It is observed that the maximum extraction yield at low temperature is pretty much reached at very short times, between 15 minutes and 1 hour. The extraction at low temperature and extended time has an insignificant increasing in the extraction yield value. The same effect is observed in the case of extraction at 200°C. Besides the release of chemically attached molecules of water, CO₂ (as a result of decomposition of benzylic acid groups present in the coal matrix), carbon oxides and hydrogen sulphide that can take place at low temperature(8), physical dissolution of coal molecules was also observed. In *Appendix 6* the results of the gas chromatography-mass spectrometry analysis of the liquids obtained after solvent extraction at 100°C and 15 minutes are shown. The chromatogram shows a series of compounds that can be considered as extracted products from coal. Besides the compounds that can be related to dehydrogenation of tetralin (i.e. naphthalene), compounds with similar structure to tetralin are observed. In this case it can be considered that the rule of thumb “like dissolves like” applies. For physical dissolution is expected that tetralin extracts compounds with similar chemical properties to its own properties.

At higher temperature (300°C) at which the active decomposing stage of coal is reached (in the case of lignites around 250°C), alongside with the physical events that are occurring also reactive dissolution is taking place.

At high temperatures as observed in *Figure 18* the rate of the solvent extraction process increases significantly. The extraction yields obtained reflect that, in fact, reactive dissolution is taking place at 350°C and 450°C. Also, as observed at low temperatures, the solvent extraction of coal at high temperatures occurs at very short times. At 15 minutes 61.7% (at 350°C) and 85.6% (at 450°C) of the extractable material obtained at extended time (3 hours) is achieved. The effect of temperature is remarkable at short times; the extraction yield at 450°C at 15 min is double of the extraction yield obtained at 350°C at the same time. On the other hand, the effect of time is significant at short times as pointed out previously, but is not outstanding for extended times at 450°C as it is at 350°C. This can be explained on the fact that 85.6% of the material that can be extracted at 450°C has been already extracted, meaning that the process at 450°C has almost reached an equilibrium state (41).²

² A version of this section has been accepted for publication. Pap.-Am. Chem. Soc., Div. Fuel Chem., 56:2 (2011) 304-305.

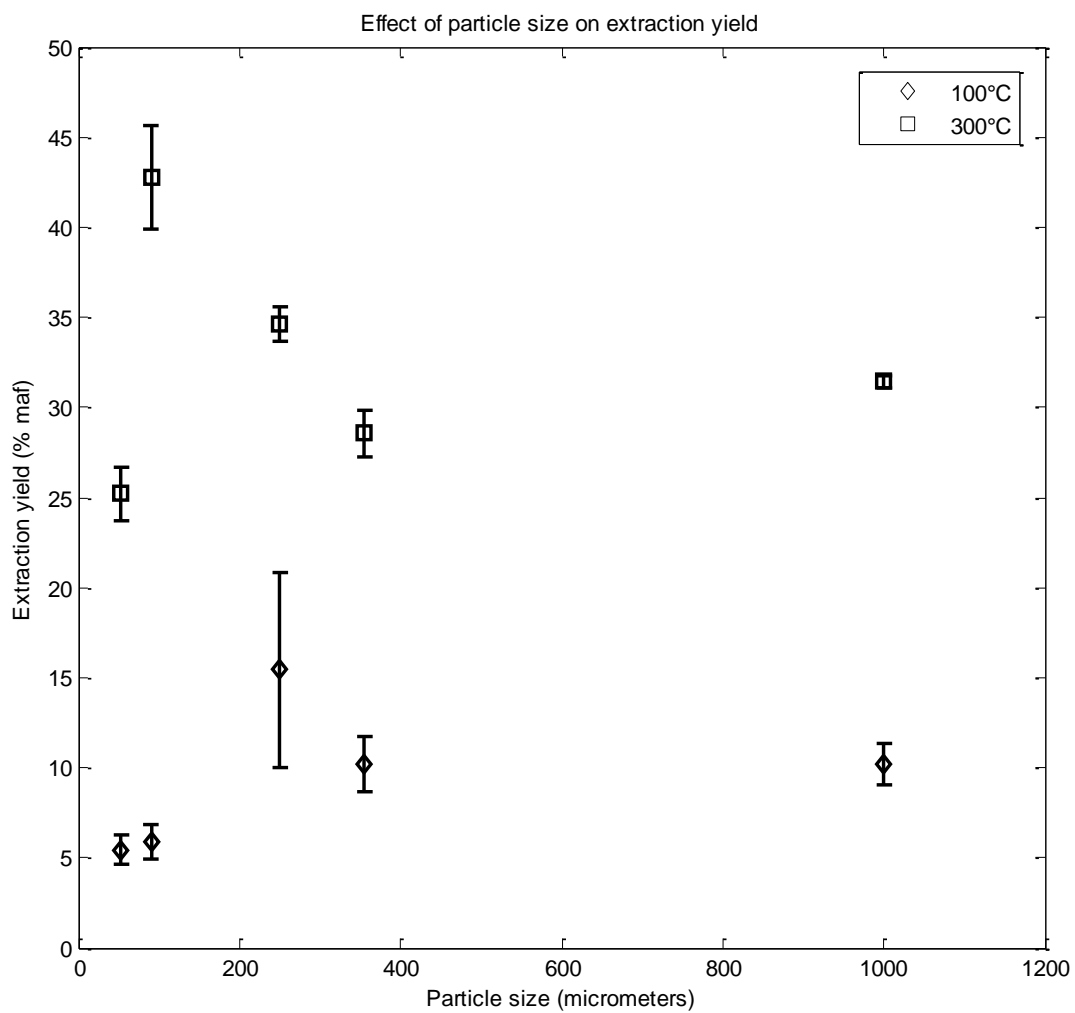


Figure 14 Effect of coal particle size on extraction yield during solvent extraction of lignite (3 hours) with tetralin at 100 and 300 °C.

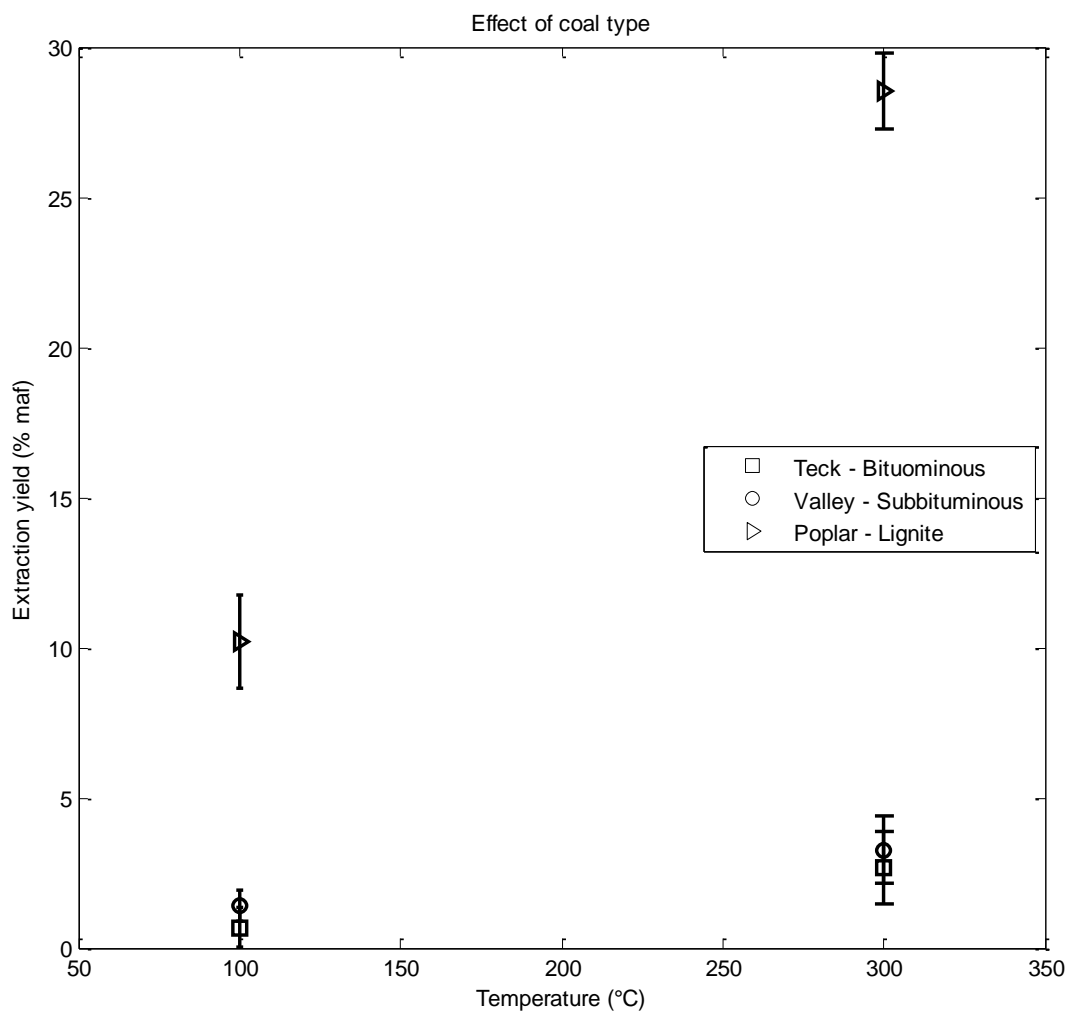


Figure 15 Effect of coal type on extraction yield during solvent extraction of three types of coal (3 hours) with tetralin at 100 and 300 °C.

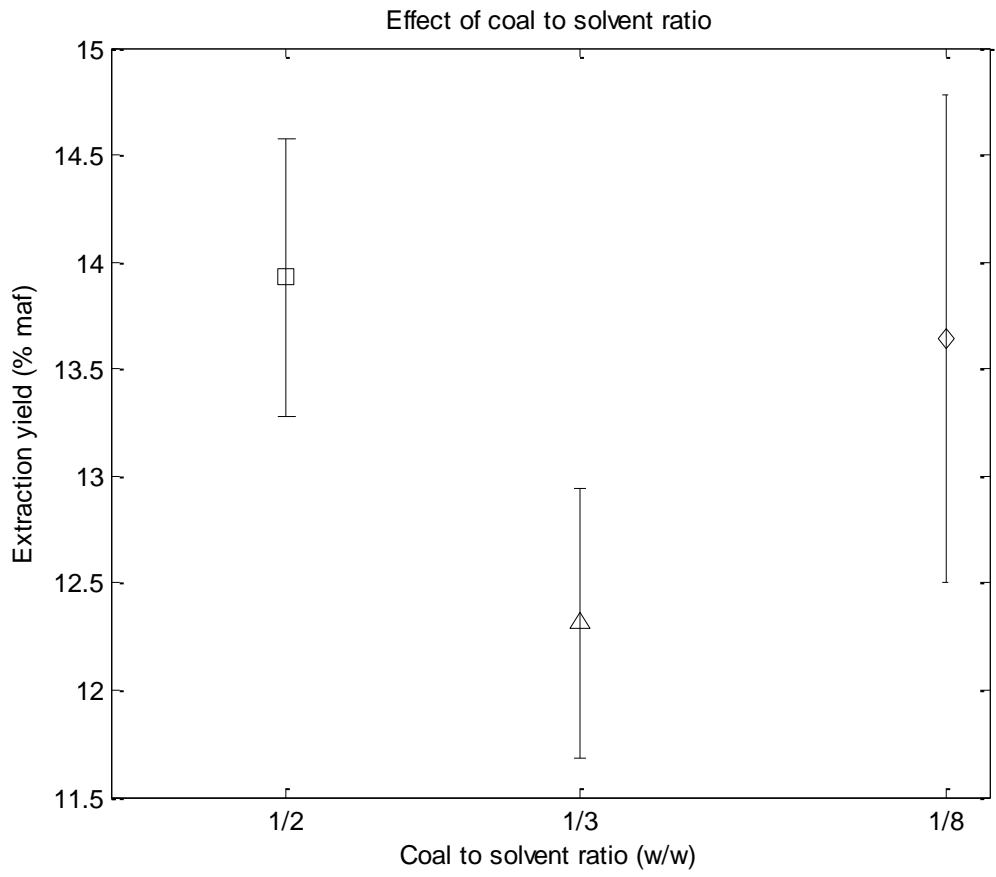


Figure 16 Effect of coal to solvent ratio on extraction yield during solvent extraction of lignite (1 hour) with tetralin at 100°C.

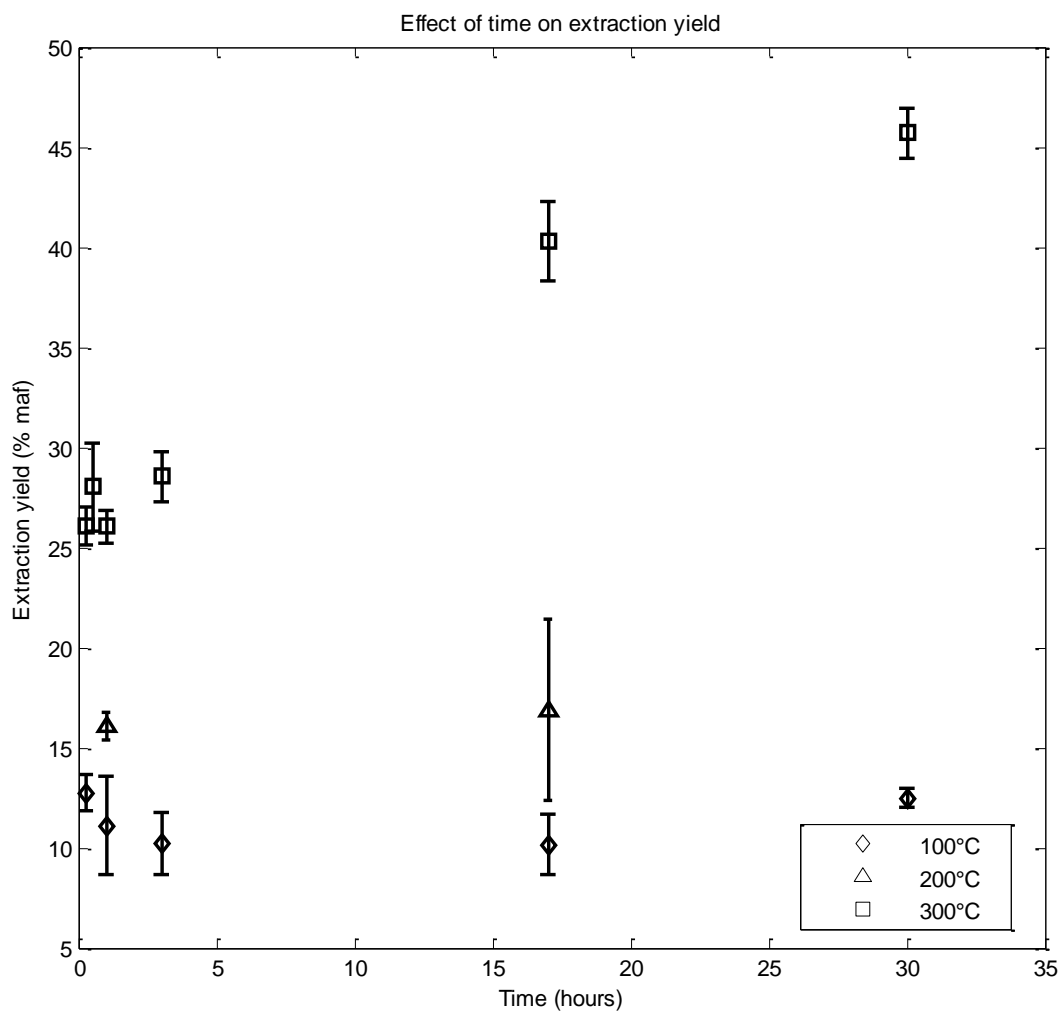


Figure 17 Effect of time on extraction yield during solvent extraction of lignite (355-1000 μm particles) with tetralin at 100, 200 and 300 $^{\circ}\text{C}$.

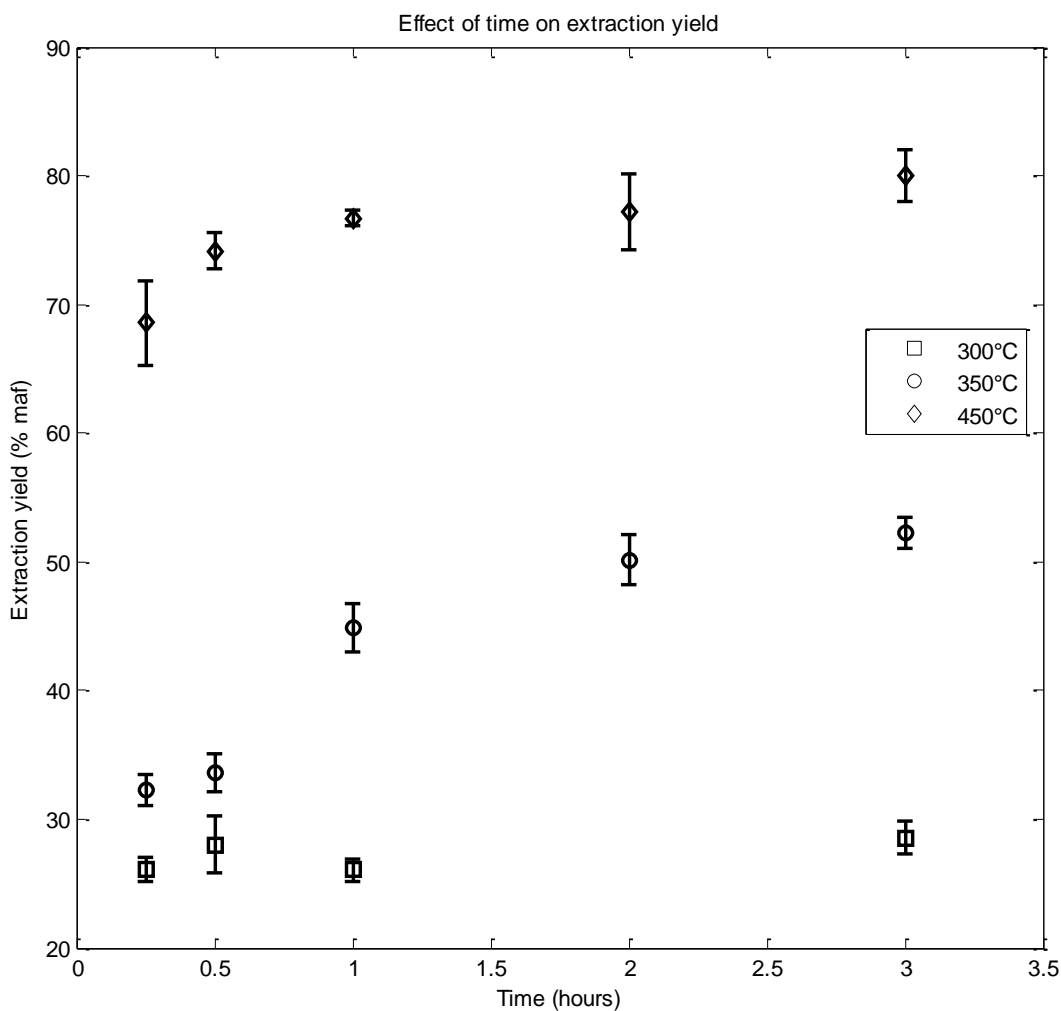


Figure 18 Effect of time on extraction yield during solvent extraction of lignite (355-1000 μm particles) with tetralin at 300, 350 and 450 $^{\circ}\text{C}$.

5.4. Performance of published models

In this section models for the physical dissolution of coal that were proposed by different authors will be tested in order to analyze if the models are able to predict the physical dissolution phenomena occurring in the solvent extraction of coal.

Isothermal Kinetic Model

In this model the authors proposed a simple model, based mainly in the material that becomes soluble in the liquid phase (coal extract) after the coal liquefaction at low temperatures (see *Figure 19*). Since coal would never become 100% soluble in the liquid phase, taking into account that the extraction is run at low temperatures, there is a

limit in the solubility that needs to be considered. The authors pointed out that coal can generate a variety of products, that are difficult to identify and therefore difficult to be mathematically modeled. A single isothermal extraction path was assumed by the authors as followed (35):

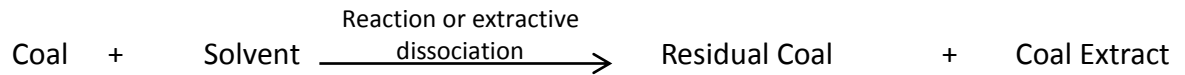


Figure 19 Isothermal extraction path proposed by Giri and Sharma.
Drawing taken from (35)

The isothermal kinetic equation for n^{th} -order proposed by authors Giri and Sharma is shown in *Equation 5*

$$\frac{dx}{dt} = k(a - x)^n$$

Equation 5 (35)

Where k is the rate constant; a , the amount of coal extract obtained at infinite time (100 hours); x , the extract obtained at time t ; and n , is the order of reaction (35).

For this practical case, the recommendation of the authors to set the coal extract at 100 hours as an infinite time was taken, but the value for parameter ‘ a ’ was obtained through extrapolation of the experimental data. The order of reaction tested by the authors ($n = 0.5, 0.66, 1.0$ and 1.34) were also evaluated in this case. The rate constant values for each order of reaction were obtained by curve-fitting the integrated form of Equation 1 vs. time, in which the slope of the line is the value of k . The best curve-fitting was obtained for $n=1$, meaning that the solvent extraction process follows a first order kinetics (35).

The results are shown in *Figure 20*, in which it can be observed that model is far from adequate for predicting the coal extraction process at low temperatures. Even though it was mentioned before that the solvent extraction process follows first order kinetics, all the different orders of reaction that were tested are shown. It is important to highlight that at short times the model presents the poorest fit, when compared against experimental data. The rate of the dissolution process observed in the laboratory is very fast, almost 50% of the material that can be dissolved (at infinite time) being solubilized in the first hour (35).

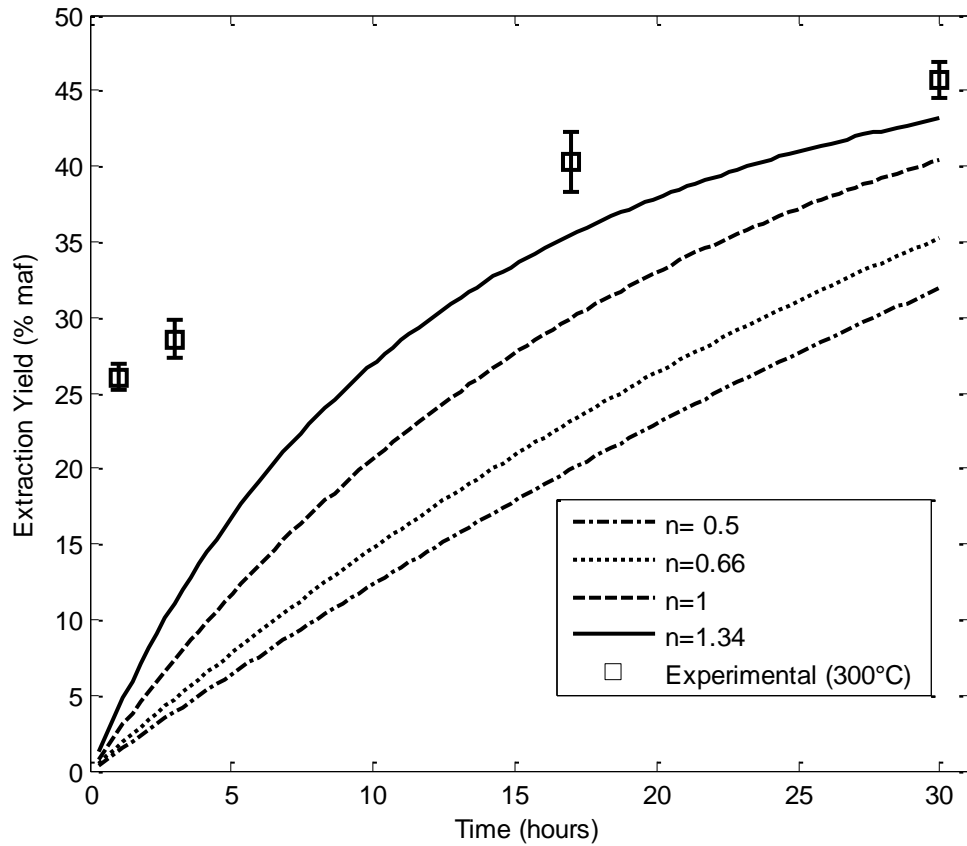


Figure 20 Isothermal kinetic model proposed by Giri and Sharma.

Shrinking Core Model

This model is based on the fact that authors observed a reduction in size of the coal particles after the solvent extraction. This means that the core of the coal particles shrinks or disintegrates. In this case it was assumed for the construction of the model that all the particles are spherical and that the extraction rate is controlled by chemical dissociation reaction (35).

The rate in terms of the reactive core was written by the authors as follows (see Equation 6) (35):

$$-kC = \frac{1}{V} \frac{dN}{dt}$$

Equation 6 (35)

Where V is the volume of the reactive core, C is the concentration of reactive molecules, dN the molecules that disappear during time and k the rate constant (35).

When V is substituted by $\frac{4}{3}\pi r_c^3$ and N by CV , therefore dN can be written as $dN=C d\left(\frac{4}{3}\pi r_c^3\right)$, the expression for the rate can be expressed as follows (35):

$$-kC = \frac{3}{r_c} \frac{dr_c}{dt}$$

Equation 7 (35)

Integrating over the radius R and t ,

$$-\int_R^{r_c} \frac{dr_c}{r_c} = \frac{k}{3} \int_0^t dt$$

Equation 8 (35)

$$-\ln \frac{r_c}{R} = \frac{k}{3} t$$

Equation 9 (35)

The *Equation 9* was written in terms of fractional conversion α by the authors, obtaining (35):

$$-\ln(1 - \alpha)^{1/3} = \frac{k}{3} t$$

Equation 10 (35)

The variable α has been defined by the authors as (35):

$$\alpha = \frac{\text{Weight loss at a given time}}{\text{Final weight loss}} = \frac{\text{Percentage extraction yield}}{\text{Percentage extraction yield at infinite time}}$$

The results of using the model proposed by Giri and Sharma to model the solvent extraction of Poplar coal at low temperature are illustrated in *Figure 21*.

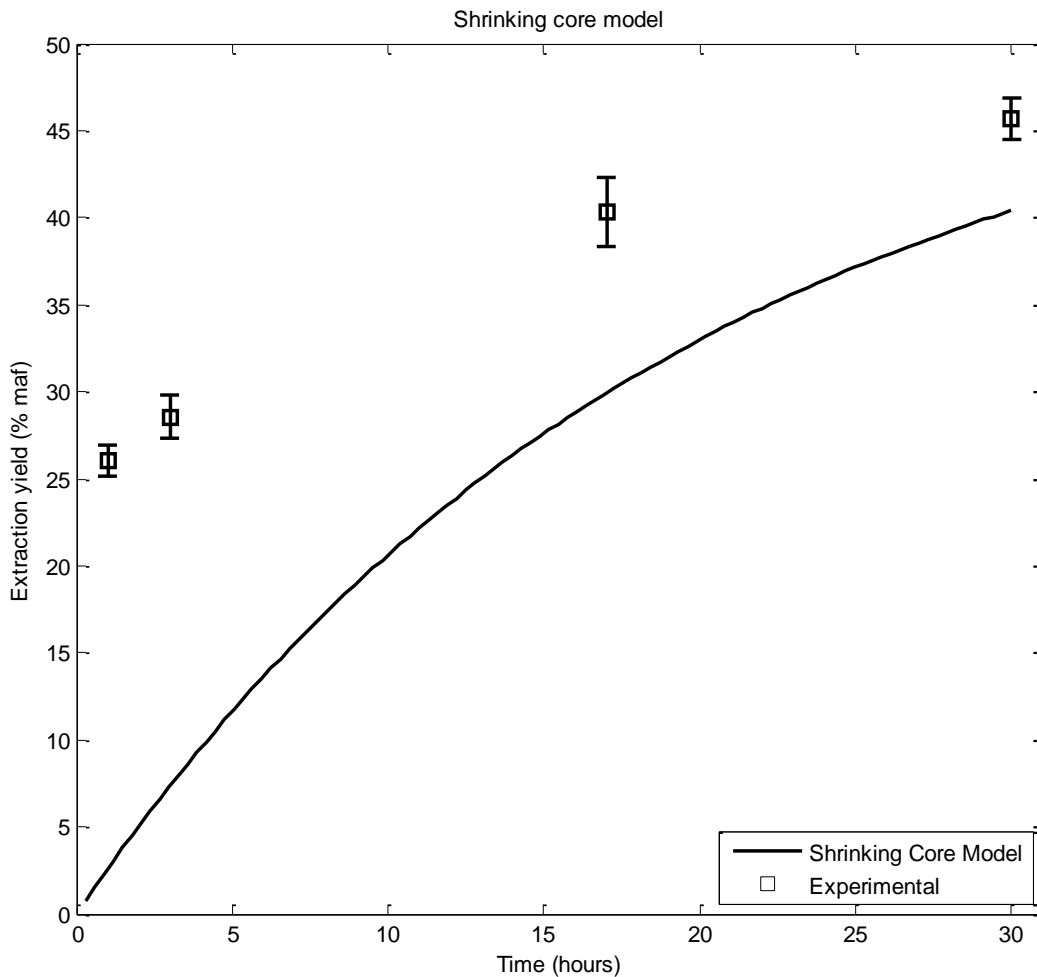


Figure 21 Shrinking core model proposed by Giri and Sharma

As observed in *Figure 21* the shrinking core model does not represent the experimental data. The poor fit of this model means that the shrinking core model cannot represent the phenomena occurring during the solvent extraction of coal at low temperature. Since *Equation 10* was obtained by integrating *Equation 7* with limits between 0 and t , *Equation 10* will have an exponential growth that would never be able to “jump” from extraction yield at time zero to extraction yield of 26.03% at time 15 minutes almost instantaneously. Unless that, the limits are re-evaluated or the modelling divided into two sections, modelling of solvent extraction process cannot be predicted with a simple model.

5.5. Modelling of physical dissolution

From the experimental data, it was observed that the process from time zero to 15 minutes is very fast, there is also a transition stage between 15 minutes and 1 hour in which the extraction yield does not increase very much. A third stage is observed especially at 300°C, where the rate decreases. From these observations, it was decided to consider the dissolution process as taking place in two steps, the first one related to physical dissolution and the second one to reactive dissolution.

In order to start modelling, it is assumed that the dissolution process of coal follows the basic deterministic model of dissolution also known as the first order model. This model is considered to be suitable for each step. The differential equation that describes the first order model is as shown in *Equation 11* (43):

$$\frac{dC}{dt} = k(C_s - C(t)), C(0) = 0$$

Equation 11

Where dC/dt is the rate of dissolution, k is a constant, C_s is the limit concentration and $C(t)$ is the concentration of the species (in solution) of interest at time t (43).

The integrated form of *Equation 11* is shown in *Equation 12* (43).

$$C(t) = C_s(1 - e^{-kt})$$

Equation 12

If *Equation 12* is rearranged and $C(t)$ is divided by C_s a new function is obtained (43):

$$F(t) = \frac{C(t)}{C_s}$$

Equation 13

The function $F(t)$ satisfies all the conditions to be a cumulative distribution function (43). In this case at time t in which $C(t) = C_s$ the function $F(t) = 1$.

For modeling purposes of solvent extraction of coal at low temperatures the following assumptions were made:

- From time zero to 0.25 hours the physical dissolution of coal takes place at a specific constant rate (albeit dependent on parameters such as temperature).

This assumption is based on the results observed in *Figure 17*. The physical dissolution is modelled using the basic deterministic model of dissolution.

- From 0.25 hours and onwards the reactive dissolution of coal takes place at a specific constant rate (different from the constant rate for physical dissolution). Reactive dissolution follows the basic deterministic model of dissolution.
- Solvent extraction of coal is a contribution of physical and chemical events (reactive dissolution) that should be reflected in the mathematical model.

For solvent extraction of coal at 300°C the previous assumptions were made and an expression that predicts the dissolution of coal at low temperatures was found and it is shown in *Equation 14*:

$$C(t) = C_{s-physical}(1 - e^{-k_p t}) + (C_{s-reactive} - C_{s-physical})(1 - e^{-k_r t})$$

Equation 14

Where $C_{s-physical}$ is the maximum concentration obtained during the physical dissolution of coal (at 0.25 hours); k_p is the constant of the physical dissolution process (determined at 0.25 hours) for which the value obtained was $28.4h^{-1}$; $C_{s-reactive}$ is the maximum concentration reached at extended times during the reactive dissolution step (after 0.25 hours), in this particular case was obtained extrapolating the experimental data to 100 hours (0.51 grams of soluble material/grams of coal (maf)); k_r is the constant of the reactive dissolution process (determined at 100 hours) for which the value obtained was $0.07h^{-1}$.

The results obtained using *Equation 14* are illustrated in *Figure 22*.

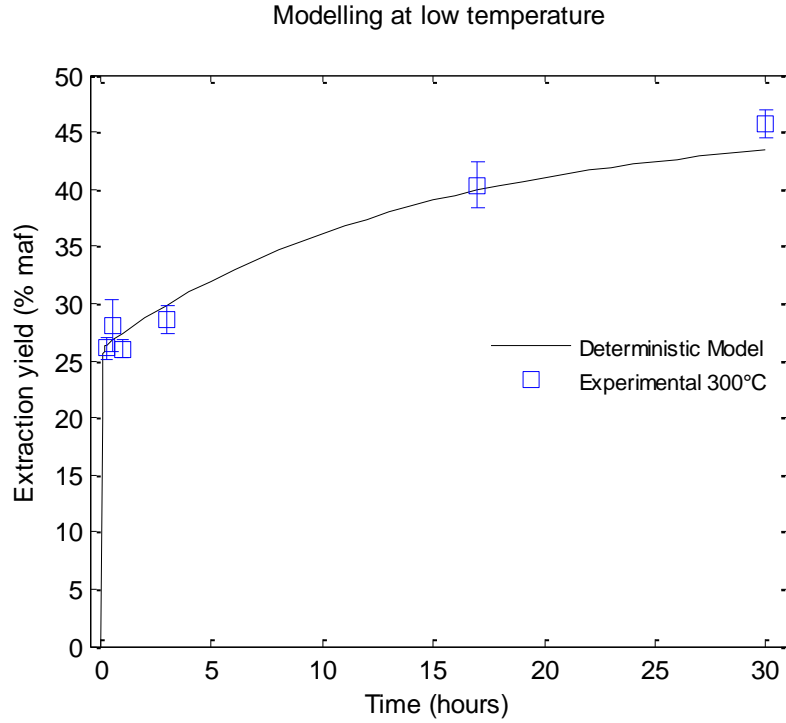


Figure 22 Deterministic model in the modelling of coal dissolution at low temperatures

It was found also a correlation between the maximum concentration obtained during the physical dissolution of coal and temperature. The maximum concentration at the physical dissolution stage presents an exponential dependence on the temperature as shown in *Figure 23*.

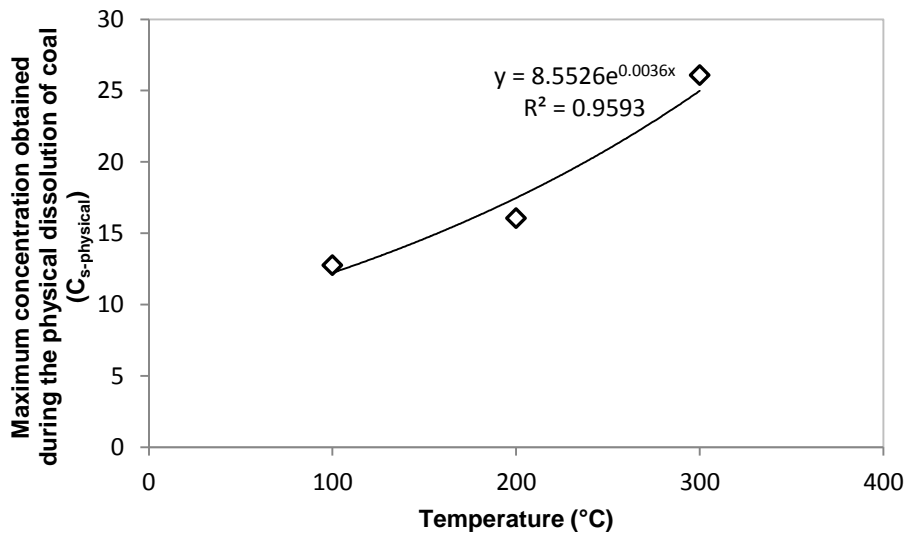


Figure 23 Correlation between maximum concentration at physical dissolution and temperature.

The discussions of this section are shown in *Section 6.5*.

5.6. Conclusion

- There was no effect of particle size in the range of 53 – 1000 μm in the extraction yield. No mass transfer limitations due to particle size were observed. However, due to the rapid physical dissolution, the observations may not rule out such effects at short contact time.
- At low temperatures physical characteristics of the coal particle (i.e pore size distribution) and chemical composition of coal (i.e. functional groups) play an important role during solvent extraction.
- Coal rank affects the coal reactivity, being confirmed in this study the statement that low rank coals are more reactive than high rank coals (20).
- There is not dissolution limitation due to solvent saturation for coal to solvent ratios in the range of 1:2 to 1:8.
- Physical dissolution dominates extraction during the first 15 minutes; whereafter reactive dissolution dominates extraction at longer exposure time.
- Reactive dissolution becomes predominant at times longer than 1 hour and more relevant as temperature increases.
- None of the literature models tested in this chapter, predict the behaviour observed for the dissolution of lignite in tetralin at 300°C. The dissolution process should be modeled by two terms: a physical dissolution term that dominates dissolution in the first couple of minutes (15 minutes selected as threshold based on current experiment) and a reactive dissolution term.

5.7. Recommendations

- The effect of particle size and mass transfer limitations during the solvent extraction of coal should be studied at short times (less than 15 minutes), since in this study no effect was observed.
- Since no effect of coal to solvent ratio was observed; for industrial process it becomes feasible to use a ratio of coal to solvent of 1:2 (possibly less) without causing any effect on the extraction yield due to solvent saturation.
- Solvent extraction of coal at times shorter than 15 minutes should be studied in order to obtain a complete time-temperature profile of the extraction process.
- The dependence of the physical and chemical dissolution rate constants on operating conditions and solvent must be established.

6. MODELLING OF CHEMICAL DISSOLUTION OF COAL

6.1. Relevance of a fundamental model

Based on the facts pointed out in the case of coal extraction kinetics based on solvent-class lumping, it can be observed that the events occurring during liquefaction at the different temperature regions are not taken into account. In most of the studies the temperature is set in the active region and the kinetic model is proposed without taking into consideration the effects at lower temperatures. Lumping of different products obtained from coal liquefaction is usually the basis of proposing a kinetic model, but in fact, most of the studies lack analyses over time-temperature to observe changes in the products that are generated. When the solvent-class lumping methodology is used, the strategy of extracting the products will ultimately define which products can be quantified and modelled.

6.2. Preliminary tests

Before we started proposing a reaction mechanism and building a kinetic model, certain characteristics of the raw coal and the products obtained after liquefaction, were tested. The purpose of these preliminary tests was to help our understanding of the physical and chemical events during the solvent extraction of coal.

The thermal behaviour of Poplar coal was studied using Thermogravimetric analysis using a Simultaneous DSC – TGA. The conditions for the experiment were set as follows:

- Heating rate: 5°C per minute.
- Atmosphere: Nitrogen
- Gas flow: 100 mL/min

In the presence of nitrogen, it is expected to observe just those effects related to thermal decomposition of coal. As can be seen in *Figure 24*, a decrease in mass takes place from the beginning of the process until around 100°C at a very fast rate. This mass loss represents the moisture loss in the coal sample. Most of the water lost below 100 °C is due to the desorption of physically adsorbed water. After 100°C until approximately 200°C the mass loss continues but at a lower rate. From 200°C and onwards the mass loss rate increases. These events observed agree with those observed by Berkowitz who identified 3 temperature dependent regions during the

thermal analysis of coal samples. In this particular case, it can be said that the active stage of Poplar coal starts at around 300°C where the mass loss rate increases due to reactive decomposition (pyrolysis).

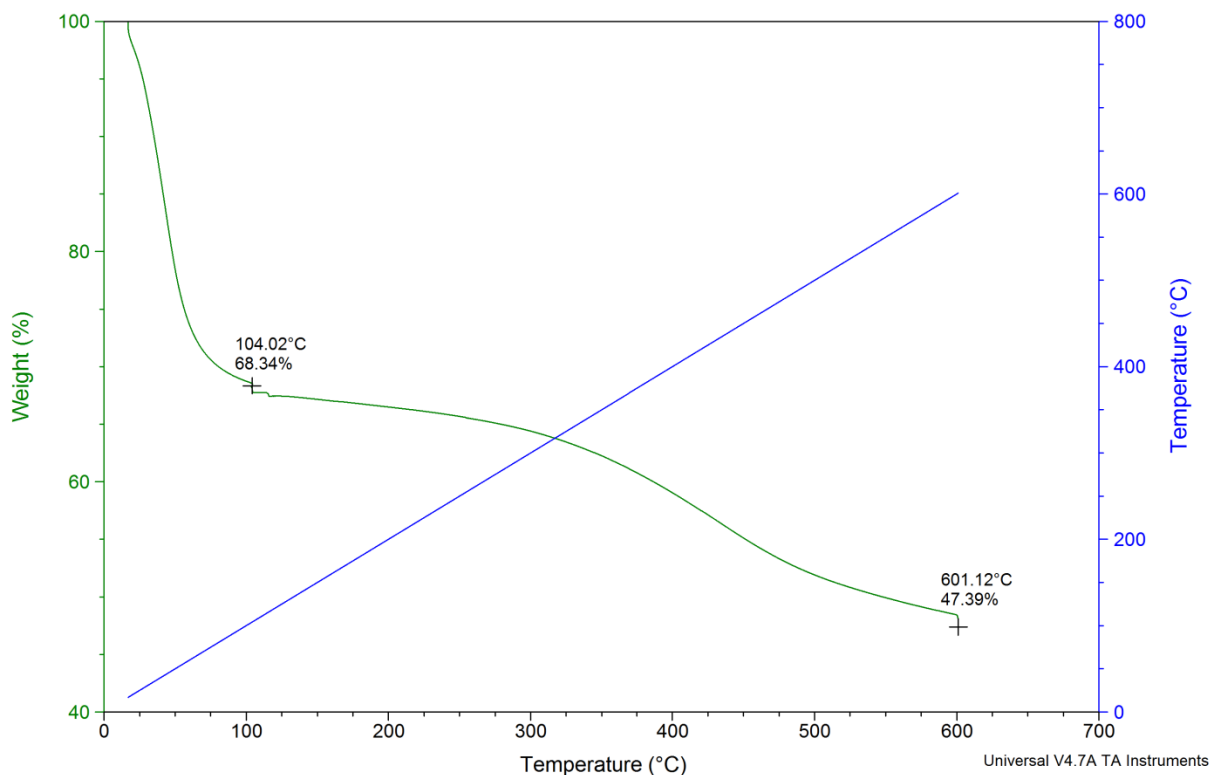


Figure 24 Pyrolysis of coal under nitrogen atmosphere obtained using Thermo-Gravimetric Analysis (TGA).

The elemental analysis of the residue collected after the solvent extraction process was done, using an elemental Vario MICRO Cube. In this case the content of carbon, nitrogen, hydrogen and sulphur were determined and the content of oxygen was calculated by difference (see *Appendix 2*). In *Figure 25* it can be noted that with increasing temperature the ratio of H/C decreases. This observation agrees with the phenomena that has been stated by different authors and explained in previous chapters, . Hydrogen is transferred to stabilize free radicals, causing some species to become hydrogen enriched and other hydrogen depleted, ultimately forming coke. The formation and capping with hydrogen of the radicals formed is favored at higher temperatures. In this case of the solid residue, it is expected to observe a reduction in the H/C ratio with respect to raw coal and residues treated at lower temperatures. At extended times (see *Figure 26*), the effect of reactive dissolution at 300°C and higher temperatures is observed; the H/C ratio keeps on decreasing as time increases, meaning that at this reaction temperature chemical events are taking place. Meanwhile,

the H/C ratio for extractions at 100°C and 200°C remains constant and around the value for the raw coal.

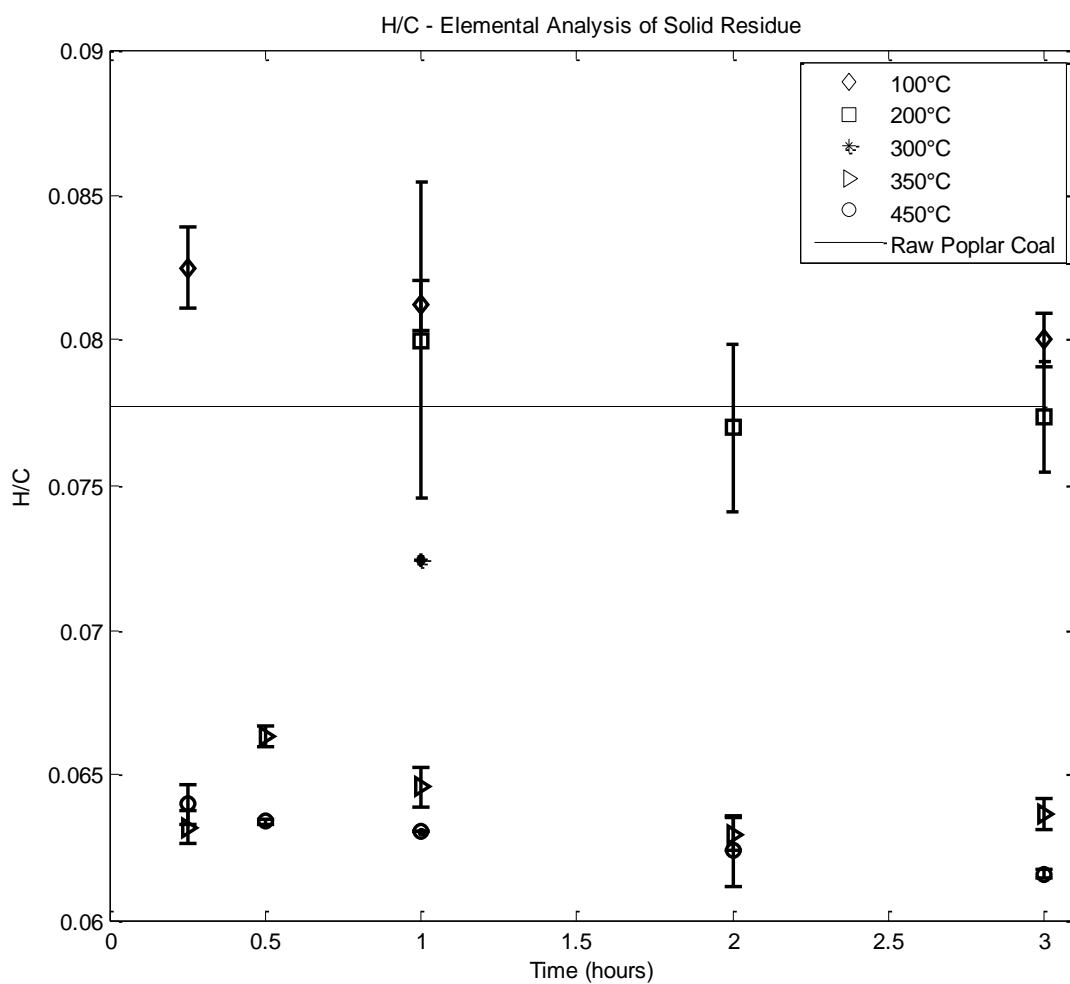


Figure 25 H/C ratio of solid residue measured using Elemental Analysis.

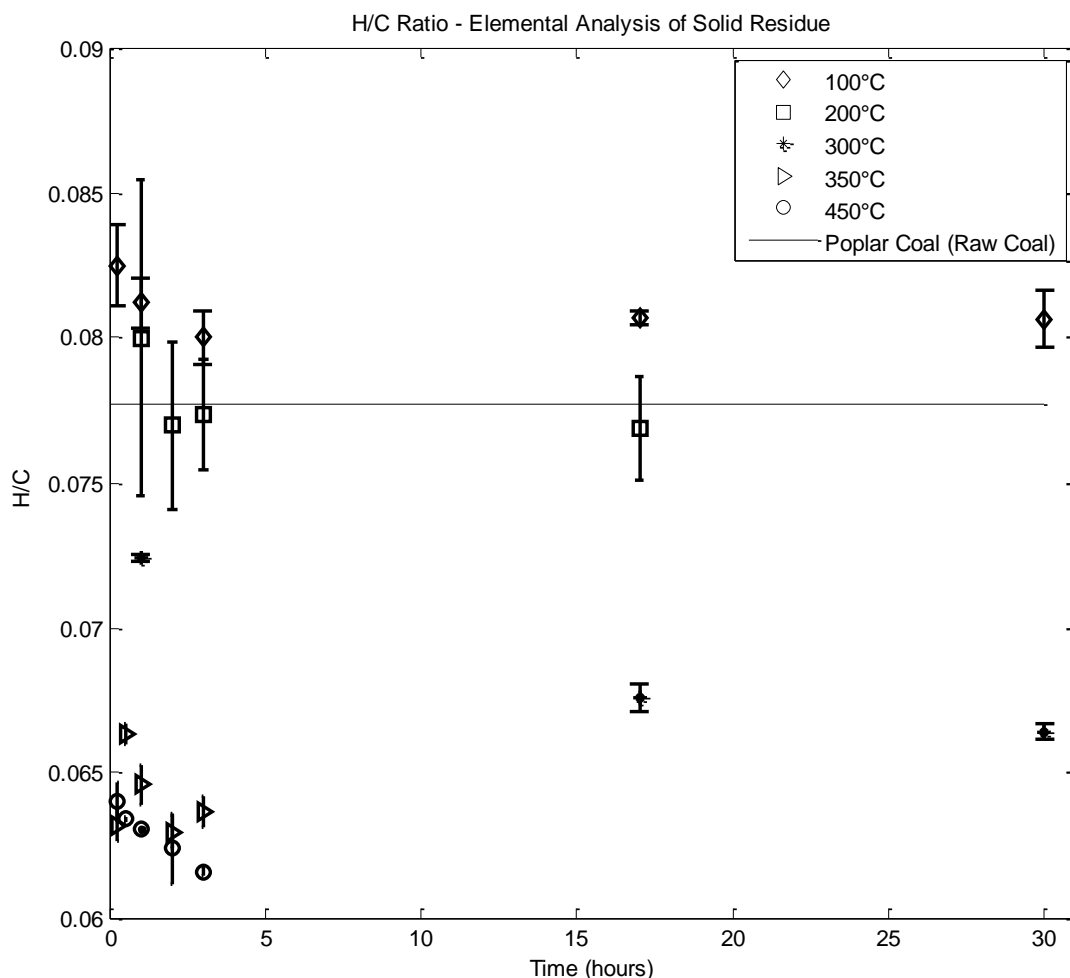


Figure 26 H/C ratio of solid residue using Elemental Analysis (extended time for extractions at low temperature)

The liquid samples (THF soluble) were analyzed using $^1\text{H-NMR}$ spectroscopy. THF from the samples was removed by evaporation, placing the samples at 55°C and 260mm Hg during 4 hours in a RotoEvaporator, previous to $^1\text{H-NMR}$ analysis. The results presented in *Figure 27* show an increase in aromatic structures as time increases for solvent extraction at 450°C . In the case of olefins, what is observed is an increase from 0.25 to 0.5 hours, and then the amount of olefins decreases as seen at 2 hours. On the other hand, aliphatic structures show a decrease over time.

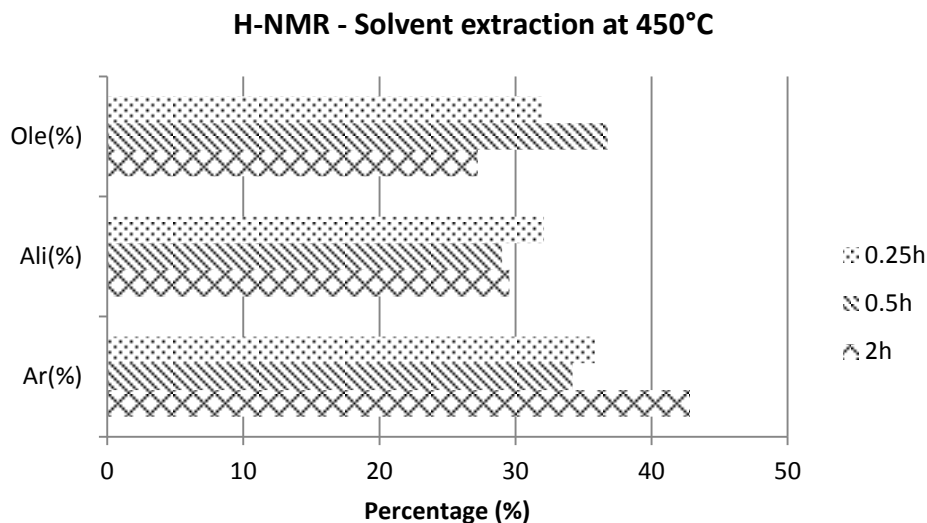


Figure 27 $^1\text{H-NMR}$ of the extracted coal dissolved in tetralin
Ole (Olefin), Ali (Aliphatic) Ar (Aromatic)

The transient increase in olefin content is likely due to hydrogen transfer from tetralin *Figure 1*, which ultimately results in the formation of naphthalene and the significant increase in aromatic content. The $^1\text{H-NMR}$ results support the mechanistic description involving hydrogen transfer from the solvent to the coal.

6.3. Low temperature regime

Rate of decomposition of coal at this stage is very slow and is characterized for releasing 'chemically combined' water, oxides of carbon and hydrogen sulfide. Molecules such as benzoic acid will decompose producing CO_2 . At this stage dehydration reactions also occur, which produce water. These decomposition reactions that take place at low temperature and a low rate, modify the coal structure and therefore subsequent thermal behaviour of coal is influenced (8). The reactions taking place at low temperature was already discussed (see *Section 3.3*).

The results in *Figure 17* make it clear that at 100 and 200 °C very little chemical dissolution takes place, if any. The extraction yield did not increase beyond that obtained by physical dissolution. The subsequent discussion will therefore focus on coal extraction at 300 °C and higher temperatures.

6.4. High temperature regime

The high temperature regime is also called the Second Stage of coal extraction or the “active stage”. It begins between ~350°C - 400°C and ends near 550°C. The reactions taking place in this temperature range has been discussed (see *Section 3.3*).

6.4.1. Experimental

Poplar coal of particle size of 355 – 1000 µm was treated with 1,2,3,4 – tetrahydronaphtalene Reagentplus 99% (Tetralin) at 350°C and 450°C. The reaction time varies from 0.25 to 3 hours. The experimental procedure has been already explained in *Section 5.2*, however for the study of the solvent extraction at high temperature the following modifications were made:

- In the case of runs at 450°C the sand bath was heated at 10°C above the reaction temperature.
- A thermocouple was introduced in one of the microreactors to observe and measure the temperature profile.

The liquid fraction was collected and the THF evaporated in a RotoEvaporator at 35rpm, 60°C and 260mm Hg. The liquid extracted coal was fractionated to obtain toluene insoluble and n-heptane insoluble products based on the ASTM 3279 procedure (50). The liquid extracted coal was first treated with toluene at a ratio of 100 grams of toluene per 1 gram of soluble material present in the liquid extracted coal. The mixture (toluene + extracted coal liquid) was put under reflux for 1 hour at slow ebullition of the mixture. The mixture was cooled down to room temperature and vacuum filtrated using glass fibre paper filter. The solid residue (toluene insoluble) was left at room temperature overnight to let the remaining toluene to evaporate. The sample weight was taken until it reached constant weight. The toluene soluble was evaporated to eliminate toluene from the mixture at 60°C and 76 mm Hg. Then the liquid sample without toluene was treated with n-heptane. The same procedure was followed to obtain the n-heptane insoluble. The n-heptane soluble was evaporated at 60°C and 120 mm Hg to eliminate the n-heptane present in the mixture.

6.4.2. Results

The results of the product characterization of the extracted coal are expressed in terms of extraction yield (% maf) that was calculated as follows:

- For toluene and n-heptane insoluble:

$$\text{Extraction yield (\% maf)} = \frac{\text{Weight of sample}_{(\text{Toluene or n-Heptane insolubles})}}{\text{Feed coal (maf)}}$$

Equation 15

The light fraction was obtained by difference as follows:

$$\text{Light fraction(maf)} = \text{Extracted coal} - \text{Toluene insoluble} - \text{nHeptane insoluble}$$

Equation 16

The light fraction (see *Equation 16*) constitutes the soluble material that still remains in solution that did not precipitate during the treatment with toluene or n-heptane.

In *Figure 28* and in *Figure 29* are shown the extraction yield of the extracted coal (coal soluble), coal insoluble and light fraction at 350°C and 450°C respectively. Coal becomes increasingly soluble as temperature and time increases. It is actually, remarkable how fast the coal is extracted into soluble material. Of the total amount of material extracted after 3 hours, at 350°C 62% and at 450°C 86% is extracted within 15 minutes.

The toluene and n-heptane insoluble fractions are shown in *Figure 30* at 350°C and in *Figure 31* at 450°C. Both toluene and n-heptane insoluble extraction yields increase with increasing time at 350°C, but in the case of extractions at 450°C the toluene insoluble fraction decreases after 0.5 hours as time further increases.

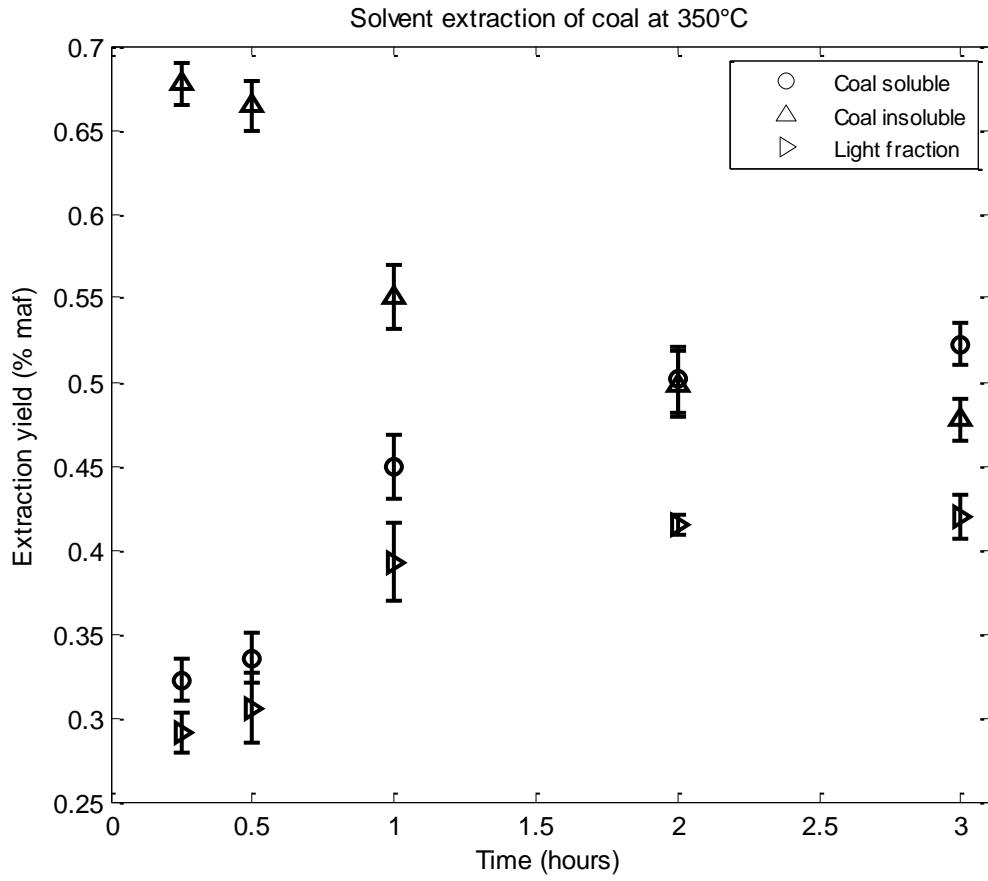


Figure 28 Experimental data for solvent extraction of coal at 350°C

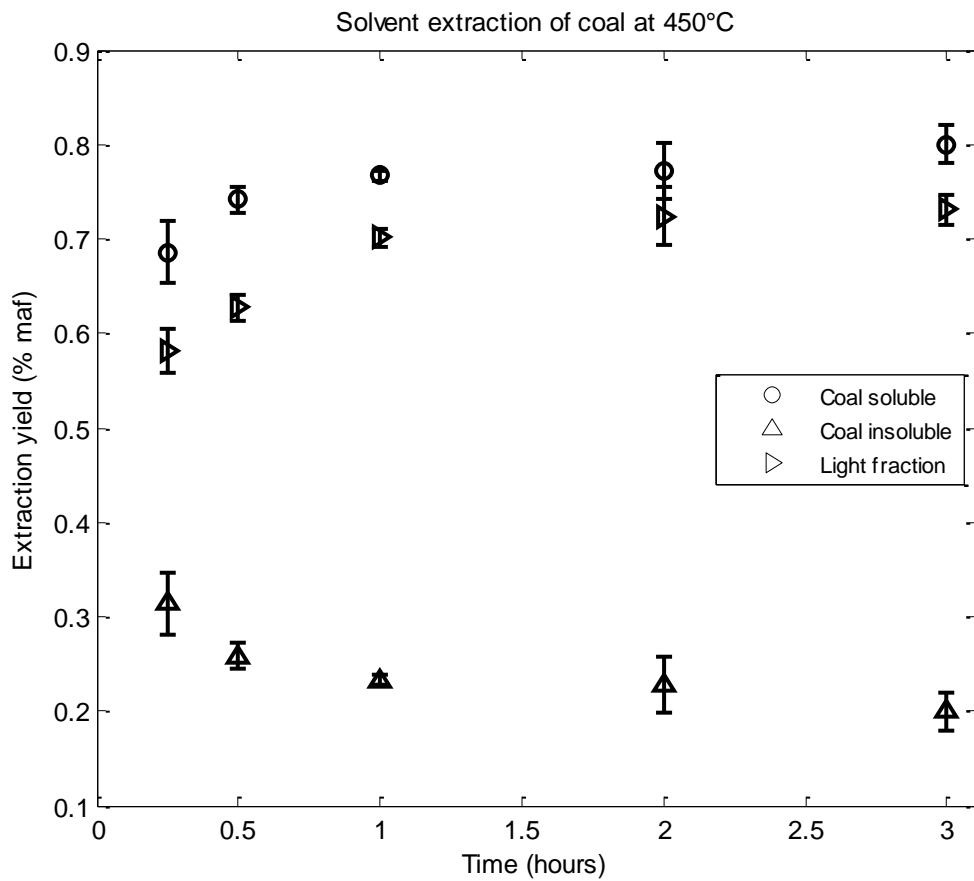


Figure 29 Experimental data for solvent extraction of coal at 450°C

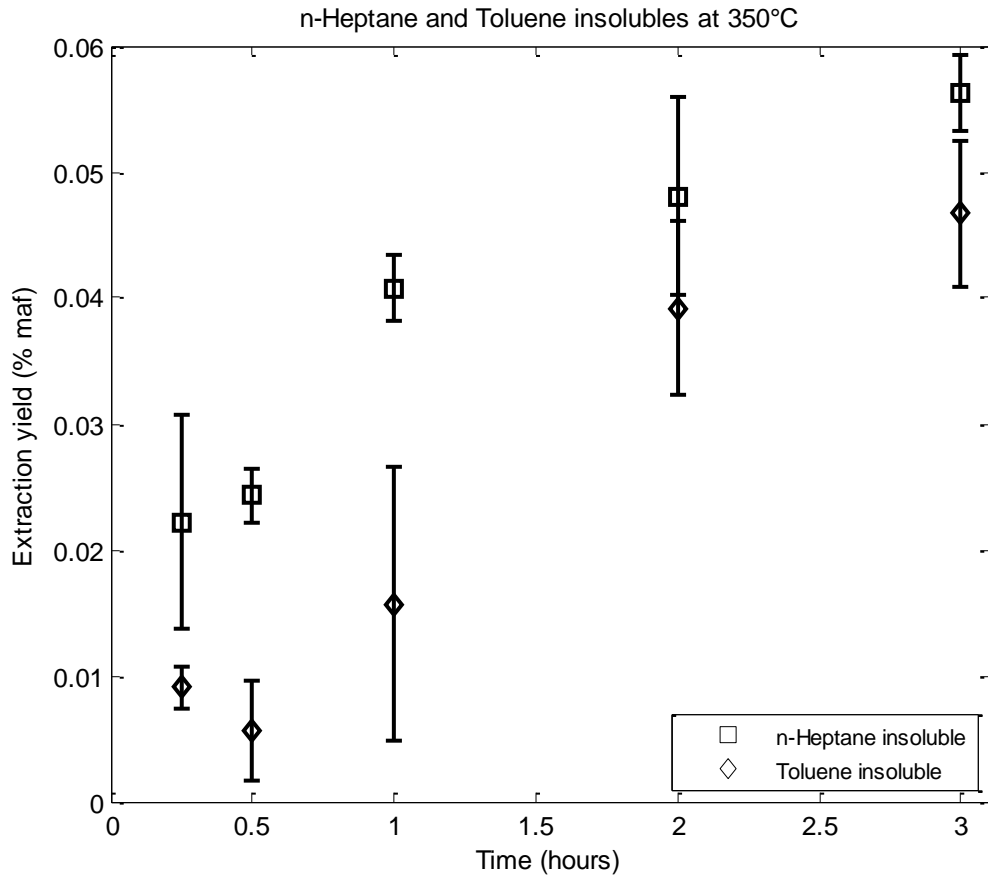


Figure 30 n-Heptane and Toluene insoluble at 350°C

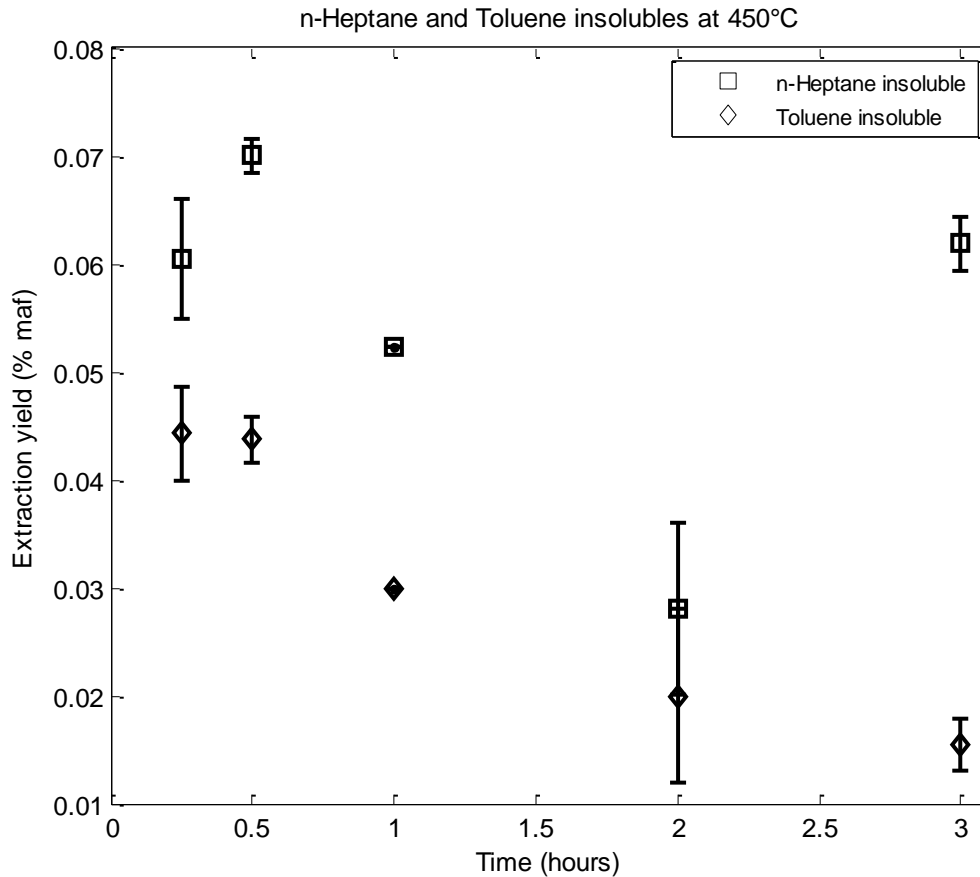


Figure 31 n-Heptane and Toluene insoluble at 450°C

6.4.3. Performance of published models

As discussed in *Section 4.2* the typical models that have been proposed in literature are: series, parallel and series-parallel of irreversible and/or reversible reactions mechanism. In this section the models proposed for lignites by Ceylan and Olcay were tested and compared against the experimental data obtained in this study. The models proposed by Ceylan and Olcay include the gas products during the coal liquefaction but do not include the insoluble coal that is generated over time. The gas products were not measured in this study, instead, the insoluble coal fraction was taken into account in the models.

In the following models the fractions are represented as follows: *C* (coal), *P* (n-heptane insoluble fraction), *A* (Toluene insoluble fraction), *O* (Light fraction), *I* (Undissolved coal)

Model A

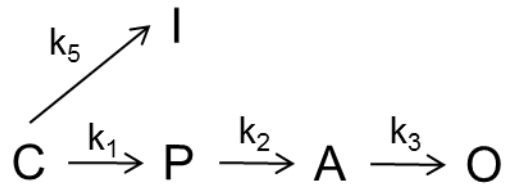


Figure 32 Model A based on the Model 1 proposed by Ceylan and Olcay
Drawing taken from (30)

Model B

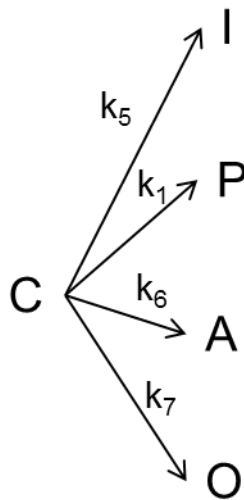


Figure 33 Model B based on the Model 2 proposed by Ceylan and Olcay
Drawing taken from (30)

Model C

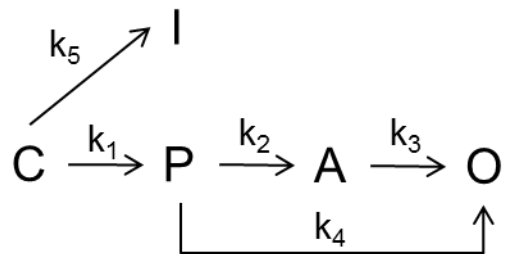


Figure 34 Model C based on the Model 3 proposed by Ceylan and Olcay
Drawing taken from (30)

Table 4 Summary of the rate constants calculated for literature models

Temperature (°C)		k_1	k_2	k_3	k_4	k_5	k_6	k_7
350	Model A	1.58	78.42	29.08	N.A.	1.86	N.A.	N.A.
	Model B	0.09	N.A.	N.A.	N.A.	1.52	0.14	1.28
	Model C	1.57	2.10	-0.38	41.63	1.70	N.A.	N.A.
	Model C*	1.57	7.16	0.00	66.09	1.70	N.A.	N.A.
450	Model A	13.95	15.11	21.05	N.A.	4.92	N.A.	N.A.
	Model B	0.26	N.A.	N.A.	N.A.	1.86	0.46	5.75
	Model C	83.69	-154.71	61.01	634.42	31.01	N.A.	N.A.
	Model C*	1.57	66.05	0.00	7.16	1.70	N.A.	N.A.

* Constraint tolerance included in the calculation

From Model A, Model B and Model C it can be observed that the limiting step is the formation of n-heptane insoluble fraction from coal. This step shows in all models the lowest reaction rate.

In the case of Model C two options were evaluated. The first one with no constraint tolerance for the reaction rates and the second one included a constraint since in the first option negative reaction rates were obtained. The negative reaction rates do not mean an erroneous result, instead, that the reaction is favoured in the opposite way. For example for Model C, the reaction rate k_3 obtained was negative as observed in *Table 4*. In this case the reaction from n-heptane insoluble fraction to light fraction at 350°C is not favoured in that direction, instead favoured in the opposite way from light fraction to n-heptane soluble fraction. In the solvent extraction process this can be explained by the fact that retrograde or condensation reactions are taking place. The graphic results of the predicted extraction yield values are shown in *Appendix 3*

When the constraint tolerance is integrated into the calculations, the value obtained for k_3 is zero, meaning that the reaction from n-heptane insoluble fraction to light fraction it does not take place.

6.4.4. Modelling of solvent extraction yield during active decomposition

The purpose for this section is to develop a mathematical model that it should be able to explain and predict the solvent extraction process during the active decomposition stage of coal. The model is built based on the results showed in *Section 6.4.2* for extractions at 350°C and 450°C.

The following steps were considered each time that a model was proposed:

1. Propose a reaction mechanism

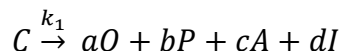
2. Write down the differential equations that describe the reaction kinetics based on the proposed mechanism.
3. Implement the differential equations in a MATLAB file.
4. An initial guess b_0 was established to start the calculations.
5. The ordinary differential equation solver ode45 from MATLAB was used to find a solution to the proposed equations.
6. The calculated extraction yields were compared against the experimental data and the sum of squared errors was calculated. Besides that, a weight matrix was included in the error criteria, since the range of extraction yield differs, especially in the case of toluene and heptane insoluble fraction for which the extraction yield values obtained are very low compared to the other 3 fractions.
7. Parameters were modified and steps 5 and 6 repeated until the error was minimized based on the least square error criteria. For this aim, the fminsearch function in MATLAB was used.
8. A vector with the solutions was written and the plots of the experimental data and the predicted data were generated.

The models proposed are based on the observations highlighted in the previous section. $^1\text{H-NMR}$ results (see *Appendix 4*) indicated that the same products are obtained either at 350°C or 450°C ; therefore, each model that is proposed is tested for both reaction temperatures. The spectra (*Appendix 4*) correspond to samples of the liquid extracted coal at the same residence time (15 minutes) and at 350 and 450°C respectively. The results show that the same products are present at both reaction times but at different proportions. Even though, the results of $^1\text{H-NMR}$ can be ambiguous due to the high content of the solvent (tetralin) in the samples.

The models are compared and discussed collectively (*Section 6.5*)

Model 1

1. Reaction mechanism proposed: An irreversible single reaction of fractional order related to the stoichiometry of the reaction



Where k_1 is the constant rate, $0 < a, b, c, d < 1$ are stoichiometric factors or intrinsic reaction order and O (light fraction), P (Toluene Insoluble), A (Heptane Insoluble) and I (Undissolved coal).

2. Reaction kinetics :

$$\frac{dC}{dt} = -k_1[C]$$

$$\frac{dO}{dt} = k_1[C]^a$$

$$\frac{dP}{dt} = k_1[C]^b$$

$$\frac{dA}{dt} = k_1[C]^c$$

$$\frac{dI}{dt} = k_1[C]^d$$

3. See *Appendix 5*
4. See *Appendix 5*
5. See *Appendix 5*
6. Solution

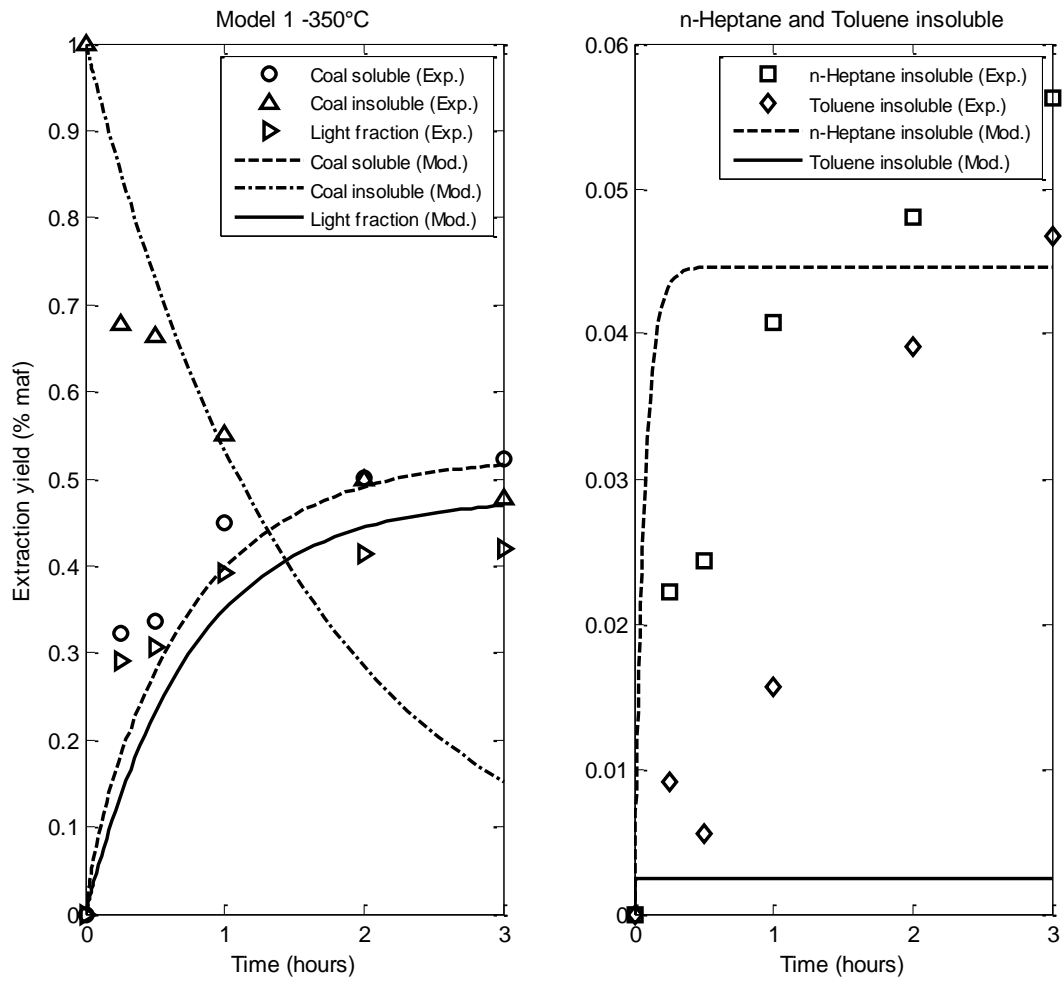


Figure 35 Model 1 at 350°C

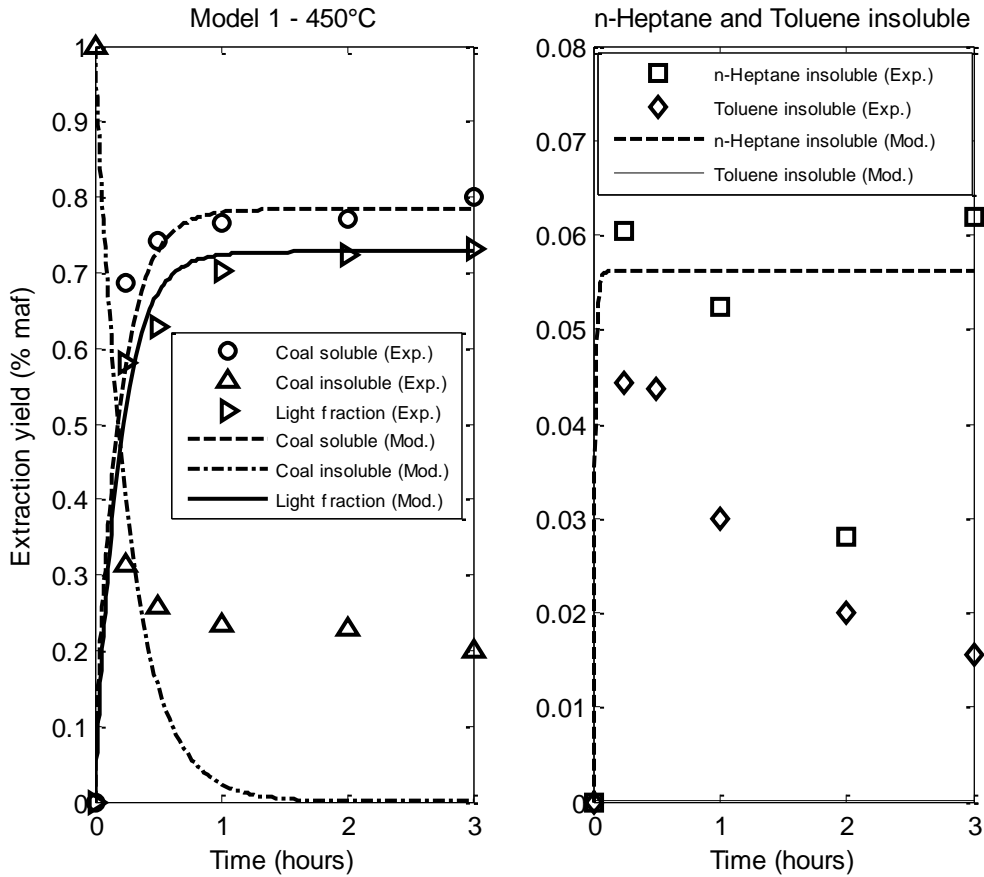
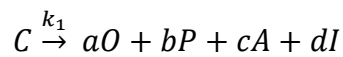


Figure 36 Model 1 at 450°C

Model 2

1. Reaction mechanism proposed: An irreversible single reaction of first order with single rate constant proportional to the product selectivity for each product.



2. Reaction kinetics:

$$\frac{dC}{dt} = -k_1[C]$$

$$\frac{dO}{dt} = k_1a[C]$$

$$\frac{dP}{dt} = k_1b[C]$$

$$\frac{dA}{dt} = k_1c[C]$$

$$\frac{dI}{dt} = k_1 d[C]$$

This model was build assuming that the reaction mechanism is of first order with respect to coal.

3. See Appendix 5
4. See Appendix 5
5. See Appendix 5
6. Solution

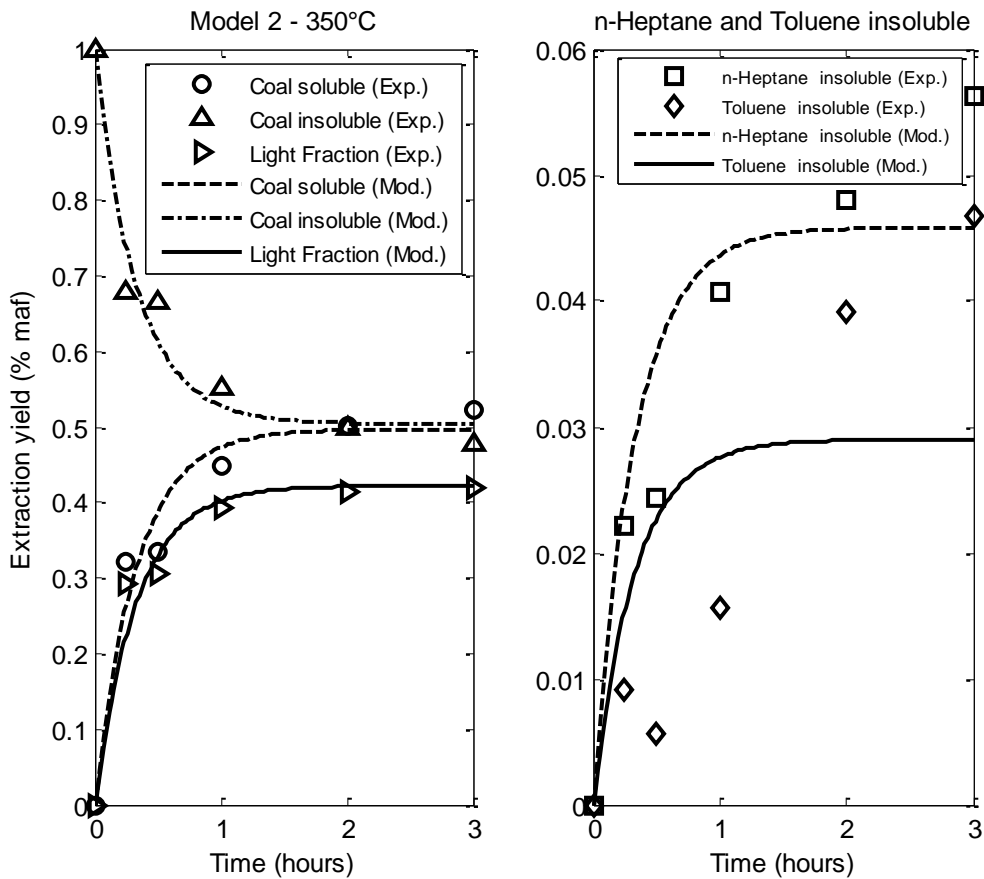


Figure 37 Model 2 at 350°C

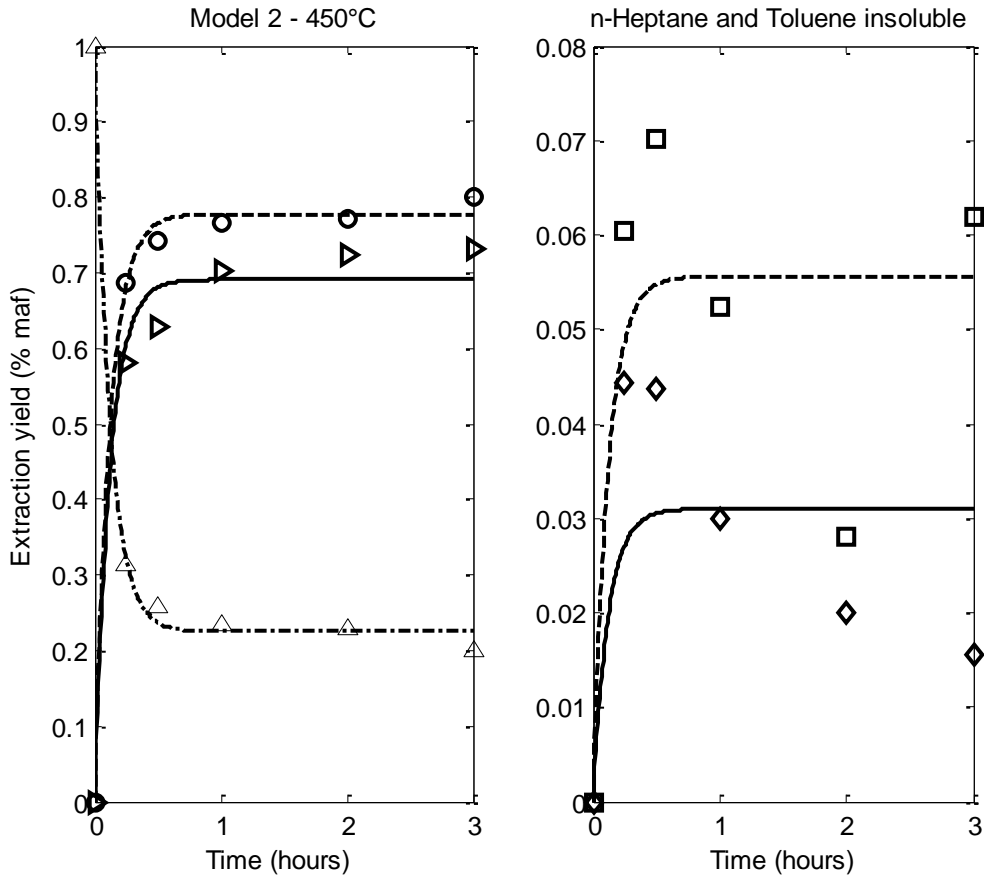
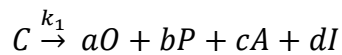


Figure 38 Model 2 at 450°C

Model 3

1. Reaction mechanism proposed: An irreversible single reaction of first order with single rate constant and fixed proportionality to each product.



2. Reaction kinetics: The stoichiometric coefficients, shown in the differential equations that are illustrated as follows, correspond to those obtained at 350°C and 3 hours.

$$\frac{dC}{dt} = -k_1[C]$$

$$\frac{dO}{dt} = k_1 0.42[C]$$

$$\frac{dP}{dt} = k_1 0.05[C]$$

$$\frac{dA}{dt} = k_1 0.06[C]$$

$$\frac{dI}{dt} = k_1 0.48[C]$$

This model differs from Model 2 in the stoichiometric factors. The stoichiometric factors have been set as the fraction obtained at 3 hours, assuming that the reaction has been completed at 3 hours.

3. See Appendix 5
4. See Appendix 5
5. See Appendix 5
6. Solution

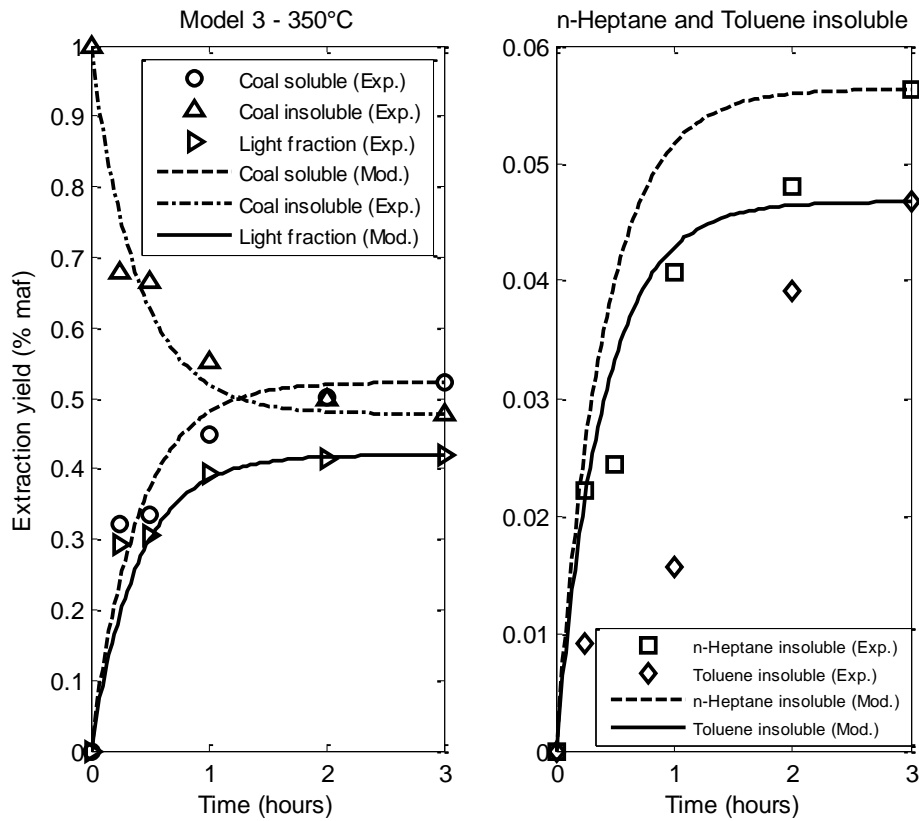


Figure 39 Model 3 at 350°C

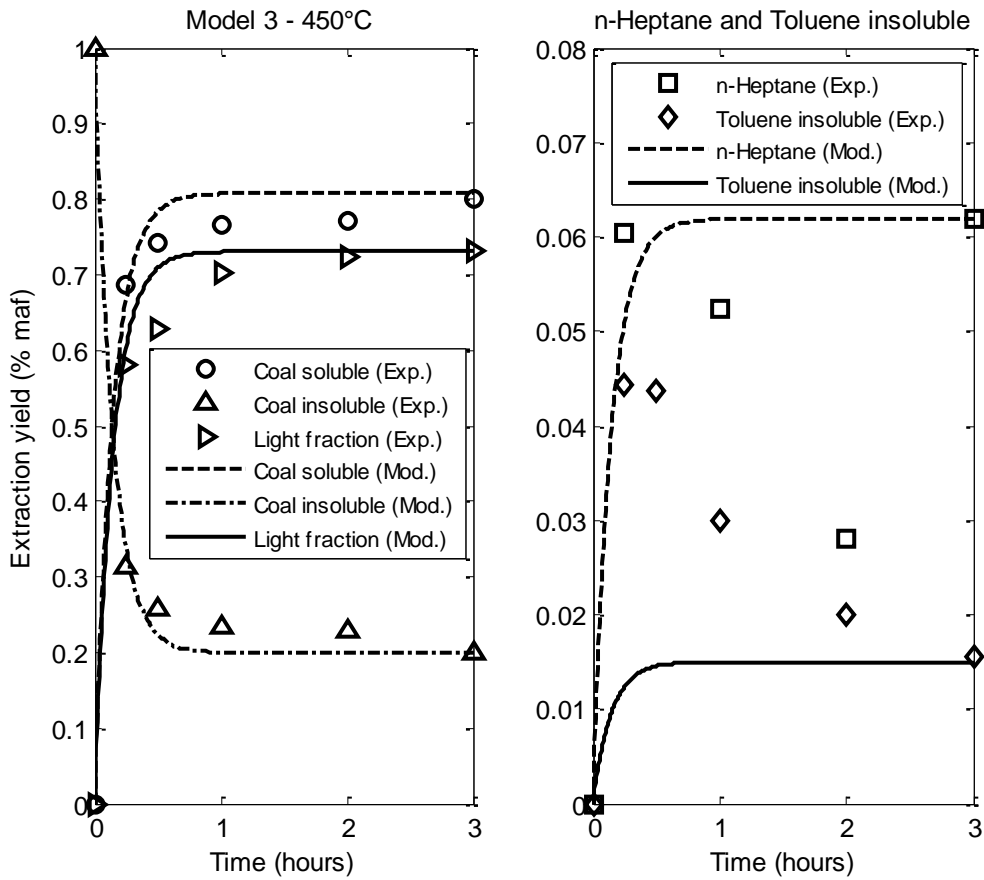
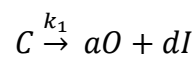


Figure 40 Model 3 at 450°C

Model 4

Model 4 was proposed based on the results observed for Models 1, 2 and 3, in which the toluene and n-heptane insoluble fraction cannot be modeled based on the single reaction mechanism proposed. In this case is observed that the toluene and n-heptane insoluble fractions are generated from a parallel reaction with constant rate k_2 as follows:

1. Reaction mechanism proposed: An irreversible set of parallel reactions of first order



2. Reaction kinetics:

$$\frac{dC}{dt} = -k_1[C] - k_2[C]$$

$$\frac{dO}{dt} = k_1a[C]$$

$$\frac{dP}{dt} = k_2b[C]$$

$$\frac{dA}{dt} = k_2c[C]$$

$$\frac{dI}{dt} = k_1d[C]$$

3. See *Appendix 5*.
4. See *Appendix 5*.
5. See *Appendix 5*.
6. Solution

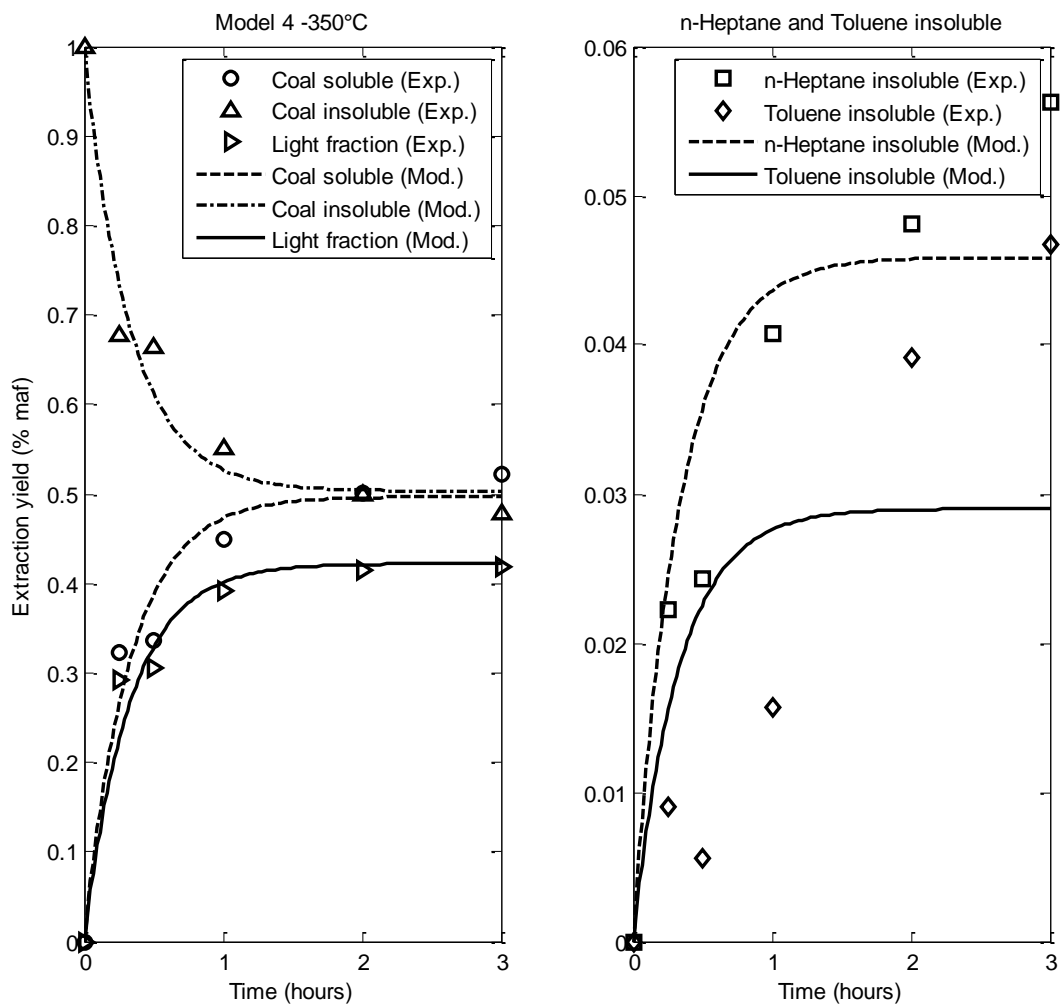


Figure 41 Model 4 at 350°C

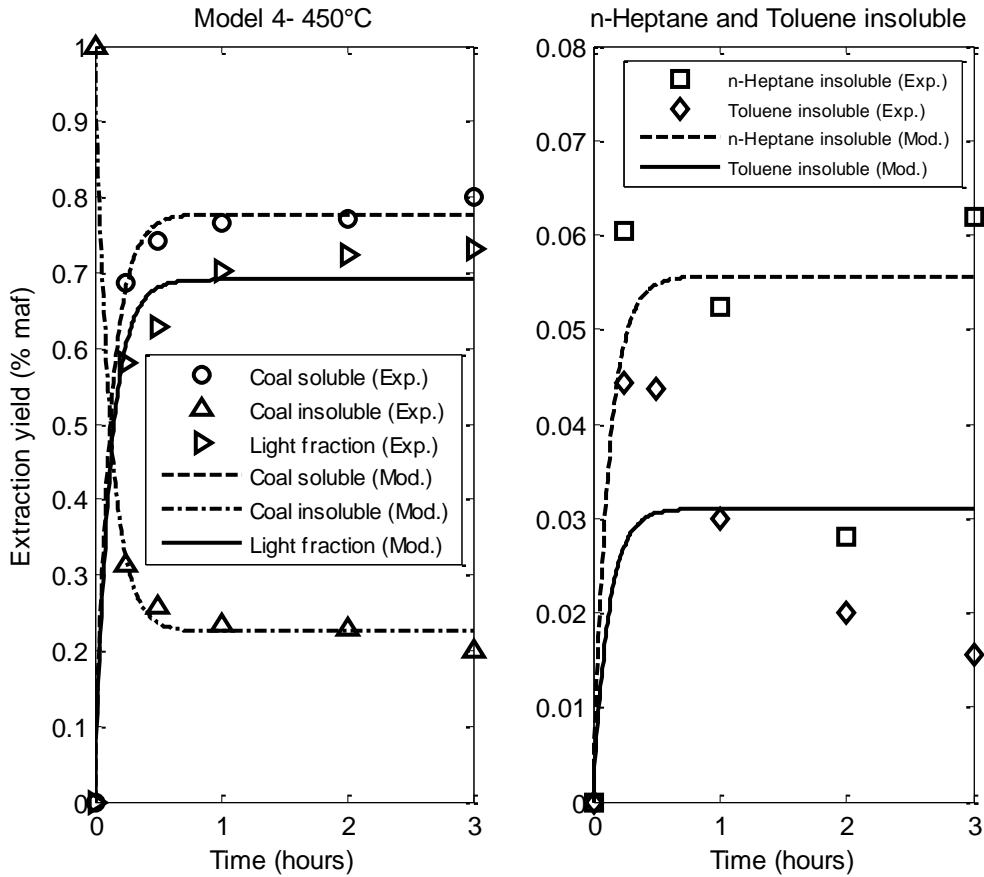
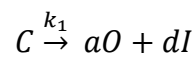


Figure 42 Model 4 at 450°C

Model 5

This model is a combination of Model 4 (using 2 sets of irreversible reactions) and Model 3 (using stoichiometric factors obtained at 3 hours).

1. Reaction mechanism proposed: An irreversible set of parallel reactions of first order



2. Reaction kinetics: The stoichiometric coefficients, shown in the differential equations that are illustrated as follows, correspond to those obtained at 350°C and 3 hours.

$$\frac{dC}{dt} = -k_1[C] - k_2[C]$$

$$\frac{dO}{dt} = k_1 \cdot 0.42[C]$$

$$\frac{dP}{dt} = k_2 \cdot 0.05[C]$$

$$\frac{dA}{dt} = k_2 \cdot 0.06[C]$$

$$\frac{dI}{dt} = k_1 \cdot 0.47[C]$$

3. See Appendix 5.
4. See Appendix 5.
5. See Appendix 5.
6. Solution

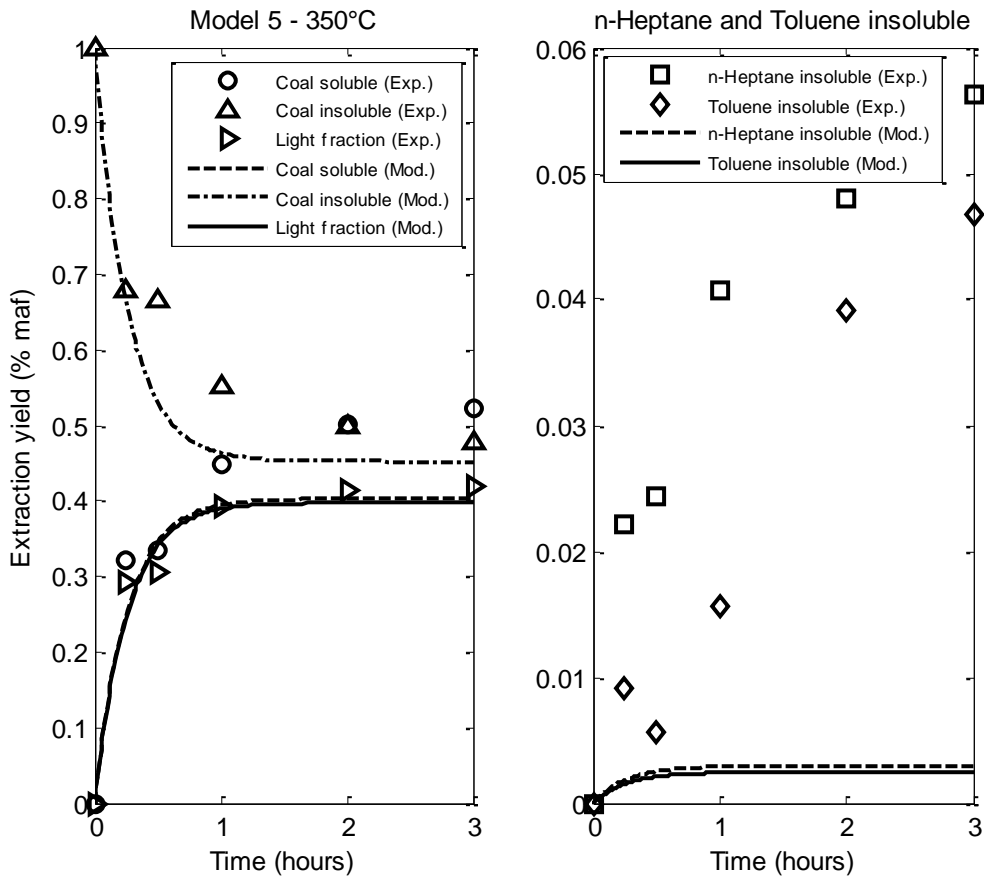


Figure 43 Model 5 at 350°C

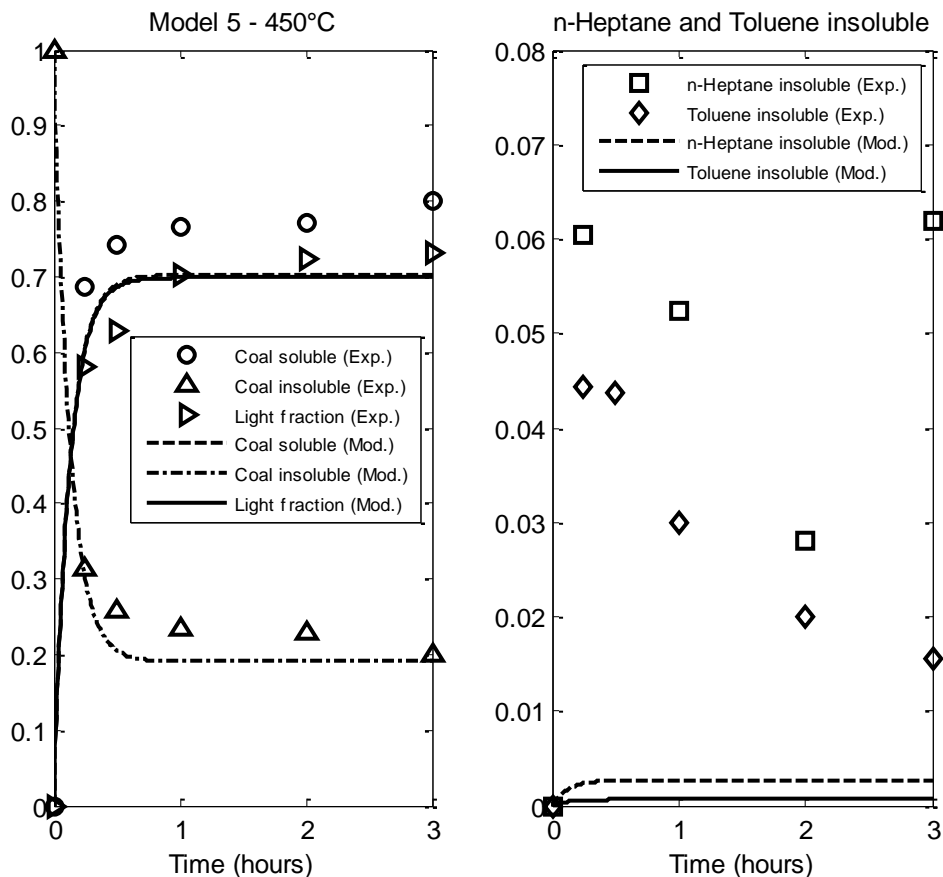


Figure 44 Model 5 at 450°C

6.5. Discussions

Low temperature regime

The process of solvent extraction of coal at low temperature is described (as observed in the experimental results) using two terms, one for physical dissolution and one for reactive dissolution.

Physical dissolution is characterized by very fast dissolution in which physical interactions between the solvent and coal takes place, as a result of this interaction a solution is obtained with the physically extractable material. This physical dissolution region is affected by temperature, as observed in *Figure 17*, and the extraction yield increases as temperature increases. Physical dissolution is rapid and it dominates extraction at short contact time. Also it is understood that at higher temperature (e.g. 300°C), the physical dissolution is essentially complete at times shorter than 15 minutes. Nevertheless, the experiments that were carried for the purpose of this study could not be run at times less than 15 minutes due to limitations of the heating rate of

the sand bath employed. The dissolution-time profile of physical dissolution could not be determined.

The reactive dissolution region is also influenced by temperature. From the results presented in *Figure 17*, it can be seen that the extraction yield after 1 hour at 100°C and 200°C remains constant, but at 300°C the extraction yield keeps on increasing after 1 hour.

Evidence that supports the fact of the reactive dissolution is taking place, can be found in the elemental analysis shown in *Figure 26*. In these results, it can be observed that the H/C ratio barely changes for extractions runs at 100 and 200°C, being close to the H/C ratio of the raw coal at different reaction times, but not for extraction at 300 °C. There is little reactive dissolution activity, and the extraction yield obtained at 100 and 200°C is related mainly to physical dissolution. Despite the dominance of physical dissolution, the presence of intermediate products from tetralin as a result of hydrogen donation is observed at 100°C and 15 minutes (see *Appendix 6*). This supports literature (8) that even at low temperature a small amount of reactive dissolution takes place, even though the temperature is not high enough to favour significant free radical formation from coal decomposition. Otherwise, the effect of tetralin can play an important role in the formation of free radicals in the coal structure, as pointed out by Chunqi et al, studied the influence of temperature and solvent on the formation of free radicals. In this paper, the authors tested various organic solvents during the coal liquefaction tracing the formation of the radicals by electron paramagnetic resonance (EPR). The formation of free radicals was detected at low temperatures using *N*-methyl-2-pyrrolidinone (NMP) increasing its intensity faster (than observed with other solvents) as temperature increased (60 – 260°C) and then decreasing (this due to capping of the radicals with hydrogen atoms). Therefore from this study it can be concluded that the mechanism of free radicals formation also depends on the solvent that is surrounding the coal during the extraction process (44).

Oppositely, the H/C ratio obtained for extractions at 300°C decreases, but at a slow rate as time increases, but not as fast as it is observed for runs at higher temperature. The change in H/C ratio is the result of breaking bonds and incorporation of hydrogen into the lighter molecules produced from the coal structure.

From the results obtained modelling the solvent extraction process and taking into account the 2 regions mentioned previously, it should be highlighted that both terms are needed to properly model the whole process of extraction. Without taking into account the events occurring at short contact times, which are dominated by rapid physical dissolution, the extraction process cannot be properly modelled. Without two terms the results obtained will be similar to those obtained when testing the models propose by Giri and Sharma presented in *Figure 19* and *Figure 20*.

High temperature regime

The solvent extraction at high temperatures leads to an increase in the extraction yield as would be expected. At 350°C the effect of extended time is more beneficial for the extraction yield. For the extractions at 450°C the process occurs very fast and 85.6% of the total extraction yield obtained at 3 hours, is achieved after only 15 minutes.

On the other hand, n-heptane insoluble fraction at 350°C keeps on increasing over the time (see *Figure 30*). In the extractions at 450°C the behaviour of the n-heptane insoluble fraction is similar to toluene insoluble fraction, a decrease in the extraction yield is observed at 1 hour until 2 hours, after then, as observed in *Figure 31*, the extraction yield at 3 hours increases with respect to the extraction yield at 2 hours. Even though the differences observed are not large, a decrease in the n-heptane insoluble fraction can be explained by its chemical composition. The n-heptane insoluble fraction is typically more polar than the toluene insoluble fraction. This polar nature is due to the presence of heteroatoms such as oxygen and sulphur. These heteroatoms form weaker bonds with carbon than the bonds carbon with carbon. The decrease of n-heptane and toluene insoluble fractions observed in *Figure 31* can indicate thermal cracking of those structures, producing lighter fractions, which agrees with the increase in the light fraction that was observed. Thermal cracking of C-O and C-S bonds take place more readily than that of C-C bonds.

As discussed in the section of low temperature regime, the change of the H/C ratio with respect to the raw coal shows evidence of the chemical activity. As presented in *Figure 25*, the decrease of the H/C ratio at high temperatures is very fast. But, it is interesting that there is no significant difference between H/C ratios at 350°C compared to 450°C. The insignificant difference between the H/C ratios at 350 and 450°C could be an indication of the formation of high molecular weight aromatic compounds.

Evidence of the free radical mechanism can be obtained from the ¹H-NMR, specially related with the mechanism of hydrogen donation by tetralin. (No attempts were made to remove tetralin from the liquid samples due to its high boiling point). As observed in *Figure 1* the intermediate products of tetralin are characterized by the formation of double bonds as a result of hydrogen donation. As this donation continues during time, it can be related with the increase of olefin like structures observed in *Figure 27*. The hydrogen donation continues towards the formation of naphthalene, in that moment there is no hydrogen that can be donated to the coal structure and olefin are observed to decrease at 2 hours of reaction time. On the other hand, as naphthalene is formed, an increase in the aromatics should be observed. This agrees with the results presented in *Figure 27* in which an increase in aromatic products is observed.

In the case of modelling solvent extraction of coal at high temperatures, it is observed that the predominant event is the reactive stage. The physical stage constitutes a relevant part of the process but occurs almost instantaneously at high temperatures, such as, for this practical purpose of modelling was not taken into account. Model 2 and Model 3 show that the solvent extraction of coal can be modelled as a single reaction with a single constant rate. Coal soluble, coal insoluble and the light fractions can be modelled using the mechanism and kinetics proposed in Model 2 and Model 3. As can be observed in *Figure 37*, *Figure 38*, *Figure 39* and *Figure 40* these models are able to predict very accurately the experimental data, meeting the requirements of termination tolerance of 1×10^{-8} , but is not able to predict n-heptane and toluene insoluble fractions. Model 4 and Model 5 are using 2 sets of parallel reactions and are also able to predict the coal soluble, insoluble and light fractions, but not as close as Model 2 and Model 3 to the experimental data. Similarly to Model 2 and 3, Model 4 and 5 failed to predict the behaviour of the n-heptane and toluene insoluble fractions. Model 1 failed to predict the extraction processes itself, none of the fractions were modelled by the mechanism and kinetics proposed for Model 1. When analyzing the values obtained for each model for the constant rate and the stoichiometric factors (see *Table 5*), Model 1 and Model 4 are rejected. The reason why the models were rejected is because the stoichiometric factors obtained are higher than 1.

Table 5 Summary of the parameters calculated for the models proposed

Temperature (°C)		k1	a	b	c	d	k2
350	Model 1	0.63	2.09	411.89	22.42	1475.09	N.A
	Model 2	3.03	0.42	0.03	0.05	0.50	N.A
	Model 3	2.50	N.A	N.A	N.A	N.A	N.A
	Model 4	0.20	6.36	0.03	0.05	7.58	2.82
	Model 5	3.69	N.A	N.A	N.A	N.A	0.21
450	Model 1	3.75	1.37	26137.81	17.82	4154.15	N.A
	Model 2	8.33	0.69	0.03	0.06	0.23	N.A
	Model 3	7.02	N.A	N.A	N.A	N.A	N.A
	Model 4	0.13	43.58	0.03	0.06	14.20	8.20
	Model 5	7.64	N.A	N.A	N.A	N.A	0.35

The n-heptane and toluene insoluble fractions were obtained in order to build a kinetic model, based on measurable lumped products. As observed in all models proposed, none of them shown a good fit for the n-heptane and toluene insoluble fractions, meanwhile the 3 fractions left (coal soluble, insoluble and light fraction) that are a “direct” result from the extraction process are well predicted by the models. This can demonstrate that a kinetic model intended to reflect the real chemistry that is happening during the solvent extraction of coal cannot be build up based on solubility basis.

One of the literature models tested (Model C), provided an interesting result when analysing the constant rates. Retrograde or condensation reaction takes place during the solvent extraction of coal. In the case of the models that were proposed in this study, retrograde reactions were not taking into account, which can lead to erroneous prediction of the n-heptane insoluble fraction.

Weller also pointed out the deficiencies and lack of understanding of the solvent extraction process of coal reflected in models that have been built up with the aim to explain the extraction mechanism. In this communication, Weller criticizes the empirical foundations that have been employed to propose a reaction mechanism. Besides, it is pointed out that the fractions obtained on “the basis of solubility” are not individual species, and those may change over time in solvent extraction of coal (45). That is, a description based on solubility does not uniquely classify molecules.

Such a change in the composition of the n-heptane and toluene insoluble fractions over time was observed in this study. The structural composition of n-heptane and toluene insoluble was studied by infrared spectroscopy using a FT-IR MB3000 (ABB) with diamond attenuated total reflectance (ATR). The analysis of the spectra was done using hierarchical cluster analysis shown in

Appendix 7. Five clusters were identified. Each cluster is constituted by a number of spectra (see Labeling in

Appendix 7) which have similarities among them. For example Cluster 1, is integrated by spectra of heptane insoluble at different residence times, at 350 and 450°C. This is an ideal situation, but when analysing the elements (spectra) that conform other clusters the following is observed:

- Cluster 2 and Cluster 4 are integrated by spectra of n-heptane and toluene insoluble. Such similarities should not be observed between n-heptane and toluene insoluble that enables these fractions to belong to the same cluster. In terms of modelling, these similarities do not support the fact that n-heptane and toluene insoluble were taken as two different lumped categories.

On the other hand, distance between the five clusters is observed. This can be interpreted as differences between the clusters. For example Cluster 1 and Cluster 2 contain elements of n-heptane insoluble each one, that differences among the clusters should not be observed. To sum up, differences in the structural composition for either n-heptane or toluene insoluble were observed. Therefore n-heptane and the toluene insoluble fraction do not exhibit the same structural composition, these fractions should not have been considered as categories for modelling.

6.6. Conclusions

- Solvent extraction of coal at low temperatures follows the basic deterministic model of dissolution or first order and can be modelled using this model taking into account two steps during the extraction: physical dissolution (at short times) and reactive dissolution (at time larger than 15 minutes approximately).
- The reaction mechanism of solvent extraction of coal can be proposed in a single reaction however, the products included in the reaction should not be obtained on basis of solubility.
- Differences in the composition of n-heptane and toluene insoluble were observed, for that reason it is inconsistent to generate a kinetic model based on products that were obtained by differences in solubility.
- The solvent extraction of coal at 350°C and 450°C can be modeled following the same reaction mechanism, obtaining a constant rate value higher for 450°C, showing the influence of the temperature in the process.

6.7. Recommendations

- It is important to obtain experimental data for times shorter than 15 minutes, in order to accurately model the physical dissolution region. For that purpose a semi-continuous reactor using preheated solvent and coal, will help to elucidate the phenomena occurring at short periods of time.
- In order to properly model the solvent extraction of coal at high temperatures, is highly recommended to test the following techniques in order to characterize the products obtained in the process:
 - Centrifugation of the products obtained, in order to obtain a wide range of products classified based on weight (46).
 - Perform a simulated distillation SimDist to characterize the products based on boiling point.

7. GENERAL CONCLUSIONS

In this study the following hypotheses were stated

1. Mass transfer limits the liquefaction process. Mass transfer limitations depend on particle size. These limitations can be observed as yield losses and the formation of high molecular weight products (recombination of free radicals, i.e., self-stabilization).
2. The kinetic description used for solvent extraction of coal cannot be formulated as a state function. The kinetic model should be formulated based on a time-temperature profile, where the time-temperature history affects dissolution.

The outcome of the study of the hypotheses presented above is:

1. Mass transfer limits the liquefaction process:
 - a. No effect of particle size was observed in the range studied (53 – 1000 μm). However, due to the rapid dissolution process of coal observed, the residence time was not short enough to observe the influence of particle size in the extraction yield.
 - b. There is no limitation on the extent of dissolution due to coal to solvent ratio in the range studied (1:2, 1:3 and 1:8). From an industrial point of view, this finding is very attractive, meaning that liquid extracts from coal can be obtained using less solvent without affecting the yield. However, the coal to solvent ratio that can be used in the industrial process could be even less than 1:2, but this scenario was not studied.
2. The kinetic description used for solvent extraction of coal cannot be formulated as a state function.
 - a. The limiting concentration reached at the end of the physical dissolution region is exponentially dependent on the temperature.
 - b. Chemical dissolution is dominant at temperatures above 300°C.
 - c. The solvent extraction of coal can be modelled as a single reaction mechanism based on a time profile obtained experimentally.

Apart from the conclusions mentioned above, the following was also concluded from this study:

- Two regions were identified during the solvent extraction process of coal: physical dissolution region and chemical dissolution region.
- The physical dissolution occurs very fast, at very short times. In this study the threshold established for the physical dissolution region was 15 minutes. However, this threshold could be less than 15 minutes. In this study, residence times shorter than 15 minutes could not be studied due to configuration of the experimental setting.
- The chemical dissolution region was observed to become noticeable at a temperature of 200°C. As temperature increased the chemical dissolution became dominant for the solvent extraction process of coal.
- The modelling of solvent extraction of coal at low temperatures (below 350°C) was performed taking into account the physical and the chemical dissolution regions.
- Two terms were included for the modelling of solvent extraction of coal. The first term describes physical dissolution, which includes a constant rate and a limiting concentration that is reached at physical dissolution conditions. The second term describes chemical dissolution, which also includes a constant rate and a limiting concentration that is reached at extended times.
- Coal reactivity is indeed affected by coal rank. Low rank coal, as observed in this case using lignite, has higher reactivity than high rank coals (subbituminous and bituminous).
- Differences in the chemical structure of n-heptane and toluene insoluble fractions over extraction time were observed. The chemical structure of the insoluble fractions was not the same at different process conditions
- Lumped categories of products obtained from liquid extracted coal on solubility basis (n-heptane and toluene insoluble fractions) are not suitable to describe the solvent extraction process of coal.
- A single reaction mechanism can describe the solvent extraction of coal. However, as it was observed in the results of testing literature models, retrograde reactions should be taken into account for proper modelling.

8. BIBLIOGRAPHY

- (1) Abichandani, J. S.; Shah, Y. T.; Cronauer, D. C.; Ruberto, R. G. Kinetics of thermal liquefaction of coal. *Fuel* **1982**, *61*, 276-82.
- (2) Do Kim, S.; Woo, K. J.; Jeong, S. K.; Rhim, Y. J.; Lee, S. H. Production of low ash coal by thermal extraction with N-methyl-2-pyrrolidinone. *Korean Journal of Chemical Engineering* **2008**, *25*, 758-763.
- (3) Larson, E. D.; Tingji, R. Synthetic fuel production by indirect coal liquefaction. *Energy for Sustainable Development* **2003**, *Volume VII No. 4*, 79.
- (4) Lee, S.; Speight, J.; Loyalka, S. In *Clean Liquid Fuels from Coal*; Handbook of alternative fuel technologies; CRC Press: Boca Raton, USA, 2007; pp 115.
- (5) Schmidt, L. D. *Engineering of Chemical Reactions (2nd Edition)*. , 454.
- (6) T. Kabe, A. Ishihara, E.E. Qian, I P. sutrisna, Y. Kabe In *Coal and Coal-Related Compounds*; Kodansha: Tokyo, 2004; .
- (7) Anonymous Wiley Critical Content - Petroleum Technology, Volume 1-2. , 352-353.
- (8) Berkowitz, N. In *An introduction to coal technology*; Academic Press Inc.: New York, 1979; .
- (9) C.Y. Wen, E. S. L. In *Coal Conversion Technology*; Addison-Wesley Publishing Company: Reading, Massachusetts, 1979; .
- (10) Mohan, G.; Silla, H. Kinetics of donor-solvent liquefaction of bituminous coals in nonisothermal experiments. *Ind. Eng. Chem. Process Des. Dev.* **1981**, *20*, 349-58.
- (11) Quann, R. J.; Jaffe, S. B. Structure-oriented lumping: describing the chemistry of complex hydrocarbon mixtures. *Ind Eng Chem Res* **1992**, *31*, 2483-97.
- (12) Schobert, H. H. The geochemistry of coal. Part I. The classification and origin of coal. *J. Chem. Educ.* **1989**, *66*, 242-null.
- (13) Mayo, F. R.; Pavelka, L. A.; Zevely, J. S.; Hirschon, A. S. Extractions and Reactions of Coals Below 100-Degrees-C .3. Comparison of Extraction Products of Illinois No-6 Coal. *Fuel* **1988**, *67*, 607-611.
- (14) Berkowitz, N.; Calderon, J.; Liron, A. Some Observations Respecting Reaction Paths in Coal-Liquefaction .1. Reactions of Coal Tetralin Slurries. *Fuel* **1988**, *67*, 626-631.

- (15) Gethner, J. S. Thermal and Oxidation Chemistry of Coal at Low-Temperatures. *Fuel* **1985**, *64*, 1443-1446.
- (16) Shaw, J. M.; Peters, E. Role of initial reaction conditions in direct coal liquefaction. *Industrial and Engineering Chemistry Research* **1989**, *28*, 1795-1801.
- (17) Shaw, J. M.; Peters, E. A general model for coal dissolution reactions. *Ind Eng Chem Res* **1989**, *28*, 976-82.
- (18) Provine, W. D.; Jung, B.; Jacintha, M. A.; Rethwisch, D. G.; Huang, H.; Calkins, W. H.; Klein, M. T.; Scouten, C.; Dybowski, C. R. A Kinetic Investigation of Coal-Liquefaction at Short Reaction-Times. *Catalysis Today* **1994**, *19*, 409-419.
- (19) Franz, J. A.; Camaioni, D. M. Radical Pathways of Coal Dissolution in Hydrogen Donor Media .2. Beta-Scission and 1,2 Aryl Migration Reactions of Radicals Derived from Methylindans and Tetralin at 327-627-Degrees-C. *J. Org. Chem.* **1980**, *45*, 5247-5255.
- (20) De Klerk, A., Ed.; In *Beyond Fisher Tropsch*; Elsevier, Ed.; 2009; pp 592.
- (21) Huang, H.; Wang, K.; Wang, S.; Klein, M. T.; Calkins, W. H. Kinetics of Coal Liquefaction at Very Short Reaction Times. *Energy Fuels* **1996**, *10*, 641-8.
- (22) Penninger, J. M. L. New aspects of the mechanism for the thermal hydrocracking of indan and tetralin. *Int J Chem Kinet* **1982**, *14*, 761-80.
- (23) Shalabi, M. A.; Baldwin, R. M.; Bain, R. L.; Gary, J. H.; Golden, J. O. Noncatalytic coal liquefaction in a donor solvent. Rate of formation of oil, asphaltenes, and preasphaltenes. *Ind. Eng. Chem. Process Des. Dev.* **1979**, *18*, 474-9.
- (24) Masuda, K.; Okuma, O.; Nishizawa, T.; Kanaji, M.; Matsumura, T. High-temperature NMR analysis of aromatic units in asphaltenes and preasphaltenes derived from Victorian brown coal. *Fuel* **1996**, *75*, 295-9.
- (25) Song, C.; Nihonmatsu, T.; Nomura, M. Effect of pore structure of nickel-molybdenum/alumina catalysts in hydrocracking of coal-derived and oil sand derived asphaltenes. *Ind Eng Chem Res* **1991**, *30*, 1726-34.
- (26) Pradhan, V. R.; Holder, G. D.; Wender, I.; Tierney, J. W. Kinetic Modeling of Direct Liquefaction of Wyodak Coal Catalyzed by Sulfated Iron-Oxides. *Ind Eng Chem Res* **1992**, *31*, 2051-2056.
- (27) Speight, J. G. Handbook of Coal Analysis., pp 191.
- (28) Shui, H.; Zhou, H. Kinetic study on the aggregation of coal soluble constituents in solution. *Fuel Process Technol* **2005**, *86*, 661-671.

- (29) Cronauer, D. C.; Shah, Y. T.; Ruberto, R. G. Kinetics of thermal liquefaction of Belle Ayr subbituminous coal. *Ind. Eng. Chem. Process Des. Dev.* **1978**, *17*, 281-8.
- (30) Ceylan, K.; Olcay, A. Kinetic rate models for dissolution of Turkish lignites in tetralin under nitrogen or hydrogen atmospheres. *Fuel Process Technol* **1998**, *53*, 183-195.
- (31) Chen, C.; Gao, J.; Yan, Y. Original preasphaltenes and asphaltenes in coals. *Fuel Process Technol* **1998**, *55*, 143-151.
- (32) Li, X.; Hu, H.; Zhu, S.; Hu, S.; Wu, B.; Meng, M. Kinetics of coal liquefaction during heating-up and isothermal stages. *Fuel* **2008**, *87*, 508-513.
- (33) Rudling, J. Simple model based on solubility parameters for liquid desorption of organic solvents adsorbed on activated carbon. *J. Chromatogr.* **1986**, *362*, 175-85.
- (34) Sanada, Y.; Honda, H. Solvent Extraction of Coal - Relation between the Yield of Extract and the Solubility Parameter of the Solvent. *Bull. Chem. Soc. Jpn.* **1962**, *35*, 1358-1360.
- (35) Giri, C. C.; Sharma, D. K. Kinetic studies and shrinking core model on solvolytic extraction of coal. *Fuel Process Technol* **2000**, *68*, 97-109.
- (36) Speight, J. G. Handbook of Coal Analysis., pp 9.
- (37) Miura, K.; Mae, K.; Hasegawa, I.; Chen, H.; Kumano, A.; Tamura, K. Estimation of Hydrogen Bond Distributions Formed between Coal and Polar Solvents Using in Situ IR Technique. *Energy Fuels* **2002**, *16*, 23-31.
- (38) Giri, C. C.; Sharma, D. K. Mass-transfer studies of solvent extraction of coals in N-methyl-2-pyrrolidone. *Fuel* **2000**, *79*, 577-585.
- (39) Landau, H. G.; Asbury, R. S. Ultimate yield of solvent extraction of coal; calculation from rate of extraction. *J. Ind. Eng. Chem. (Washington, D. C.)* **1938**, *30*, 117.
- (40) Asbury, R. S. Action of solvents on coal. Extraction of Edenborn coal by benzene at elevated temperatures. *J. Ind. Eng. Chem. (Washington, D. C.)* **1934**, *26*, 1301-6.
- (41) Murcia, C. F.; Hernandez, M. R.; Gupta, R.; de, K., Arno. Solvent extraction of coal at low temperature: influence of time and particle size. *Prepr. Symp. - Am. Chem. Soc., Div. Fuel Chem.* **2011**, *56*, 304-305.
- (42) Kucukbayrak, S.; Haykiri-Acma, H.; Ersoy-Mericboyu, A.; Yaman, S. Effect of lignite properties on reactivity of lignite. *Energy Convers. Manage.* **2000**, *42*, 613-626.

- (43) Čupera, J. Mathematical models of dissolution, Masarykova Univerzita, Brno, Czech Republic, 2009.
- (44) Li, C.; Takanohashi, T.; Saito, I.; Iino, M.; Moriyama, R.; Kumagai, H.; Chiba, T. The behavior of free radicals in coal at temperatures up to 300 C in various organic solvents, using in situ EPR spectroscopy. *Energy and Fuels* **2002**, *16*, 1116-1120.
- (45) Weller, S. W. Kinetics of Coal Liquefaction: Interpretation of Data. *Energy Fuels* **1995**, *9*, 384-5.
- (46) Eyssautier, J.; Levitz, P.; Barbier, J.; Espinat, D.; Barre, L. In *In Asphaltene aggregation behaviors through mass and composition polydispersity*; American Chemical Society: 2011; , pp FUEL-372.
- (47) ASTM Standard D3173-11, "Moisture in the Analysis Sample of Coal and Coke," ASTM International, West Conshohocken, PA, 2011, DOI: 10.1520/D3173-11, www.astm.org.
- (48) ASTM Standard D3173-11, "Ash in the Analysis Sample of Coal and Coke from Coal," ASTM International, West Conshohocken, PA, 2011, DOI: 10.1520/D3174-11, www.astm.org.
- (49) ASTM Standard D3175-11, "Volatile Matter in the Analysis Sample of Coal and Coke," ASTM International, West Conshohocken, PA, 2011, DOI: 10.1520/D3175-11, www.astm.org.
- (50) ASTM Standard D3175-11, "Standard Test Method for n-Heptane Insolubles," ASTM International, West Conshohocken, PA, 2007, DOI: 10.1520/D3279-07, www.astm.org.

9. APPENDIXES

Appendix 1 – List of equipment

- Fluidised Bath SBS-4
Brand: TECHNE
With temperature controller TC-8D

- Furnace for ash analysis
Brand: Barnstead Thermolyne

- Vacuum oven
Brand: Thermo Scientific
Model 6259

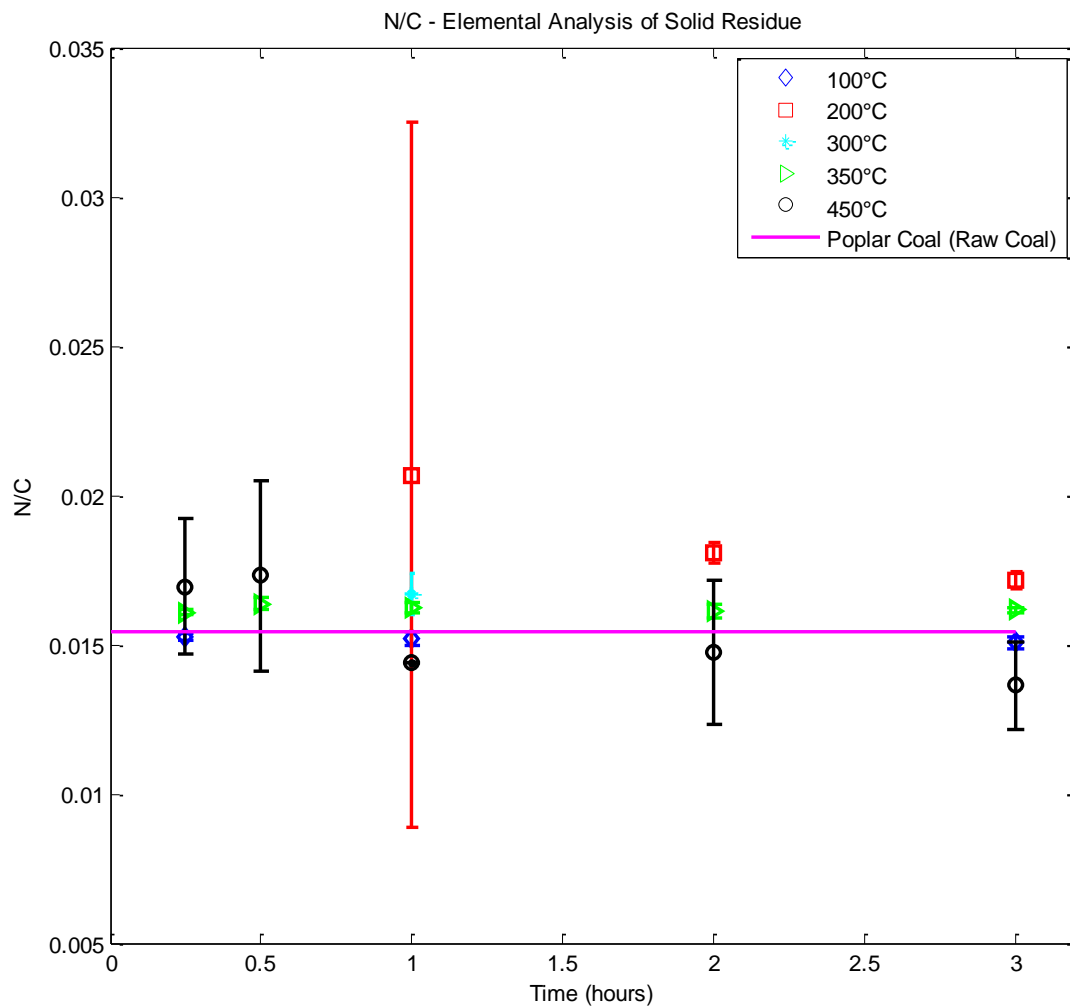
- Rotoevaporator
Brand: Heidolph Instruments GmbH & Co
Type Basis Hel-VAP ML
With Rotavac vario pumping unit

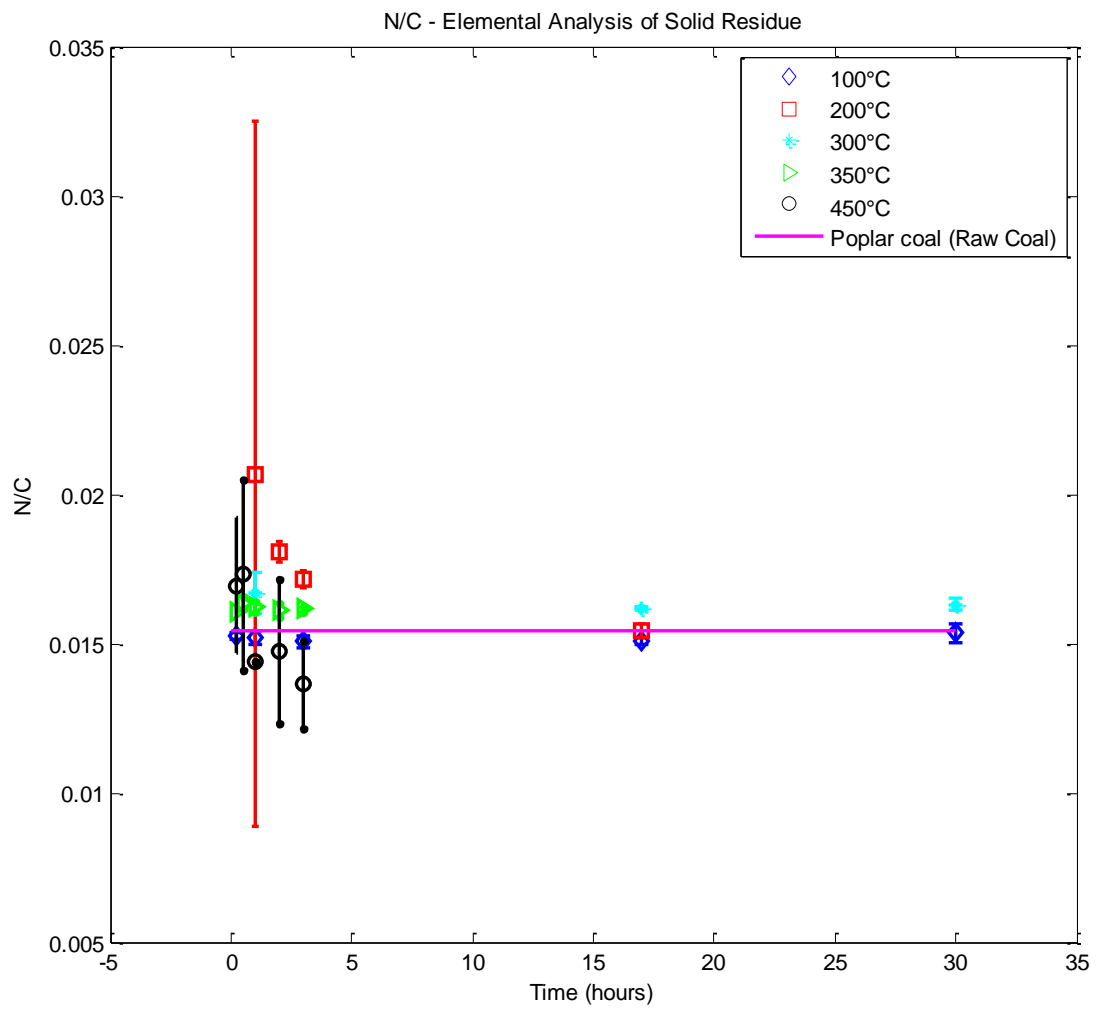
- Stainless steel microreactor
Capacity: 15 mL
DN: 10mm
Fittings provided by Swagelok

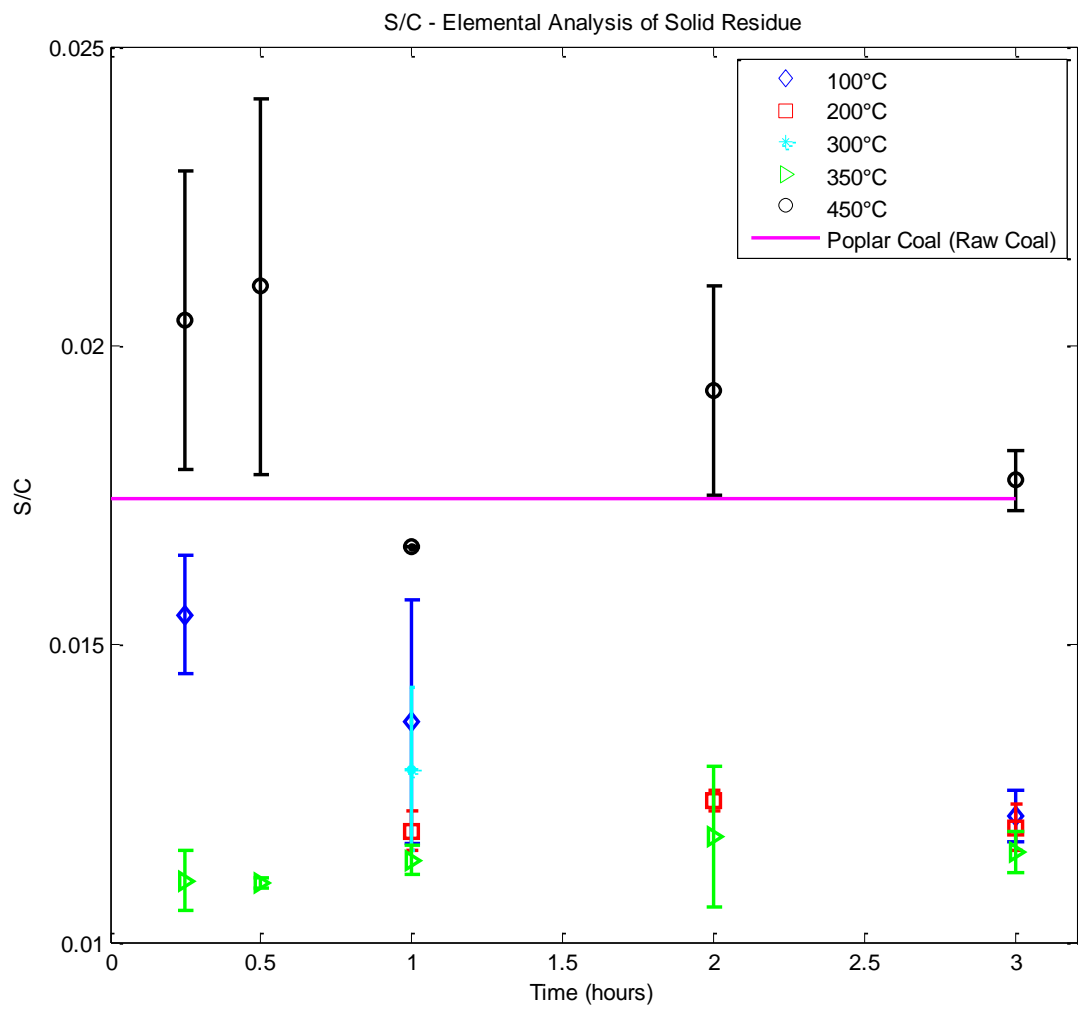
- TGA – SDT Q600
Simultaneous DSC – TGA
Brand: T.A

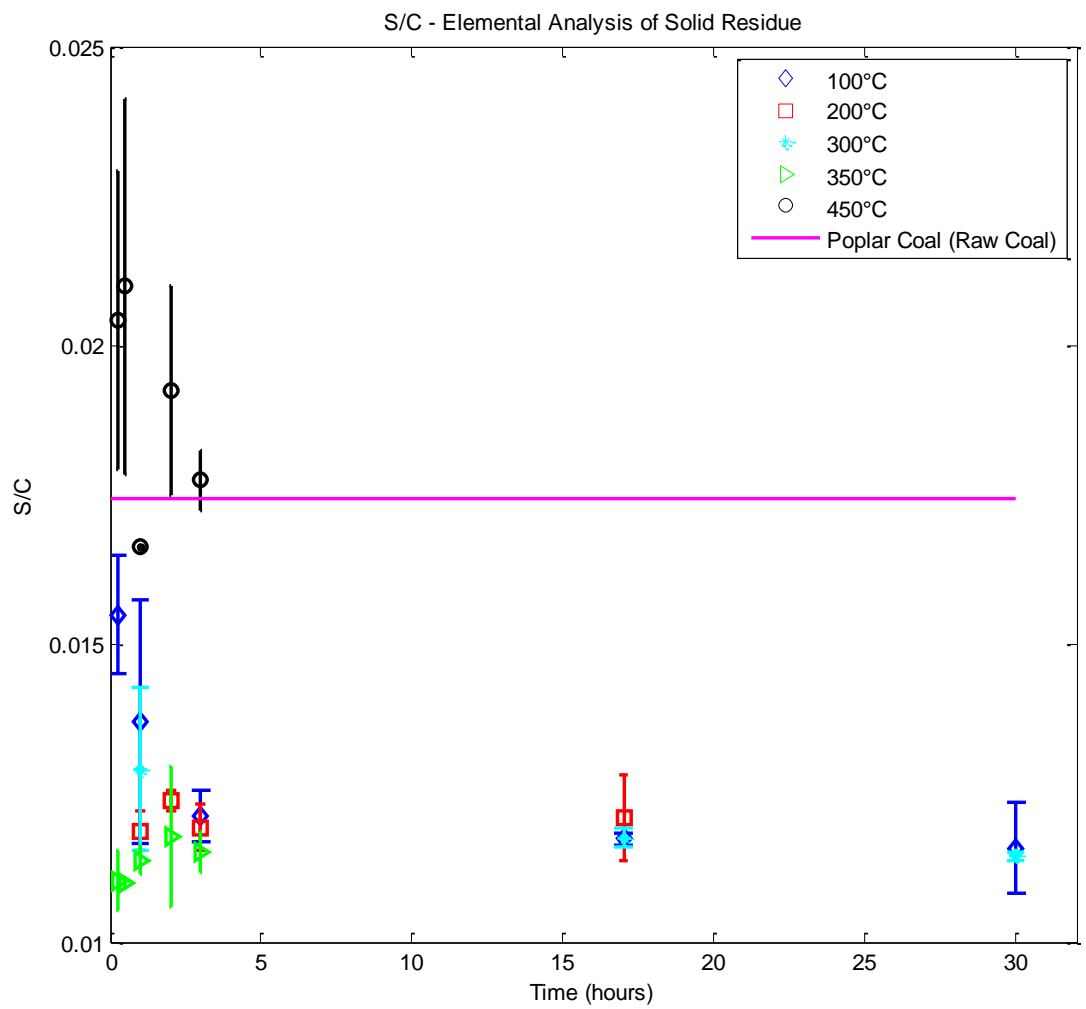
- FTIR MB 3000
With MIRacle™ ATR – PIKE Technologies
Multi-Reflection Attenuated Total Reflectance
Software: Horizon MB
Brand; ABB Inc

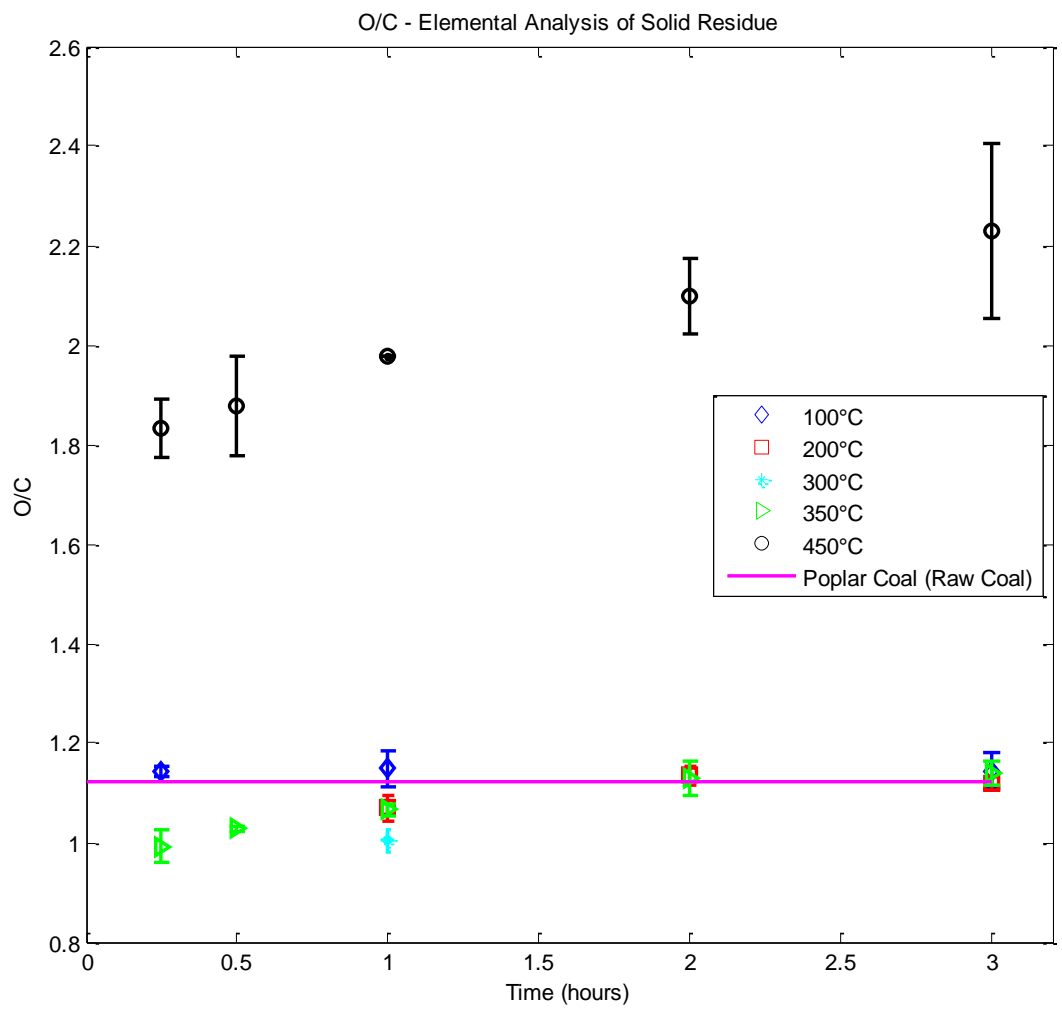
Appendix 2 – Elemental analysis of the solid residue (coal insoluble)

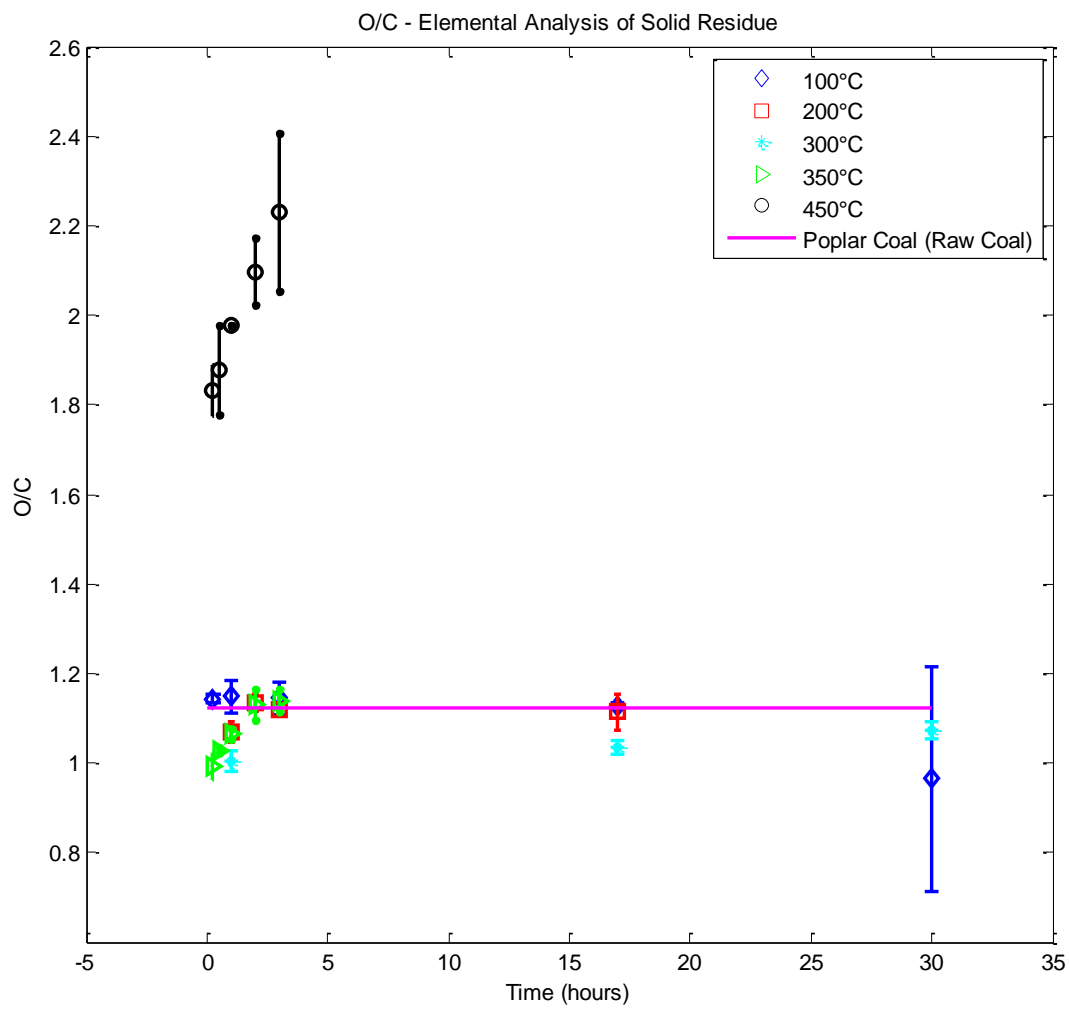




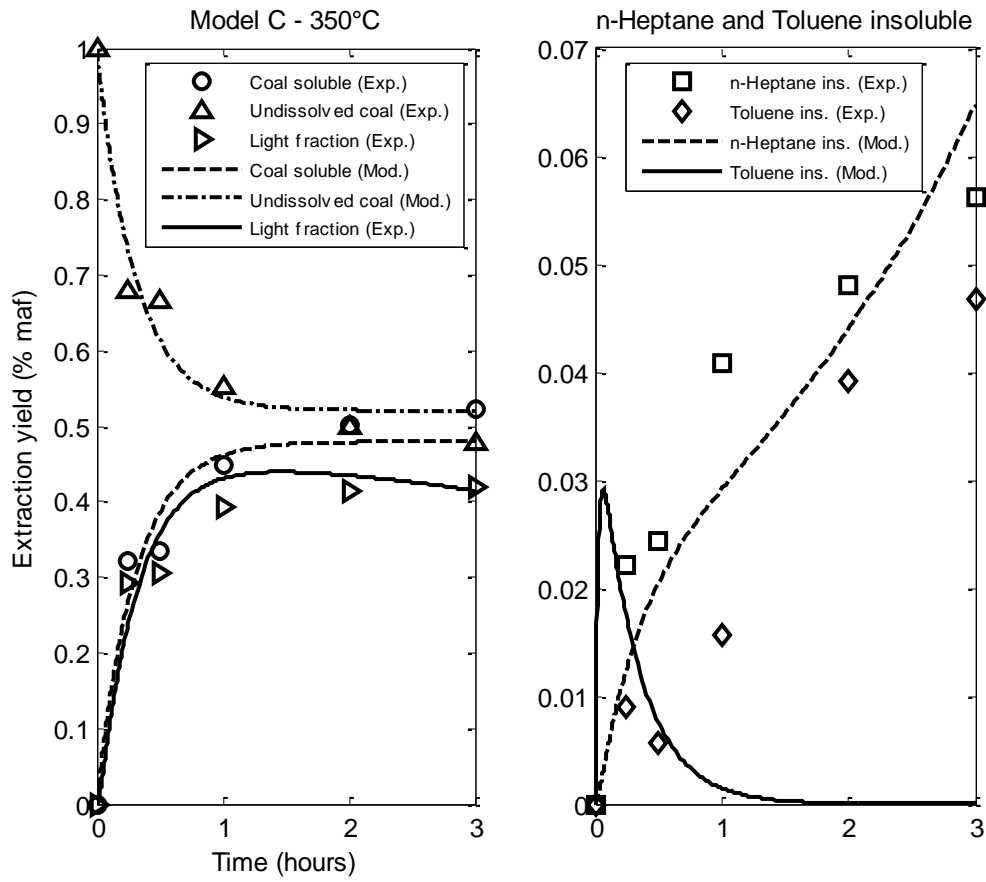




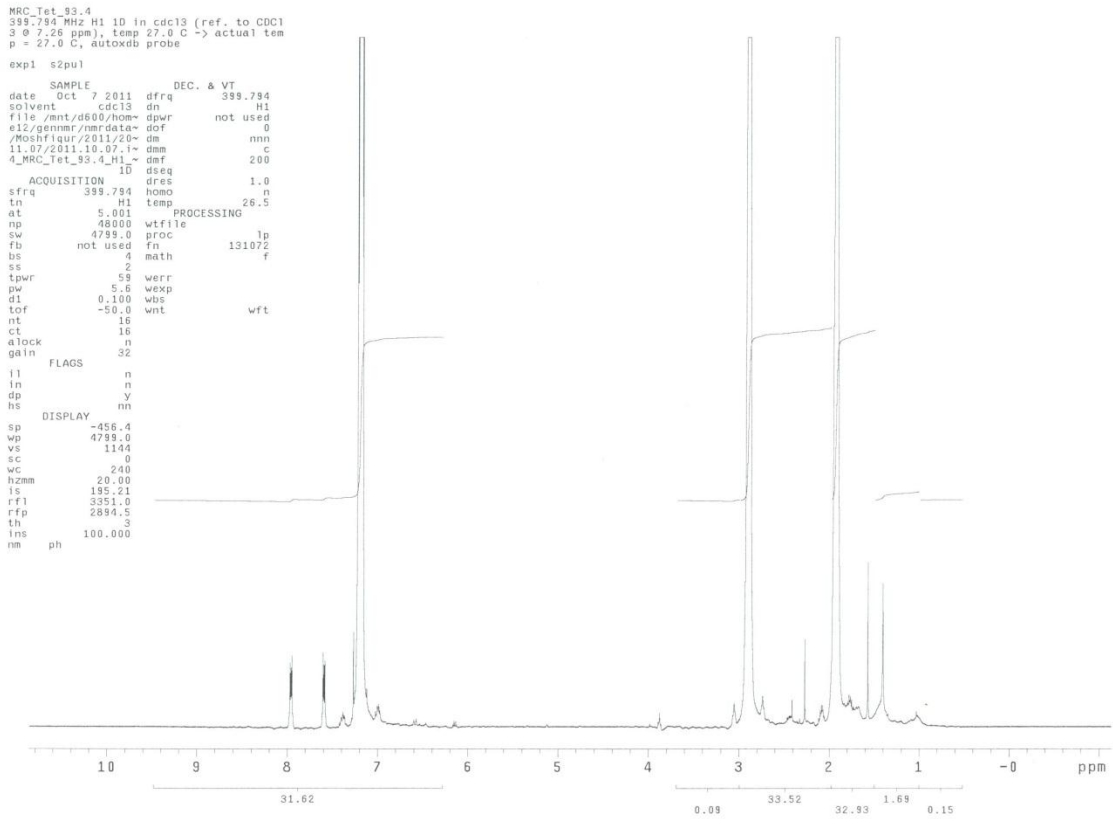




Appendix 3 Graphic representation of the extraction yield predicted by Model C (no constrain tolerance)



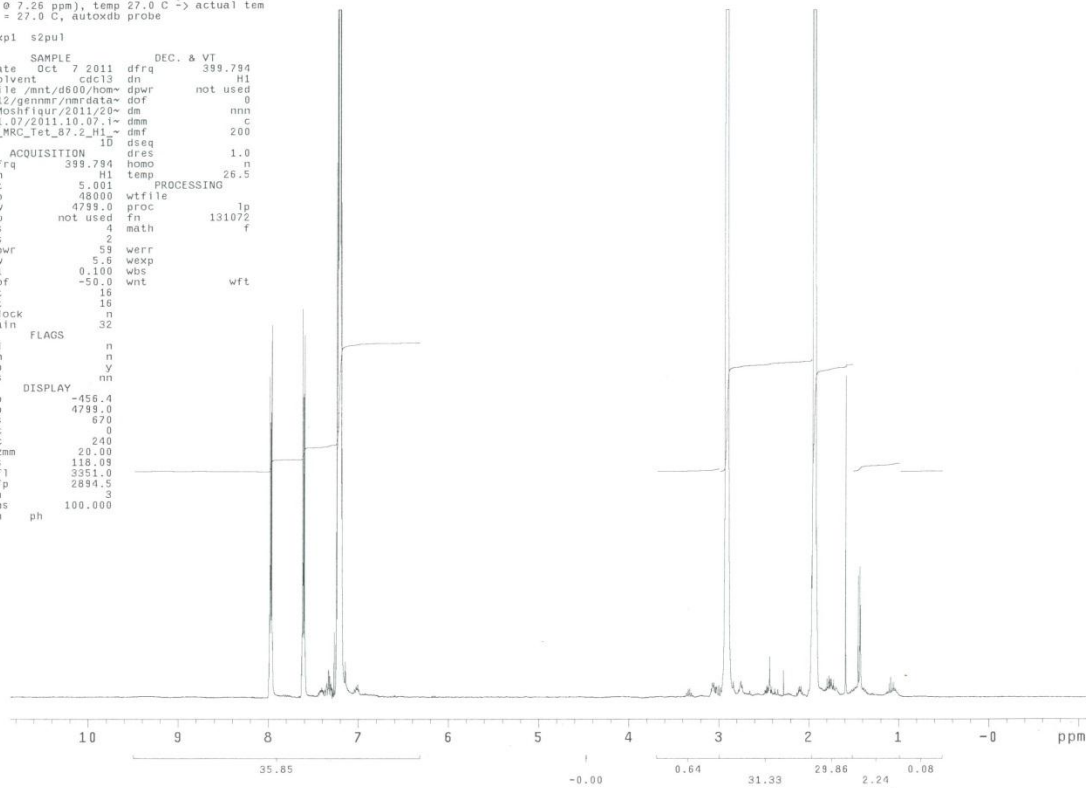
Appendix 4 – ¹H-NMR analysis of the liquid coal extracted



MRC_Tet_87.2
 399.794 MHz H1 D in cdc13 (ref. to CDC1
 3 @ 7.26 ppm), temp 27.0 C -> actual tem
 p = 27.0 C, autotdb probe

```

exp1 s2pu1
SAMPLE          DEC. & VT
date    Oct 7 2011  dfrq    399.794
solvent  cdc13      dn      H1
file    /mnt/d600/hom~ dpwr  not used
e12/genmr/nmrdata~ dof    0
/Moshfigur/2011/20~ dm    nnn
11.27/2011-10.07.1~ dmm    c
4_MRC_Tet_87.2_H1~ dmf    200
ACQUISITION    10      dseq    1.0
sfrq    399.794      homo    n
tn      H1          temp    26.5
at      5.001      PROCESSING
np      48000      wfile
sw      4799.0      proc    1p
fb      not used   fn      131072
bs      4          math    f
ss      2
tpwr    59        werr
pw      5.6       wexp
dl      0.100     wbs
tof     -50.0     wnt      wft
nt      16
ct      16
atock   n
gain    32
FLAGS
il      n
in      n
dp      y
hs      nm
DISPLAY
sp      -456.4
wp      4799.0
vs      670
sc      0
wc      240
hzmm    20.00
fs      118.09
rf1     3991.0
rfp     2894.5
th      3
lms     100.000
nm      ph
  
```



Appendix 5 - MATLAB code for the models proposed

Model 1

Reaction kinetics:

```
function dxdt = CarolinaModel1(t,x,b)

% x = variables
% b = constants

dxdt = [-b(1)*x(1);
        b(1)*(x(1)^b(2));
        b(1)*(x(1)^b(3));
        b(1)*(x(1)^b(4));
        b(1)*(x(1)^b(5));];
```

Solver:

```
%% TO CALL and Optimize
%
% b0 = [0.02 1 2 1 3]
% BB = fminsearch(@(b) MinErrorCar(b),b0);
%
%%
```

```
function myError = MinErrorCar(b0,x0)
```

```
% Xexp, Texp
load MyExpData
```

```
b = b0;
%x0 = Xexp(1,:);
```

```
MYOptions = odeset('Reltol', 2.3e-14);
```

```
[T, x] = ode45(@(t,x) CarolinaModel1(t,x,b), Texp, x0, MYOptions);
```

```
y(:,1)= x(:,2)+x(:,3)+x(:,4);
y(:,2)= x(:,4);
y(:,3)= x(:,3);
y(:,4)= x(:,1)+x(:,5);
y(:,5)= x(:,2);
```

```
% plot(T,x)
[MyLen, MyLen2] = size(Xexp);
%w = ones(MyLen2,1);
w = 1./mean(Xexp);
```

```
myError = 0;
```

```
for i = 1:5
    myError = myError + ((Xexp(:,i) - y(:,i))' * diag(w(i)*ones(MyLen,1)) * (Xexp(:,i) - y(:,i)));
end
```

```
%disp(myError);
%myError = (Xexp - x) * (Xexp - x)';
```

Plot

```
% Plot

x0 = [1; 0; 0; 0; 0;];

%optOptions = optimset('TolFun', 1e-8);
optOptions2 = optimset('MaxFunEvals',200);

%BB = fminsearch(@(b) MinErrorCar(b,x0),b0);
%BB = fminsearch(@(b) MinErrorCar3(b,x0),[1],optOptions);
BB = fminsearch(@(b) MinErrorCar3(b,x0),[1],optOptions2);

figure
subplot (1,2,1)
plot(Texp,Xexp(:,1),'or')
hold on
subplot (1,2,2)
plot(Texp,Xexp(:,2),'sb')
hold on
subplot (1,2,2)
plot(Texp,Xexp(:,3),'dk')
subplot (1,2,1)
plot(Texp,Xexp(:,4),'^m')
subplot (1,2,1)
plot(Texp,Xexp(:,5),'>g')

MYOptions = odeset('Reltol', 2.3e-14);

[T, x] = ode45(@(t,x) CarolinaModel1(t,x,BB), [0 3], x0, MYOptions);
y(:,1)= x(:,2)+x(:,3)+x(:,4);
y(:,2)= x(:,4);
y(:,3)= x(:,3);
y(:,4)= x(:,1)+x(:,5);
y(:,5)= x(:,2);

subplot (1,2,1)
plot(T,y(:,1),'--r')
subplot (1,2,2)
plot(T,y(:,2),'--b')
hold on
subplot (1,2,2)
plot(T,y(:,3),'-k')
subplot (1,2,1)
plot(T,y(:,4),'-m')
subplot (1,2,1)
plot(T,y(:,5),'-g')
```

Model 2

Reaction kinetics:

```
function dxdt = CarolinaModel2(t,x,b)

% x = variables
% b = constantes

dxdt = [-b(1)*x(1);
        b(1)*b(2)*x(1);
        b(1)*b(3)*x(1);
        b(1)*b(4)*x(1);
        b(1)*b(5)*x(1);];
```

Solver

```
%% TO CALL and Optimize
%
% b0 = [0.02 1 2 1 3]
% BB = fminsearch(@(b) MinErrorCar(b),b0);
%
%%

function myError = MinErrorCar2(b0,x0)

% Xexp, Texp
load MyExpData

b = b0;
%x0 = Xexp(1,:);

MYOptions = odeset('Reltol', 2.3e-14);

[T, x] = ode45(@(t,x) CarolinaModel2(t,x,b), Texp, x0, MYOptions);

y(:,1)= x(:,2)+x(:,3)+x(:,4);
y(:,2)= x(:,4);
y(:,3)= x(:,3);
y(:,4)= x(:,1)+x(:,5);
y(:,5)= x(:,2);

% plot(T,x)

[MyLen, MyLen2] = size(Xexp450);
%w = ones(MyLen2,1);
w = 1./mean(Xexp);

myError = 0;

for i = 1:5
    myError = myError + ((Xexp(:,i) - y(:,i))' * diag(w(i)*ones(MyLen,1)) * (Xexp(:,i) - y(:,i)));
end

%disp(myError);
%myError = (Xexp - x) * (Xexp - x)';
```

Plot:

```
% Plot

x0 = [1; 0; 0; 0; 0];

optOptions = optimset('TolFun', 1e-8);
%optOptions2 = optimset('MaxFunEvals',200);

%BB = fminsearch(@(b) MinErrorCar2(b,x0),b0);
BB = fminsearch(@(b) MinErrorCar2(b,x0),b0,optOptions);
%BB = fminsearch(@(b) MinErrorCar3(b,x0),[1],optOptions2);

figure
subplot (1,2,1)
plot(Texp,Xexp(:,1),'or')
hold on
subplot (1,2,2)
```

```

plot(Texp,Xexp(:,2),'sb')
hold on
subplot(1,2,2)
plot(Texp,Xexp(:,3),'dk')
subplot(1,2,1)
plot(Texp,Xexp(:,4),'^m')
subplot(1,2,1)
plot(Texp,Xexp(:,5),'>g')

MYOptions = odeset('Reltol', 2.3e-14);

[T, x] = ode45(@(t,x) CarolinaModel2(t,x,BB), [0 3], x0, MYOptions);
y(:,1)= x(:,2)+x(:,3)+x(:,4);
y(:,2)= x(:,4);
y(:,3)= x(:,3);
y(:,4)= x(:,1)+x(:,5);
y(:,5)= x(:,2);

subplot(1,2,1)
plot(T,y(:,1),'-r')
subplot(1,2,2)
plot(T,y(:,2),'-b')
hold on
subplot(1,2,2)
plot(T,y(:,3),'-k')
subplot(1,2,1)
plot(T,y(:,4),'-m')
subplot(1,2,1)
plot(T,y(:,5),'-g')

```

Model 3

Reaction kinetics:

```

function dxdt = CarolinaModel3(t,x,b)

% x = variables
% b = constantes

dxdt = [-b(1)*x(1);
        b(1)*(0.419515)*x(1));
        b(1)*(0.046728)*x(1);
        b(1)*(0.056294)*x(1);
        b(1)*(0.477464)*x(1);];

```

Solver:

```

function myError = MinErrorCar3(b0,x0)

% Xexp, Texp
load MyExpData

b = b0;
%x0 = Xexp(1,:);

MYOptions = odeset('Reltol', 2.3e-14);

[T, x] = ode45(@(t,x) CarolinaModel3(t,x,b), Texp, x0, MYOptions);

```

```

y(:,1)= x(:,2)+x(:,3)+x(:,4);
y(:,2)= x(:,4);
y(:,3)= x(:,3);
y(:,4)= x(:,1)+x(:,5);
y(:,5)= x(:,2);

% plot(T,x)

[MyLen, MyLen2] = size(Xexp);
%w = ones(MyLen2,1);
w = 1./mean(Xexp450);

myError = 0;

for i = 1:5
    myError = myError + ((Xexp(:,i) - y(:,i))' * diag(w(i)*ones(MyLen,1)) * (Xexp(:,i) - y(:,i)));
end

%disp(myError);
%myError = (Xexp - x)' * (Xexp - x);

```

Plot:

```

% Plot

x0 = [1; 0; 0; 0; 0;];

optOptions = optimset('TolFun', 1e-8);

%BB = fminsearch(@(b) MinErrorCar3(b,x0),b0Model3);
BB = fminsearch(@(b) MinErrorCar3(b,x0),b0,optOptions);

figure
subplot(1,2,1)
plot(Texp,Xexp(:,1),'or')
hold on
subplot(1,2,2)
plot(Texp,Xexp(:,2),'sb')
hold on
subplot(1,2,2)
plot(Texp,Xexp(:,3),'dk')
subplot(1,2,1)
plot(Texp,Xexp(:,4),'^m')
subplot(1,2,1)
plot(Texp,Xexp(:,5),'>g')

MYOptions = odeset('Reltol', 2.3e-14);

[T, x] = ode45(@(t,x) CarolinaModel3(t,x,BB), [0 3], x0, MYOptions);
y(:,1)= x(:,2)+x(:,3)+x(:,4);
y(:,2)= x(:,4);
y(:,3)= x(:,3);
y(:,4)= x(:,1)+x(:,5);
y(:,5)= x(:,2);

subplot(1,2,1)
plot(T,y(:,1),'-r')
subplot(1,2,2)
plot(T,y(:,2),'-b')
hold on
subplot(1,2,2)
plot(T,y(:,3),'-k')
subplot(1,2,1)
plot(T,y(:,4),'-m')
subplot(1,2,1)

```

```
plot(T,y(:,5),'-g')
```

Model 4

Reaction kinetics

```
function dxdt = CarolinaModel4(t,x,b)
```

```
% x = variables  
% b = constantes  
%b6 = k2
```

```
dxdt = [-b(1)*x(1)-b(6)*x(1);  
        b(1)*b(2)*x(1);  
        b(6)*b(3)*x(1);  
        b(6)*b(4)*x(1);  
        b(1)*b(5)*x(1);];
```

Solver

```
function myError = MinErrorCar4(b0,x0)
```

```
% Xexp, Texp  
load MyExpData
```

```
b = b0;  
%x0 = Xexp(1,:);
```

```
MYOptions = odeset('Reltol', 2.3e-14);
```

```
[T, x] = ode45(@(t,x) CarolinaModel4(t,x,b), Texp, x0, MYOptions);
```

```
y(:,1)= x(:,2)+x(:,3)+x(:,4);  
y(:,2)= x(:,4);  
y(:,3)= x(:,3);  
y(:,4)= x(:,1)+x(:,5);  
y(:,5)= x(:,2);
```

```
% plot(T,x)  
[MyLen, MyLen2] = size(Xexp);  
%w = ones(MyLen2,1);  
w = 1./mean(Xexp);
```

```
myError = 0;
```

```
for i = 1:5  
    myError = myError + ((Xexp(:,i) - y(:,i))' * diag(w(i)*ones(MyLen,1)) * (Xexp(:,i) - y(:,i)));  
end
```

```
%disp(myError);  
%myError = (Xexp - x) * (Xexp - x)';
```

Plot

```
% Plot
```

```
x0 = [1; 0; 0; 0; 0];
```

```
optOptions = optimset('TolFun', 1e-8);
```

```
BB = fminsearch(@(b) MinErrorCar4(b,x0),b0,optOptions);
```

```

%BB = fminsearch(@(b) MinErrorCar4(b,x0),b0Model4);

figure
subplot (1,2,1)
plot(Texp,Xexp(:,1),'or')
hold on
subplot (1,2,2)
plot(Texp,Xexp(:,2),'sb')
hold on
subplot (1,2,2)
plot(Texp,Xexp(:,3),'dk')
subplot (1,2,1)
plot(Texp,Xexp(:,4),'^m')
subplot (1,2,1)
plot(Texp,Xexp(:,5),'>g')

MYOptions= odeset('Reltol', 2.3e-14);

[T, x] = ode45(@(t,x) CarolinaModel4(t,x,BB), [0 3], x0, MYOptions);
y(:,1)= x(:,2)+x(:,3)+x(:,4);
y(:,2)= x(:,4);
y(:,3)= x(:,3);
y(:,4)= x(:,1)+x(:,5);
y(:,5)= x(:,2);

subplot (1,2,1)
plot(T,y(:,1),'-r')
subplot (1,2,2)
plot(T,y(:,2),'-b')
hold on
subplot (1,2,2)
plot(T,y(:,3),'-k')
subplot (1,2,1)
plot(T,y(:,4),'-m')
subplot (1,2,1)
plot(T,y(:,5),'-g')

```

Model 5

Reaction kinetics:

```
function dxdt = CarolinaModel5(t,x,b)
```

```

% x = variables
% b = constantes
%b2 = k2

```

```

dxdt = [-b(1)*x(1)-b(2)*x(1);
        b(1)*(0.419515)*x(1);
        b(2)*(0.046728)*x(1);
        b(2)*(0.056294)*x(1);
        b(1)*(0.477464)*x(1);];

```

Solver

```
function myError = MinErrorCar5(b0,x0)
```

```

% Xexp, Texp
load MyExpData

```

```

b = b0;
%x0 = Xexp(1,:);

MYOptions = odeset('Reltol', 2.3e-14);

[T, x] = ode45(@(t,x) CarolinaModel5(t,x,b), Texp, x0, MYOptions);

y(:,1)= x(:,2)+x(:,3)+x(:,4);
y(:,2)= x(:,4);
y(:,3)= x(:,3);
y(:,4)= x(:,1)+x(:,5);
y(:,5)= x(:,2);

% plot(T,x)
[MyLen, MyLen2] = size(Xexp);
%w = ones(MyLen2,1);
w = 1./mean(Xexp);

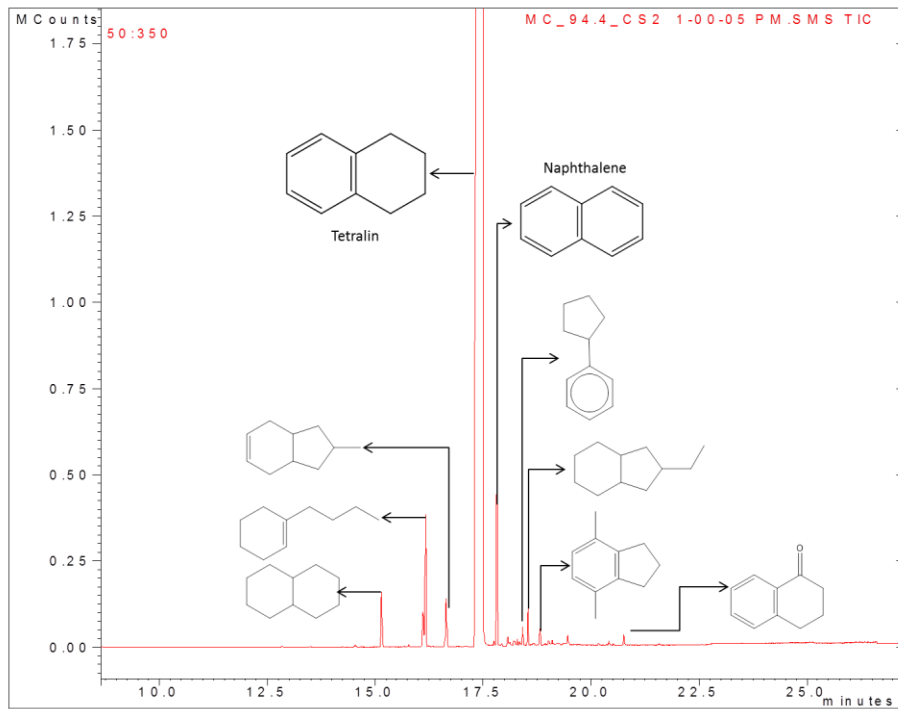
myError = 0;

for i = 1:5
    myError = myError + ((Xexp(:,i) - y(:,i))' * diag(w(i)*ones(MyLen,1)) * (Xexp(:,i) - y(:,i)));
end

%disp(myError);
%myError = (Xexp - x) * (Xexp - x)';

```

Appendix 6 - GC of extracted liquid at 100°C and 15 minutes



Appendix 7 Cluster analysis of the FTIR spectra of n-heptane and toluene insoluble fractions

Labeling of the spectra:

NO.	T/°C	t/min	solvent	NO.	T/°C	t/min	solvent	NO.	T/°C	t/min	solvent
1	350	15	heptane	14	450	15	heptane	27	350	30	toluene
2		15		15		60		28		60	
3		15		16		60		29		60	
4		30		17		60		30		120	
5		30		18		120		31		120	
6		30		19		120		32		120	
7		60		20		180		33		180	
8		60		21		180		34		180	
9		120		22	350	15	450	35	toluene	30	
10		120		23		15		36		30	
11		120		24		15		37		120	
12		180		25		30		38		120	
13		180		26		30		39		180	

Clustering analysis

